Cell Type-Selective Regulation of Food Intake and Novelty Driven Investigatory Behavior by Neurons of the Mouse Medial Prefrontal Cortex

Brandon Anthony Newmyer

Richmond, VA

B.S., Radford University, 2012

A Dissertation presented to the Graduate Faculty

of the University of Virginia in Candidacy for the Degree of

Doctorate of Philosophy

Department of Neuroscience

University of Virginia

August, 2019

Douglas A. Bayliss, PhD (Chair)

Michael M. Scott, PhD

Mark P. Beenhakker, PhD

Wendy J. Lynch, PhD

Ali D. Güler, PhD

Acknowledgements

The following work would not have been possible without the continuous support of my mentor, Dr. Michael Scott. I realize that you took a calculated risk taking me under your wing as your first graduate student and I hope that I have lived up to your expectations. Together, we have developed and refined numerous protocols, designed countless studies, and our work has revealed novel findings that are truly fascinating. It's been a long ride, sometimes arduous, often exhausting, but never dull. Thank you for pouring into me; your mentorship has truly helped me develop my technical and writing skills and become a better scientist. I've learned that I am academically capable of more than I ever thought possible. Your persistent positivity, even in the face of seemingly endless streams of negative data, helped me get through the tough times.

I'd also like to thank each of my fellow lab members who have since moved on. Phil Lambeth, thank you for showing me the ropes and for your endless enthusiasm and excitement for science; both are powerful motivators. Dr. Dan Warthen and Dr. Jon Joy-Gaba, thank you both for teaching me countless techniques throughout the years and being good friends. Dr. Ron Gaykema, you will forever be remembered in my heart as the local god of all things histological. Watching you innovate on the fly to refine and improve various methodologies was truly inspiring and is an invaluable skill that I hope I have refined in myself from watching- and learning from you.

To committee member Dr. Mark Beenhakker and his graduate students Dr. Peter Klein and Katie Salvati, I am forever appreciative of all the time and resources you shared with me. I learned so much from working in your lab, and will be continually reminded of "the power of positive thinking" thanks to Mark. To the rest of my committee, Dr. Doug Bayliss, Dr. Wendy Lynch, Dr. Ali Güler, and Dr. Chien Li, thank you all for the time you spent with me discussing my project and all of the valuable insight and suggestions you provided. Every committee meeting was truly an enjoyable experience for me, filled with thought-provoking discussion and encouragement. You all helped me get excited about the science I was conducting and stay motivated. Dr. Ruth Stornetta, thank you so much for all the time you spent teaching me about microscopy. I realize that you are always very busy, yet you always seemed eager and willing to answer my questions and teach me; I appreciate you for all that you do for all of the students in the department. I also want to acknowledge Dr. Tolu Odumosu; you're one of the kindest, wisest, and most patient people I have ever met. In the last seven years, you've taught me so much and been such a great friend, and I also appreciate your advice and input as I worked to design microcircuitries to be used in electrophysiological recording. To my good friend, Akin Odeleye: you listened to me complain and helped me through internal difficulties on countless occasions and you always made everything we did in school more enjoyable.

I am eternally grateful for my undergraduate mentor, Dr. Mark Cline, who took me in and introduced me to neuroscience research on my very first day of college as a freshman. Dr. Cline installed a passion in me for neuroscience research, helped me grow a tremendous deal as a student and a person, and it is solely because of his tutelage that I was able to make it to graduate school. He provided guidance to me on countless levels, from classwork help to how to present complex scientific ideas to general audiences, how to write scientifically, how to carry myself professionally, and more, in addition to being a true friend at any hour of the day. I am forever thankful for everything he has done and continues to do for me.

Lastly, thank you to all of the friends I have made during my time in Charlottesville and to my family for their unwavering support through the highs and lows of graduate school. I couldn't have done it without you and I love you all.

Index of Abbreviations

5CSRTT	5-Choice Serial Reaction Time Task
5HT	Serotonin
AAV	Adeno-associated Virus
Acb	Nucleus Accumbens
AcbC	Accumbens Nucleus, Core
ACC	Anterior Cingulate Cortex
ACh	Acetylcholine
AIC	Agranular Insular Cortex
AMG	Amygdala
ARC	Arcuate
Au1	Primary Auditory Cortex
BE	Binge Eating
BLA	Basolateral Amygdala
CB	Calbindin
CCK	Cholecystokinin
CeA	Central Amygdala
CeL	Lateral Division of the Central Nucleus of the Amygdala
CeM	Amygdala, Central Nucleus
CeM	Medial Division of the Central Nucleus of the Amygdala
ChAT	Choline Acetyltransferase
CPA	Conditioned Place Avoidance
CPP	Conditioned Place Preference
CR	Calretinin
CT	Circadian Time
DA	Dopamine
DM	Dorsomedial Hypothalamic Nucleus
DR	Dorsal Raphe Nucleus
DREADD	Designer Receptors Exclusively- Activated by Designer Drugs
Ent	Entorhinal Cortex
EYFP	Yellow Fluorescent Protein
Fmi	Forceps Minor Corpus Callosum
FR	Fixed Ratio
FS	Fast Spiking
GI	Granular Insular Cortex
HCD	High Calorie Diet
HIP	Hippocampus
IL	Infralimbic Cortex
IMD	Intermediodorsal Thalamus
IN	Interneuron
IZ	Interaction Zone
LC	Locus Coeruleus
LH	Lateral Hypothalamus
LS	Lateral Septum
MD	Medial Thalamic Nucleus
MO	Medial Orbital Cortex
mPFC	Medial Prefrontal Cortex
NBM	Nucleus Basalis of Meynert
NE	Norepinephrine
NPY	Neuropeptide Y
OC	Olfactory Cortex
OFC	Orbital Frontal Cortex
PAG	Periaqueductal Gray
PF	Perifornical Area of Hypothalamus
PFC	Prefrontal Cortex
PL	Prelimbic Cortex
PR	Progressive Ratio
PV	Parvalbumin
PVN	Paraventricular Nucleus
PYR	Pyramidal Neuron
S1	Primary Somatosensory Cortex
SN	Substantia Nigra
SOM	Somatostatin
SSFO	Stabilized Step-Function Opsin
V1	Primary Visual Cortex
VIP	Vasoactive Intestinal Peptide
vM1	Vibrissal Motor Cortex
VTA	Ventral Tegmental Area

List of Figures and Tables

Table of Contents

Chapter 1: Introduction

Overview

The prevalence of obesity in the United States has skyrocketed in the last 60 years from 13% of the population in 1960 to almost 40% in 2016, currently affecting over 93 million US adults (Center for Disease Control). Excessive palatable food intake consumption is a significant contributor to the development of obesity in otherwise healthy individuals. Thus, understanding the central mechanisms that govern hedonic food intake is essential in developing novel hypotheses that lead to treatments for this disorder.

Hunger exists as one of the most primitive and powerful urges that we experience, governed by a multitude of interconnected pathways within the brain and by connections between the brain and periphery. The hypothalamus in particular sits in a position to receive signals from the gut to centrally regulate homeostatic hunger and satiety perception. However, in higher mammals, food intake is not exclusively homeostatically driven, but is instead governed by higher cognitive regions through hedonics and emotion. Indeed, rats sated on a normal chow diet will continue to eat when presented with palatable food (reviewed in Cowin et al., 2011), and cues that predict food can stimulate food intake independent of physiological hunger (Reppucci and Petrovich, 2012). Together, these studies help illustrate the complexities of food intake regulation; peripheral and hypothalamic signaling drive physiological food intake, while food intake driven by psychological factors is mainly controlled by various cortical nuclei. Homeostatic and hedonic pathways must be centrally integrated to ultimately drive the decision to eat. The prefrontal cortex (PFC) is critical to this integration, coordinating information through long-range connections to many different brain regions to drive goal-directed behavioral output, such as food intake (reviewed in Mannella et al., 2013). This dissertation will briefly summarize our current scientific understanding of the PFC with respect to its role in the regulation of food

intake as well as other complex behaviors, in addition to how our laboratory has made progress within this field to better our understanding of specific neuronal mechanisms that drive PFC-mediated food intake and other behaviors that affect ingestion.

1.0 PFC Structure

The last cortical area to arise in evolutionary history, the PFC comprises the outer layer of the most rostral portion of the frontal lobe (i.e. the prefrontal lobe) and is exclusive to the mammalian brain (Teffer and Semendeferi, 2012). There appears to be correlation between PFC size and cognitive complexity across species; the human PFC occupies a much larger region of the cerebral cortex than other mammalian counterparts, but shares similar organization to those of other primate species (Miller et al., 2002). With respect to cytoarchitectonics in humans, the PFC is composed of Brodmann areas 9, 10, 11, 12, 46, and 47 (Teffer and Semendeferi, 2012). Despite that extensive research aimed at elucidating PFC function utilizes rodents as animal models, functional mapping of the primate PFC directly onto rodent cortical areas has proven challenging. Morphological differences between the brains of these two organisms result in no one area in rodents fulfilling the gross anatomical position occupied by the primate PFC, yet the medial wall of the rat cortex subserves behavioral functions homologous to those regulated by the PFC in primates (reviewed Brown and Bowman, 2002). Thus, elucidating behavioral function in this cortical region in rats can provide translational insight into cognitive processing in primates.

In the rodent, the PFC encompasses several cortical areas and can be further subdivided based on structural and functional data: the anterior cingulate- (ACC), prelimbic- (PL), infralimbic- (IL), and dorsal peduncular cortices comprise the medial prefrontal cortex (mPFC), while the orbital frontal cortex (OFC) contains the dorsolateral, lateral, medial, and ventral orbital cortices (Logue et al., 2014). The presence of cortical granular layer IV also delineates the PFC from surrounding cortical areas in primates, though this layer is absent in

non-primate species (Uylings et al., 2003). Thus, identifying the specific cortical boundaries of the PFC across species has been challenging due to the lack of a single functional or anatomical definition of this area.

1.01 Afferent and Efferent PFC Projections

The PFC was defined in 1948 as the cortical projection area to the mediodorsal thalamic nucleus (Rose and Woolsey, 1948), but it has since been demonstrated that PFC projects and receives projections from a multitude of nuclei and that attempting to classify the area by single criterion is inadequate. Indeed, while striking morphological differences within the PFC exist between the rat and human, they do share many common projections and functional roles.

The PFC receives no direct input from the periphery and thus sensory information is relayed through afferents spanning from the brainstem to other cortical areas. In addition to the bidirectional connections that exist between the PFC and the medial thalamic nucleus (MD), the visual- (V1), auditory- (Au1), somatosensory- (S1), granular insular- (GI), and olfactory cortices (OC) all relay information to various PFC subregions (Barbas, 1992). Specifically, the lateral portions of the mPFC predominately receive visual, auditory, and somatosensory information while gustatory and olfactory afferents target the more rostral OFC (Barbas, 2000). The PFC sends direct projections to the lateral septum (LS, Johnson et al., 1968) and also projects to- and receives afferents from the amygdala (AMG), which forms three main loops of interaction targeting:

1) the agranular insular cortex (AIC, defined as PFC dorsal to the rhinal sulcus),
2) the IL, and the PL in rodents, and
3) an additional 2 loops including the OFC and ACC in primates (Mannella et al., 2013).

The ventral mPFC forms a striato-cortical loop with the nucleus accumbens (Acb, reviewed in Manella et al. 2013, Del Arco and Mora, 2008). Not all of these mPFC-Acb projections are glutamatergic; Lee et al. in 2014 found that fast-spiking PV cells in the mPFC project to the Acb.

In the diencephalon, the lateral hypothalamus (LH) receives PFC afferents (Petrovich et al., 2005), while the entorhinal cortex (Ent) receives afferents from both the PFC and the hippocampus (HIP) and thus serves a communicative relay between the two. The ventral tegmental area (VTA) in the midbrain also shares reciprocate projections with the PFC. The PFC receives norepinephrine (NE) inputs from the locus coeruleus (LC), serotonergic (5HT) inputs from the dorsal raphe nucleus (DR), and cholinergic inputs from the nucleus basalis of Meynert (NBM) in the basal forebrain (Logue and Gould, 2014). Figure 2 provides a schematic of these mPFC projections.

1.02 Neurons of the PFC

Many distinct neuronal subtypes comprise the complex PFC neural network. As in other neocortical areas, neurons of the PFC are arranged in six layers (I-VI, Markram et al., 2004). Approximately 70-80% of neocortical neurons are glutamatergic pyramidal (PYR) neurons, which function as the primary excitatory cells of the PFC (Garcia-Lopez et al., 2006). They reside predominantly in layers III and V and are morphologically distinguishable from other cell types, as their name implies, by their triangular-shaped somas (Markram et al., 2004, Garcia Lopez et al., 2006). Other hallmark features include a single axon, one large apical dendrite, multiple basal dendrites, and the presence of dendritic spines, which facilitate the ability of PYR neurons to integrate information from massive quantities of neighboring cells. Indeed, the average human PYR neuron can receive over 30,000 regulatory inputs; many of which target the apical dendrite, which can have upwards of 6000 dendritic spines (Megias et al., 2001, Laberge and Kasevich, 2007).

The remaining 20-30% of neocortical neurons are comprised of many diverse subclasses of interneurons (INs), the majority of which are GABAergic, which through complex synergies with each other and PYR neurons govern PYR excitatory output (Markram et al., 2004). Sometimes referred to as ‘local circuit neurons,’ their axons tend to project laterally across cortical columns

but not into white matter to synapse in other brain regions, thus restricting their innervations to neurons within the neocortex. Marked differences exist between IN subclasses with respect to their morphologies and their physiological functions. Within the PFC, at least four of these subclasses exist (Markram et al., 2004, Marin, 2012):

- *Basket cells*, so named because of their basket-like appearance around PYR neuron somata, comprise approximately 50% of INs. These cells are fast-spiking (FS, Kawaguchi and Kondo, 2003) and can be further subdivided into large, small, and nest basket cells.
    - *Large basket cells* are widely distributed through cortical layers and can express calbindin (CB), neuropeptide Y (NPY), cholecystokinin (CCK), calretinin (CR), parvalbumin (PV), and somatostatin (SOM), but do not express vasoactive intestinal peptide (VIP).
    - *Small basket cells* also distribute through layers I-VI and have particularly densely arborized axons that, in contrast to other IN subtypes, seldom cross cortical layers. They can be identified by their expression of VIP.
    - *Nest basket cells* are less understood than other basket cell subtypes, only being identified as a separate subclass of basket cells in 2002 (Wang et al.). They have less axonal branching than other basket cells and express all of the aforementioned chemical markers expressed by other basket cell subtypes, with the exception of CR and VIP.
- *Bipolar cells*, spanning layers II-VI, are so named because of their distinct morphology; a majority of these cells express both VIP and GABA (Kubota et al., 1994).
- *Martinotti cells* are non-FS and characterized by their long axons projecting to layer I from layers II through VI, as well as their elaborate dendritic trees. They express SOM but not PV nor VIP.

- *Chandelier cells* have characteristic axon boutons resembling elegant light fixtures and span cortical layers II-VI. They express either one or both PV and CB and are non-FS (Kawaguchi and Kondo, 2003).

1.03 Local PFC Neuron Connectivity

A popular research strategy in recent years is to selectively isolate and target INs by their molecular definitions, which is advantageous for two main reasons:

1. Three major subpopulations of INs that comprise nearly 85% of all cortical neurons are uniquely defined by the markers they express: SOM, PV, or VIP (Rudy et al., 2011).
2. Experimentally targeting neurons by these markers is both reliable and replicable.

Within these three main IN subpopulations, interconnectivities and physiological functions can be mapped through a synthesis of recent data from different research groups (Figure 1):

- PV-expressing GABAergic large basket- and chandelier cells tightly couple to PYR somata and proximal dendrites to synchronize their integrated synaptic output (Kawaguchi and Kondo, 2003, Cardin et al., 2009, Somogyi et al., 1983).
- SOM-expressing Martinotti cells function as disinhibitors- through projections to VIP and PV neurons and as inhibitors of PYR neurons through direct projections to their dendrites (Kawaguchi and Kondo, 2003).
- The majority of VIP-expressing GABAergic bipolar cells, through projections to SOM-, CB-, and PV-expressing neurons but not PYR neurons, exhibit disinhibitory action with respect to PYR output; that is to say, VIP neuron activation through inhibition of PV neurons increases PYR output (Hioki et al., 2013, reviewed in Pfeffer 2014). A smaller subpopulation of these cells that co-express choline acetyltransferase (ChAT) project

directly to L2-3 PYR cells and thus function as inhibitors of PYR output (Obermayer et al., 2018). This suggests that mPFC VIP output is diverse and that VIP cells function beyond disinhibition; indeed their circuitries appear to be much more complex.

Much of our knowledge of cortical IN circuitries has been gained from work in areas of the mouse neocortex outside of the PFC. Because their circuitries are arranged similarly, we can therefore gain insight into mPFC circuitry through examining other cortical areas. For example, In the visual cortex, Karnani et al. (2016) demonstrated that VIP and SOM INs typically fire in large groups. Firing of a small group of these INs recruits firing of a larger population, accomplished via several mechanisms:

- SOM cells lack within-population inhibition, while this is scarce but not absent in VIP cells.
- In VIP cells:
    - One (GABAergic) subpopulation facilitates population disinhibition through inhibition.
    - Another (cholinergic) subpopulation excites other local VIP cells via acetylcholine (ACh) release.

These data reveal that further subpopulations exist within IN subpopulations defined by VIP, PV, and SOM markers. Metrics used to readily classify these subpopulations remain undefined, making studying them via selective manipulations more difficult.

While mapping these IN connectivities has only recently begun and is thus likely oversimplified as described above, it is important to note the unique disinhibitory role of some VIP cells that likely govern net PFC output through disinhibition of excitatory PYR cell output (Pfeffer, 2014), as these neurons are the focus of much of our experiments described below in the following chapters.

1.2 PFC Function

Some of the earliest studies probing PFC functions utilized brain lesioning in animals, a technique that offers a relatively simple way to examine the necessity of normal PFC function in various behaviors. Perhaps the most classical lesioning example occurred accidentally in 1848 when railroad worker Phineas Gage suffered destruction of a large portion of his left frontal lobe, resulting in stark changes in his social behavior for the remainder of his life (O'Driscoll and Leach, 1998).

Indeed, the PFC has a broad range of functions pertaining to higher cognitive processing, functions that have implications in planning and decision making, moderating social behavior, and orchestrating thoughts and actions in accordance with internal goals (Miller et al., 2002, Yang and Raine, 2009). Among other high-order association areas, the PFC is unique in its dense direct projections to motor control systems, which put it at a position to directly initiate execution of selected goals. These 'goal-making' decisions involve integration of sensory information, as well as memory and emotion as it relates to the choice at hand, based on information received from the visual cortex, AMG, HIP, ACC, and LH (Petrovich et al., 2005). Mannella in 2013 proposed a new model based on review of then-current literature illustrating how the PFC interacts with these other brain regions to drive behavior:

1. The motivational value of a stimulus is encoded by the AMG and HIP.
2. Acb integrates homeostatic signaling from the hypothalamus with motivational value from the AMG and HIP.
3. The PFC communicates with the Acb to select a behavioral outcome.

The PFC's targeting of both excitatory and inhibitory neurons in these same regions illustrates the region's involvement in selection of relevant signals while simultaneously suppressing those irrelevant to the goal being pursued. This concept has been illustrated directly in human subjects, as individuals with lateral PFC damage due to stroke were shown to be unable to

follow conversations in a noisy room due to their inability to ignore irrelevant auditory stimuli (Barbas, 2010).

Summarily, PFC projections are as diverse and far spanning as are the functions of this brain region. The majority of the work presented in this dissertation focuses on how one specific mPFC neuronal subtype, VIP-expressing neurons, affect both food intake and novelty valuation. Thus, our current understanding of PFC involvement in these specific processes will be reviewed further below.

1.21 The PFC and Salience

The brain is constantly bombarded with external stimuli. The ability to detect the salience of a stimulus, i.e. its quality of being particularly noticeable or important, is essential to an organism's ability to sort relevant information from noise. In order to survive, the brain must be able to focus limited cognitive bandwidth on the most pertinent stimuli at any given moment (Uddin 2014): a mouse must be able to identify viable food sources within its environment as well as detect and be able to react fast enough to evade an attack from a predator. The PFC is an important component of this 'salience network.' An important concept to note is the difference between *salience* and *value*: while value is associated with a positive stimulus, i.e. something the animal finds pleasurable or rewarding, salience as an index of the importance of stimulus, be it positive or negative. While increasing value can increase salience, increasing salience does not necessarily increase value.

Noradrenergic projections from the PFC to the Acb are necessary in motivational salience, a process that regulates the strength of goal-seeking behavior, i.e. how much risk is the animal willing to take and how much energy is it willing to exert in the pursuit of a reward (reviewed in Puglisi-Allegra and Ventura, 2012). Depleting prefrontal cortical NE in rats impaired amphetamine-induced DA outflow in the Acb and abolished drug-induced conditioned place preference (CPP) (Ventura et al., 2003), while this same NE depletion also abolished

conditioned place avoidance (CPA) to a pharmacological aversive stimulus, lithium chloride, in mice (Ventura et al., 2007). Together, these data demonstrate NE release in the PFC is critical for attribution of motivational salience to both appetitive and aversive stimuli.

Similar findings were observed when using highly salient non-pharmacological stimuli. Selective mPFC NE depletion impaired both CPP associated with white chocolate and CPA associated with intermittent pulsating light (Ventura et al., 2008). Interestingly, in this same study Ventura et al. found that NE release in the mPFC was proportionate to the salience of the stimulus and that mPFC NE depletion impaired CPP to highly- but not mildly salient stimuli. They also demonstrated that perceived salience of a stimulus can change depending on context, which in turn can change how the PFC responds to the same stimulus under different conditions: food restriction resulted in increased concentrations of mPFC NE, comparable to what was observed when fed mice consumed highly palatable white chocolate. This increase was not simply due to increased palatability associated with fasting; food restriction also elevated the mPFC NE response to a mildly salient stressor to similar levels of non-fasted mice exposed to a highly salient stressor. Taken together, these results demonstrate that the mPFC NE response to a stimulus in an index of the motivational salience of the stimulus, which is dependent on the internal state of the organism. Broadly, there is greater involvement of the mPFC in the pursuit of food reward if the food is palatable, i.e. more rewarding and thus more salient. The same is true of other stimuli unrelated to food intake; the more salient a stimulus, whether it be appetitive or aversive, the more active PFC-Acb circuitries become.

1.22 Novelty Affects Salience

Novelty can strongly modulate motivation in addition to salience. Midbrain dopamine (DA) neurons and their downstream targets that influence motivation to initiate behavior also respond to a novel stimulus with increased firing; these neurons habituate when novel stimuli become familiar (Schultz 1998). Manipulating the DA system in both rodents and primates has

resulted in changes in novelty-seeking behaviors; pharmacologically blocking DA reuptake enhanced novelty-seeking in primates (Costa et al., 2014), while DA D4 receptor KO mice exhibited reduced exploration of novel stimuli, compared to control counterparts (Dulawa et al., 1999). Animals inherently show a novelty bias, a preference for novel over familiar items. Novelty itself can have reward value: rats were observed to lever press for a novel flashing light stimulus that had no otherwise beneficial value (Reed et al., 1996). Additionally, novelty can also enhance DA signaling that predicts reward potential without itself being rewarding (Krebs et al., 2009, reviewed in Duzel et al., 2010). The HIP is thought to play a key role in the detection of salience based on novelty, through a loop with VTA DA neurons (Lisman and Grace, 2005).

1.23 Calculating Salience – How is the PFC Involved?

As briefly mentioned in section 1.2, Manella et al. (2013) compiled data from many studies to formulate a working hypothesis explaining how the brain calculates salience and executes goal-directed behavior. The AMG is primarily responsible for coding the appetitive or aversive value of an unconditioned stimulus. Novelty value of this same stimulus is represented within the HIP. The Acb synergizes these values in addition to information about homeostatic state from the LH and the ARC, while the PFC communicates to the Acb internal representations of attainable outcome based on the stimulus. Integration then occurs at the Acb based on information from all of these sources, which forms a stimulus' current salience. The process as a whole is supported by VTA DA inputs to various components of the network. The Acb is then thought to communicate with the PFC to select the outcome with the highest salience.

1.24 Manipulating Salience via the PFC

The dopaminergic regulation of glutamatergic output from the PFC to the Acb drives motivational salience broadly and regulates drug seeking behavior (Sanchez et al., 2003). Brenhouse et al. in 2008 revealed that adolescent rats, which are inherently more sensitive to

cocaine CPP than both younger and older counterparts, have higher relative levels of D_1 receptor expression in the PFC. Authors could block cocaine-induced CPP with PFC microinjection of a D_1 antagonist in these animals, while dose-dependently increasing preferences for cocaine-associated environments with D_1 agonist microinjections into the PFC. While these data associate increased sensitivity to addictive behaviors during adolescence with changes in PFC D_1 receptor expression, they more broadly demonstrate that manipulating PFC circuitry can regulate attribution of salience.

While they did not experimentally manipulate salience directly, Ahn and Philips (1999) observed how context could change the salience of food in rats, and how these changes were associated with changes in PFC DA concentrations. Briefly, they examined mPFC and Acb DA levels through microdialysis while rats underwent a sensory-specific satiety protocol. DA levels in the mPFC and Acb increased when hungry rats consumed a palatable food (diet 1), and these levels decreased as rats approached satiety. When presented again with diet 1, the now sated rats consumed far less and mPFC DA levels remained low, but when presented with a novel palatable diet (diet 2), these animals ate significantly more of the diet and mPFC DA levels increased once more. These results suggest that as food is consumed, its salience decreases proportionate to an increase in satiety, which was associated with decreased mPFC and Acb DA levels. Sated rats consumed diet 2 due to enhanced novelty-associated salience (relative to diet 1); rise in mPFC DA was also observed during diet 2 consumption. These data again illustrate that perceived salience is context-dependent and is associated with changes in PFC activity.

Because appetite regulation involves both physiological and psychological components and an organism's decision to pursue and consume food requires synthesis of hedonic and homeostatic signaling spanning the entire brain, it is thus not surprising that the PFC plays an important role in appetite regulation.

1.25 Food Intake

In one of the earliest studies probing appetitive function of the PFC, Ursin et al in 1969 demonstrated that rhesus monkeys with dorsolateral frontal lesions maintained a preference for a familiar laboratory diet instead of novel, palatable food sources. These findings were largely confirmed in rats in 1975, when Kolb and Nonneman demonstrated that lesions in different parts of the PFC result in varying changes in feeding behavior. Specifically, OFC lesions decreased basal food and water intake, while mPFC lesions increased "finickiness," i.e. aversion to novel food sources, sparing familiar food intake. The valuation of food is a critical component that affects the decision to eat. Taken together, the results from these early studies demonstrate a regulatory role for the PFC in feeding across the valuation spectrum of the food source in question; food can be considered of lower value when the food is familiar and presented in a home cage environment to non-fasted animals, and this value can increase as either palatability or novelty increases.

1.25.1 Food Valuation

The role for the PFC in the concept of food valuation has been more extensively probed in recent years as research technology has advanced. As reviewed by Manella et al. (2013), both the OFC and mPFC present expected value of different behavioral options at the time of decision-making, which serve as inputs into the decision-making process that then allow the animal to choose an outcome to maximize expected gains (Padoa-Schioppa and Assad, 2006). Brain activity in these regions has been mapped using fMRI data in humans after food presentation; researchers demonstrated that food value is represented by different patterns of OFC activity (Suzuki et al., 2017). Stimulating the right side of the dorsolateral PFC in humans during a food valuation task resulted in a decrease in value assigned to the food stimulus (Camus et al., 2009). In rats, Feenstra and Botterblom (1996) demonstrated using microdialysis a 130-150% increase in extracellular DA concentration in the mPFC following exposure to a

novel environment and during food consumption after fasting, demonstrating a role for the PFC in situations where an external stimulus is highly valued. These data also illustrate how the relative value of a stimulus changes in the PFC depending on the homeostatic state of the animal; the inherently low value of a familiar chow can increase dramatically as hunger increases.

1.25.2 Food Foraging

The PFC has also been implemented in food foraging behavior. In rats, ACC lesions caused impaired memory-based foraging (Seamans et al., 1995) and decreased amount of food collected in food foraging tests (Li et al., 2012). Caracheo in 2013 investigated this concept further, demonstrating abrupt changes in ACC firing patterns and complexity when rats switched from foraging in a novel environment to exploiting food reward. A separate study used neurotoxic lesions in the mPFC to demonstrate its necessity in learned enhancement of food consumption (Petrovich, 2007), a behavior that could be comparable in humans to food craving. Effort-based decision making also involves the PFC: ACC lesions in rats reduced their willingness to expend effort to obtain a highly valued reward when a smaller reward was attainable with less effort (Rudebeck et al., 2006). While aforementioned OFC and mPFC lesioning studies revealed roles for the PFC in both novel and familiar food intake, these studies summarily demonstrate roles for the PFC in acquiring food and in making decisions to expend considerable effort in the pursuit of food reward.

1.25.3 Appetitive Learning

The mPFC is critical in appetitive learning, i.e. performing tasks that result in food reward. When rats experienced conditioned stimulus learning (learning to pair an auditory tone with food reward), increased c-Fos immunoreactivity was observed in PL; this was also apparent in AMG to PL projections, indicating a role for the AMG-PL pathway in appetitive learning (Keefer and Petrovich, 2017). This type of learning also requires both D1 and NMDA

receptors in the mPFC; antagonizing either of these receptor subtypes in rats impaired acquisition of lever press behavior for food reward (Baldwin et al., 2002). Several groups have investigated the opioid system within the mPFC with respect to motivation to obtain food reward. Stimulating mPFC μ-opioid receptors increased breakpoint on a progressive ratio (PR) operant schedule (Mena et al., 2013), while chemical antagonism of these receptors via microinjection of naloxone (a high-affinity μ-opioid receptor antagonist) reduced operant responding for a palatable food reward (Blasio et al., 2014). Interestingly, this effect was selective for palatable food; when repeated with normal chow, no change in operant responding was observed. This study was the first to suggest that mPFC circuitry specific to hedonic feeding may exist.

1.25.4 Context-Driven Food Consumption

Feeding can be regulated by cues other than metabolic factors; hungry rats trained to associate a cue with food consumption will then eat more of the same food in a sated condition when presented with the same cue. The mPFC regulates this learned behavior; rats having undergone neurotoxic mPFC lesions decreased context-driven food consumption in a behavioral arena in which they were acclimated to perform this task, while the lesion did not affect free feeding in the animal's home cage environment or body weight (Petrovich et al., 2007). These data support that the mPFC functions in regulating psychological- instead of homeostatic feeding behavior. Recalling that mPFC-AMG communication is required in appetitive learning, it is likely that the lesioning procedure used in this study disrupted these communicative pathways which could suggest that deficits in recalling cue-associated behavior may underlie observed changes in cue-associated feeding.

1.25.5 Unconditioned Feeding

Both D1 and μ-opioid receptors within the mPFC also appear to regulate unconditioned free feeding. Pharmacological stimulation of mPFC μ-opioid receptors increased free-feeding on chow in both fasted and sated rats, in addition to selectively increasing carbohydrate

preference, even in animals with a pre-established fat preference (Mena et al., 2011). Optogenetic stimulation of D1 mPFC neurons increased free-feeding on chow, while optogenetic inhibition of these cells had the opposite effect (Land et al., 2014). While these data summarily implicate mPFC opioid- and DA receptor signaling in food intake, interpretation at a local circuit level is complicated in that both local GABAergic INs as well as glutamatergic PYR cells that project to other regions express μ-opioid and DA receptors (Anastasiades et al. 2018, Steketee, 2003).

1.26 Differential Roles for the IL and PL in Behavior

Because the majority of my thesis focuses on how the behavioral functions of one specific subset of mPFC neurons differ between the IL and the PL cortices, a brief review of our current understanding of these two mPFC subdivisions will be first be presented.

The IL and PL share some commonality but also differ greatly with respect to their efferent anatomical projections (summarized in Figure 3). In 2004, Robert Vertes used anterograde anatomical tracing to elucidate differential projections of the IL and the PL in the rat. Vertes argued that the differential projection patterns of the IL and PL agree with their differential roles in behavior: the IL is heavily involved in visceromotor functions such as the regulation of heart rate and blood pressure (Burns and Wyss, 1985, Verberne et al., 1987). Many of IL targets in the forebrain subsequently project to regions in the brainstem that regulate the autonomic nervous system, further implicating the IL in autonomic function. Conversely, the PL has roles in regulation of the limbic system and cognition. The PL is critical to working memory: bilateral PL lesions impaired performance in a delayed-foraging task in rats (Seamans et al., 1995).

1.26.1 “Stop/Go” Signaling Hypothesis: IL vs. PL Dichotomy

Dichotomous behavioral roles for the IL and PL have been demonstrated with respect to fear expression and both drug- and natural reward-seeking behaviors.

- **Fear Expression**: By independently manipulating both regions within the same study, Vidal-Gonzalez et al. in 2006 demonstrated that IL activation via microstimulation reduced a conditioned fear response in rats, while PL activation enhanced this response. Authors reasoned that this could be explained by differential projections between these two regions that subsequently interacted with the AMG in different ways: PL neurons projected directly to the basal AMG, which subsequently excites the medial division central nucleus of the AMG (CeM) to enhance fear behavior. Oppositely, IL neurons project to INs in the lateral division of the central nucleus of the AMG (CeL), which in turn directly inhibits the CeM, decreasing fear behavior.
- **Drug-Seeking Behavior**: Pharmacological PL lesions were associated with both decreased cocaine-seeking behavior in rats (Di Pietro et al., 2006), and decreased cocaine reinstatement after periods of drug abstinence (Pelloux et al., 2013). Optogenetically inhibiting PL-Acb projections decreased cocaine reinstatement behavior, suggesting the PL influences reinstatement behavior through interactions with the Acb (Stefanik et al., 2013). Activation of the IL with microinjection of glutamate agonist, AMPA, inhibited reinstatement of cocaine seeking after extinction in rats (Peters et al., 2008). Together, these data indicate opposing roles for the PL and IL in this behavior: the PL drives-, while the IL suppresses cocaine seeking.
- **Pursuit of Natural Reward:** In rats trained to lever-press for sucrose reward on cue, bilateral PL inactivation via microinjection of GABA agonists decreased cue-induced neuronal activity in the Acb and subsequently decreased lever-press behavior (Isihikawa et al, 2008). Pharmacological inactivation of the IL increased incorrect responding (increased pressing of a lever not associated with sucrose reward (Ghazizadeh et al., 2012)), while a separate study demonstrated that IL lesions increased premature responding for food reward in a five-choice serial reaction time task (5CSRTT) (Chudasama et al., 2003). These data suggest separate mechanisms through which the IL and PL govern reward-seeking

behavior; the PL drives reward-seeking behavior while the IL prevents negative behavior, i.e. behavior that reduces the receipt of a reward. It is thus likely that continuous synergism between these two regions ultimately determine behavioral outcome.

1.26.2 Behavioral Heterogeneity: Distinct Populations Drive Diverse Behavioral Functions

The data above collectively support a "Stop/Go" model for behavioral roles of the IL and PL: the PL is the "green light" enhancing behavioral execution, while the IL is the "stop sign" driving behavioral inhibition. However, numerous other studies have produced conflicting results that provide evidence for an imperfect behavioral mapping of these regions to concrete "Stop/Go" signaling (reviewed extensively by Moorman et al., 2015).

While Muir et al. demonstrated that IL lesions increased motor impulsivity in the 5CSRTT, non-selective optogenetic inhibition in the same area had the opposite effect, reducing impulsivity (Hardung et al., 2017). In the same study, non-selective optogenetic inhibition of the PL increased operant responding, while other work suggests that probable increased PL excitation (through increased DA-receptor expression) produces the same effect (Sonntag et al., 2014). Together, these data suggest that regulation of complex behavior involves multiple subpopulations of neurons that differentially regulate "Stop/Go" functions within both the PL and IL. The specific subpopulations targeted differed widely across these studies, and little work yet exists investigating how defined subpopulations of PL and IL neurons effect behavior. Thus, performance of cell-specific neuronal manipulations, in studies such as ours discussed below, will help to further elucidate the mechanisms driving complexities in the IL vs. PL regulation of behavior.

1.3 Behavioral Specificity of mPFC Interneurons

The local network of PFC INs shape PYR output to ultimately drive behaviors reviewed above in section 1.2. As described in 1.03, three major subpopulations of INs exist that comprise nearly 85% of all cortical neurons: SOM, PV, and VIP cells (Rudy et al., 2011). To

elucidate specific behavioral roles for these subpopulations, researchers have microinjected Cre-dependent adeno-associated viruses (AAVs) into genetic mouse strains that selectively express Cre recombinase in any one particular cell type. This allows for virus expression with both site- (depending upon injection coordinates) and cell (depending on genetic strain) specificity. Additionally packaged into these viral vectors are often cellular machineries that when transcribed allow for artificial manipulation of the cell populations of interest, through the use of light (optogenetics) or chemicals (chemogenetics). This section reviews current knowledge of the behavioral specificities of these three major molecularly-defined subclasses of PFC INs.

1.31 PV Cells, Gamma Oscillations, and Attention Processing

Functional MRI studies in humans have revealed that gamma oscillations in the PFC and other regions of the cortex increase linearly under working memory load (Howard et al., 2003). Behaviors correlated with changes in gamma power have been examined in mice: driving mPFC-lateral septum projections at gamma frequencies (40-80Hz) in a free-feeding model facilitated food approach behavior and shortened the time it took mice to reach a food zone without changing actual food consumption; thus, mPFC gamma oscillations were associated with increased performance in a food-related learning task (Carus-Cadavieco et al., 2017). PV cells have key roles in generating these gamma oscillations (Buzsaki and Wang, 2012) and optogenetically silencing mPFC PV cells was sufficient to disrupt mPFC gamma oscillations and decrease attentional processing (Kim et al., 2016). Specifically, Kim et al. found that mPFC PV neurons showed increased and sustained firing when a mouse was engaged in an operant task that required attention to a cue and a correct response to obtain a food reward, i.e. a situation requiring goal-driven attentional processing. They further demonstrated that cognition (measured by performance of goal-directed behavior) could be shifted either negatively (through optogenetic inhibition of mPFC PV cells) or positively (by optogenetically

driving this same subpopulation at gamma frequencies). Together, these data demonstrate both a prominent role for PV cells in synchronization of mPFC output, and the ability of this subpopulation to affect attention and goal-directed behavior.

1.32 mPFC INs in Working Memory

Oscillatory synchrony in both gamma (40-80Hz) and theta (4-12Hz) frequencies between the mPFC and HIP are enhanced during working memory tasks in rats (Hallock et al., 2016, Jones and Wilson, 2005). Abbas et al. in 2018 examined this circuitry in more detail to discover potential roles for mPFC PV and SOM cells in generation of these neuronal rhythms and subsequent behaviors. They demonstrated that optogenetically silencing SOM but not PV cells decreased performance during a working memory task in mice, and that this inhibition disrupted mPFC-HIP synchrony previously demonstrated to be critical for working memory. Authors hypothesized that the ability of SOM- but not PV cells to modulate this behavior may be attributed to differences in their local projection profiles: PV cells target PYR soma primarily (Kvitsiani et al., 2013); while SOM cells target PYR distal dendrites to gate PYR cell inputs (Gentet et al., 2012, reviewed in section 1.01). Thus, SOM cells regulate long-range inputs from the lateral septum to the mPFC. Taken together with section 1.31, these data demonstrate roles for both PV and SOM cells in specific behaviors and further illustrate that these neurons sit upstream of- and are responsible for shaping the activity of mPFC PYR cells, ultimately affecting behavior.

In addition to their roles in driving the “action” stages of working memory-related tasks, INs are also critical during the delay period in these tasks; indeed, working memory involves a brief period of memory retention, during which mPFC activity is greatly increased (Liu et al., 2014), but temporal roles for IN subclasses greatly differ. Kim et al. examined mPFC PV and SOM cells during a spatial working memory task that involved a delay period before the test mouse was allowed to freely pursue a food reward (Kim et al., 2016b). They found PV cells

were only weakly activated in a target-dependent manner during this delay period and were strongly inhibited by reward, while SOM cells were strongly activated in a target-dependent manner during the delay period and only a portion were inhibited by reward (The test mouse either correctly or incorrectly pursued the reward. Target-dependent manner = increased activation correlated to choice accuracy). Integrating these data with what we know about SOM cell morphology suggests that these cells play an important role in maintaining the context of working memory; as they mainly target distal PYR dendrites, they are well positioned to selectively modulate information processed by PYR cells. Meanwhile, PYR soma-targeting PV cells are better positioned to function as a gain control for PYR cells: while PV cells were more uniformly active through the delay period and did not show the same specificity for choice accuracy as did SOM cells, selective PV optogenetic stimulation (and thus downstream PYR inhibition) trended to suppress behavioral performance. These two subclasses also responded differently to reward: PV but not SOM cells significantly reduced their firing rates following reward delivery. Authors reasoned that suppression of inhibition occurring through decreased PV activity, a situation favorable for synaptic plasticity, was likely a mechanism through which mPFC-driven learning occurred.

In monkeys, bilateral mPFC lesions impaired performance in a task that involved a delay between a visual cue and subsequent response, while performance in a visually guided task was unaffected. These data suggest that the mPFC is important for memory maintenance (Funahashi et al., 1993). Further data from Kamigaki and Dan (2017) showed that optogenetic activation of either SOM or PV cells (causing PYR cell suppression) greatly decreased-, while VIP activation (causing PYR activation) increased working memory performance. These data suggest that VIP neurons, positioned directly upstream of- and sending inhibitory projections to SOM and PV cells, are well positioned to govern working memory behavior.

1.33 PV and SOM Cells Shape Social Behaviors

In 2011, researchers in the Deisseroth lab developed a new kind of optogenetic tool, the stabilized step-function opsin (SSFO), which allowed for prolonged (30 min) optogenetic activation that was not specific to one particular firing frequency, as was previously the case with traditional channelrhodopsins. They used this tool to selectively excite and inhibit PYR cells and PV cells and examined effects on social behavior in mice (Yizhar et al., 2011). Exciting mPFC PYR cells virtually abolished social investigation of a novel mouse and a conditioned fear response, while having no effect on novel object exploration or exploration of a novel open field. Interestingly, while reducing mPFC output through PV stimulation did not affect these behaviors, combinatorial excitation of PYR and PV cells resulted in social investigatory behavior significantly reduced from that of controls, but not to the magnitude of mice who underwent PYR cell excitation exclusively. These data demonstrate that excitatory/inhibitory balance can be restored through elevation of inhibitory tone, which in turn affects behavior. More broadly, these data demonstrate the complexities of PFC regulation of behavior: stimulating PFC neurons via Yizhar's SSFO paradigm affected only a specific subset of social behaviors. While exclusive PV cell stimulation did not affect behavior, stimulating these cells and thus increasing inhibitory tone did significantly shape PYR-driven changes in social interaction.

Just recently, members of the same group used designer receptors exclusively activated by designer drugs (DREADDs) to pharmacogenetically inactivate either SOM or PV cells in the mPFC and observe effects on social avoidance behavior (Xu et al., 2019). Inactivation of SOM cells decreased social avoidance behavior (researchers observed increased social interaction with a previously aversive novel mouse). Recalling our current understanding of mPFC local network connectivity (Figure 1), SOM cells project to and directly inhibit PV cells. Indeed, authors in this study demonstrated that SOM excitation inhibited PV cells and thus increased PYR excitation. These data also align with previous work, in that increased mPFC excitation is associated with decreased social investigatory behavior. This output is modulated by both PV

and SOM cells; selectively manipulating these specific neuronal subtypes shape PYR output and effect social behavior. However, roles for VIP INs in social behavior, prior to our work, had to our knowledge not been investigated.

1.34 VIP Cells Are Key Players in Sensory Processing

In 2013, Pi et al. combined optogenetic stimulation with single-cell recording techniques to probe VIP function in the auditory cortex during an auditory discrimination task, which required that mice differentiate between two different auditory stimuli that were paired to either reward or punishment. They found that both positive and negative reinforcement signals strongly activated VIP cells, which subsequently activated behaviorally relevant subpopulations of PYR cells (Pi et al., 2013). These results were recapitulated in the mPFC using real-time calcium imaging to characterize the differential activities of the three major molecularly-defined subclasses of inhibitory INs in the mPFC, SOM-, PV-, and VIP-expressing cells, in real time during a similar task (Pinto and Dan, 2015). SOM neurons were primarily active during motor action, i.e. licking for water reward, PV neurons responded equally to sensory cues, motor action, and trial outcome, and VIP neurons responded most robustly to action outcome, whether it was rewarding or aversive. Authors reasoned that mPFC VIP neurons function as both **pre-synaptic** drivers of- and **post-synaptic** responders to goal-directed behavior:

- **Pre-synaptically**, VIP cells function as the main disinhibitory regulators of PYR output.
- **Post-synaptically**, VIP cells respond following action outcome, functioning to relay feedback signals to update outcome value in real time.
- These cells subsequently activate specific downstream subpopulations of PYR cells, which allows for goal-directed behavioral change as the stimulus value is updated.

It's important to consider this concept within Mannella's broader goal-directed behavior hypothesis (outlined in 1.2 and 1.23): the mPFC uses information from the Acb, HIP, and AMG to update the salience value of a stimulus in real-time. As they receive a diverse array of extracortical inputs, mPFC VIP cells are likely first-order synthesizers of this information, which subsequently modulate PFC output, through disinhibition, based on the ever-changing value of external stimuli.

Similar to trends observed by Kamigaki and Dan in the mPFC (reviewed in section 1.32), optogenetically stimulating VIP cells had opposing effects compared to both PV- and SOM stimulation in the visual cortex; VIP stimulation improved- while both PV and SOM stimulation decreased visual contrast perception in mice (Cone et al., 2019). These data suggest that VIP INs may be essential in visual perception, a hypothesis further validated by work by Batista-Brito et al. in 2017: mice that underwent VIP cell-specific early postnatal disruption of 2 genes critical for IN maturation (Neuregulin 1 and its IN-specific receptor, ERBB4) exhibited reduced sensory responses in cortical PYR neurons that compromised both sensory processing and visual learning. A separate study revealed that locomotion activated VIP cells (via nicotinic projections from the basal forebrain) while suppressing SOM cells in the visual cortex (Stryker, 2014); the observation of direct SOM inhibition by VIP cells was confirmatory of earlier work by Pffefer et al. in 2013. Lee et al. (2013) demonstrated how VIP cells work within the circuitry linking the primary vibrissal motor cortex (vM1) to the primary somatosensory cortex (S1); PYR cells projecting from S1 to vM1 primarily target VIP cells in S1, which through inhibition of vM1 SOM cells, process and relay excitatory information critical to sensory processing. These data summarily demonstrate critical roles for VIP INs in auditory and visual processing and support the overarching cortical circuit hierarchy presented in Figure 1; VIP cells function as disinhibitory regulators of excitatory output.

1.35 mPFC Neuronal Activity During Foraging vs. Consumption

Our laboratory was the first to probe appetitive functionality of specific mPFC cell subtypes in an effort to better understand mPFC-driven food intake regulation at a circuit level. We first sought to examine how different mPFC neuronal subpopulations were differentially engaged during both the pursuit of food reward and food consumption (Gaykema et al., 2014). We found that free-feeding of a highly-palatable diet was associated with a two-fold increase in mPFC PYR cell activation in the ACC, PL, and IL, while foraging for- but not consuming this same diet resulted in a quadruple-fold increase in activation of these cells, relative to control counterparts. We also looked at activity changes in three major IN subclasses during these feeding challenges: PV, SOM, and VIP cells. The greatest changes in IN activity were observed in VIP cells, the activity of which increased during both foraging for- and free access to palatable food. These results suggest a role for VIP neurons in appetitive behavior and support earlier work referenced above by Caracheo et al. (2013) that revealed differential firing patterns in the ACC when foraging vs feeding. The changes observed in this study could perhaps be attributed to changes in ACC VIP activity.

1.36 Pharmacologically Increasing mPFC Excitatory Output Affects Food Motivation

We next sought to manipulate specific neuron subpopulations directly; using DREADDs, we investigated how increasing net mPFC output through mPFC PYR cell stimulation affected appetitive behaviors (Warthen et al., 2016). Stimulating mPFC PYR cells enhanced both operant responding for palatable food reward and reinstatement of food-seeking behavior, but did not affect free-feeding on either standard chow or a calorically-dense, highly palatable diet. We also found that stimulating these cells reduced impulsive behavior during operant responding for food reward. These data were unique in that they highlighted a role for the mPFC in feeding situations that involved high levels of cognitive demand, while we observed no effect on feeding when animals did not have to work for food. These data are also copacetic with

findings by Kamigaki and Dan (reviewed in 1.32). PYR activation by optogenetically activating VIP cells in V1 increased performance in a delayed-response operant task, while our DREADD stimulation of mPFC PYR cells also improved performance in a task-specific manner: treated animals both increased operant responding for food reward and decreased impulsive responding that resulted in withholding of food reward.

1.37 Interpreting Our Findings: VIP Cells Likely Govern mPFC Food Intake Regulation

Our data concerning mPFC PYR cells contrast other earlier work demonstrating that the mPFC could indeed regulate free feeding through stimulation of either mPFC DA- or μ-opioid receptors. However, these discrepancies can be reconciled by examining the localization of DA- and μ-opioid receptors within the mPFC. A characterization of rat cortical μ-opioid receptor expression revealed that they were restricted to GABAergic INs in layers II-IV of most of the outer cortical layer, including the PFC. Double-staining for characteristic IN markers revealed that 92% of μ-opioid receptor-expressing INs co-expressed VIP (Taki et al., 2000); thus, VIP neurons may be responsible for the decreases in binge-like feeding after mPFC mu-opioid receptor antagonization (Blasio et al., 2014) in addition to the changes in free-feeding observed after optogenetic stimulation (Mena et al., 2011). Interestingly, a considerable population of mPFC VIP cells also expresses D1 receptors (Anastasiades et al., 2018), further suggesting that VIP cells also play an important role in mPFC food intake regulation. These data, coupled with the increased mPFC VIP neuronal activation we observed during both palatable food consumption and food foraging behavior, strongly infer roles for VIP cells in regulating various aspects of feeding behavior.

1.38 Further Elucidation of PFC Feeding Circuitry

In this dissertation, my primary objective was to test the hypothesis that mPFC VIP cells had the potential to regulate food intake. Specifically, I sought to examine how VIP subpopulations within the IL versus the PL could affect food intake differentially (Chapters 2 and

3). Given that communication between the PFC and Acb is critical in motivational salience (reviewed in 1.21), it is thus likely that engagement of this particular pathway may be ultimately responsible for the behavioral changes that we observed when driving PYR cells directly (section 1.36). Thus, I also examined the necessity of this direct projection in the regulation of novel social- and object-driven exploratory behavior, as well as palatable food intake (Chapter 4). Much of my work focused on how various PFC manipulations regulated acute, binge-like consumption of highly-palatable food. While several other studies have highlighted specific genes capable of regulating binge-like eating, considerably less is known about how natural genetic variation can shape this behavior. Thus, I lastly examined differences in palatable food consumption across multiple strains of genetic inbred mice traditionally used in preclinical research (Chapter 5).

1.9 Figures

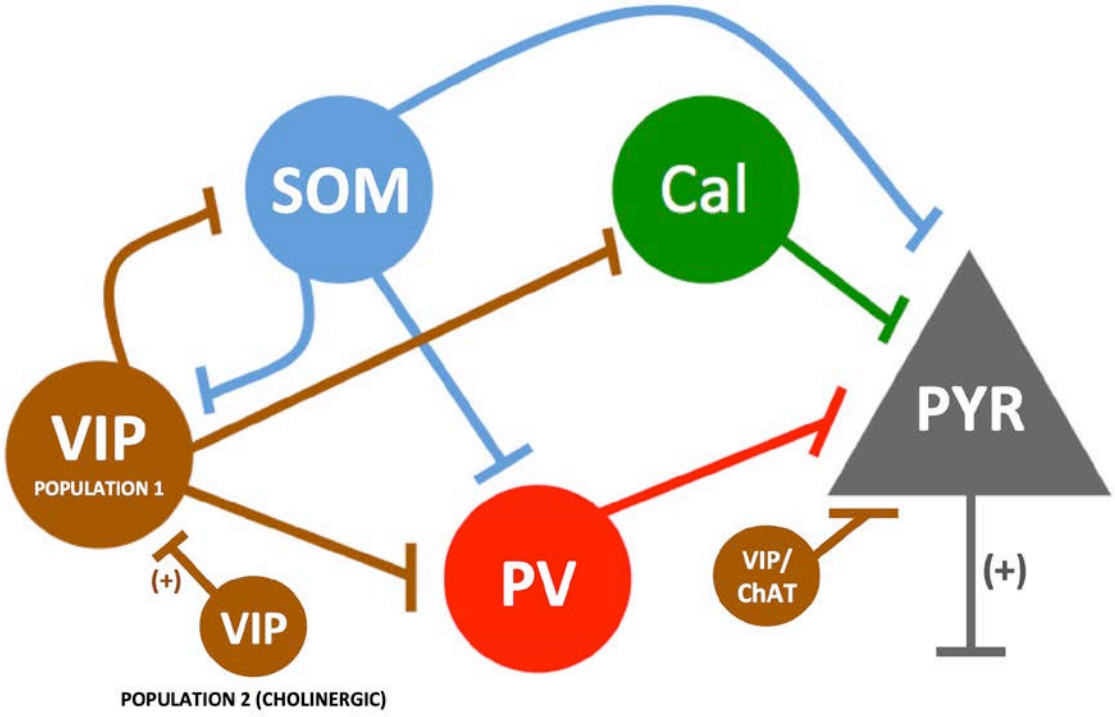

Figure 1. Schematic representation of PFC interneuron connectivities. Based on data from Pfeffer et al. 2013, Hioki et al. 2013, Kepecs et al. 2013, Deisseroth et al. 2009,, Obermayer et al., 2018, , Karnani et al., 2016. All projections are inhibitory unless denoted by (+).

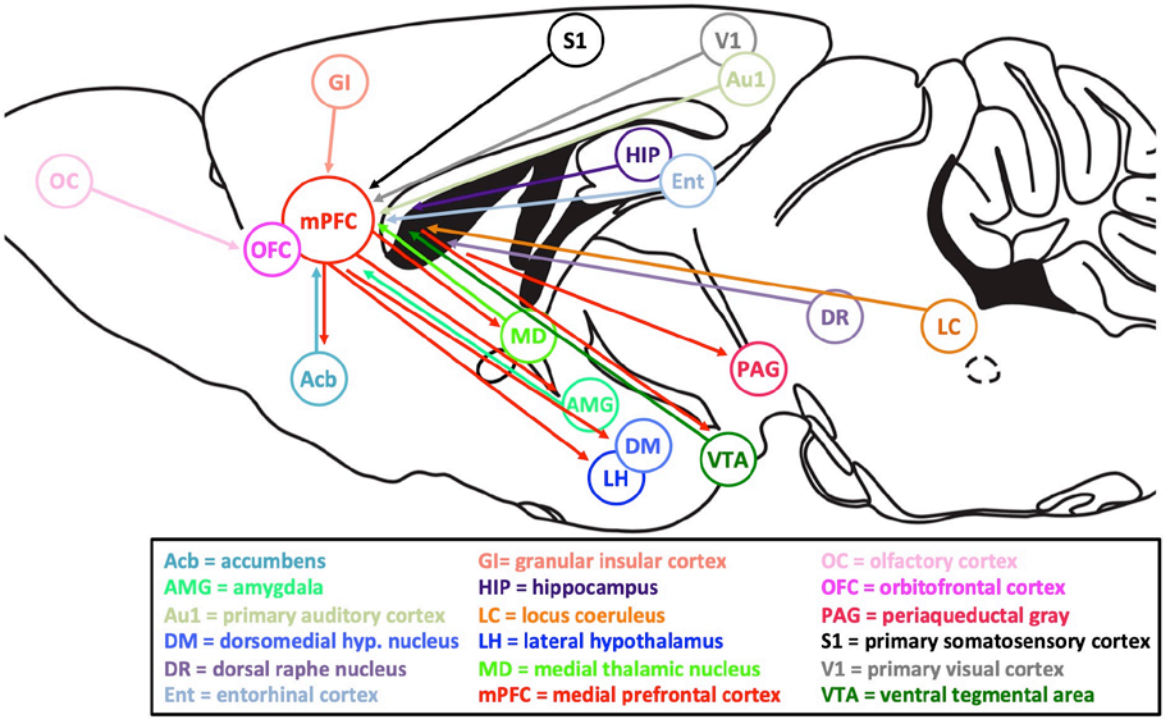

Figure 2. Schematic overview of the main afferents and efferents of the PFC, displayed over a sagittal section of the mouse brain. All nuclei are in their approximate rostral-caudal locations. Arrows denote efferent projections, color coordinated to the nuclei from which they project. Based on data from Barbas 1992, Barbas 2000, Johnson et al., 1968, Mannella et al., 2013, Del Arco and Mora, 2008, Lee et al., 2014, Logue and Gould, 2013.

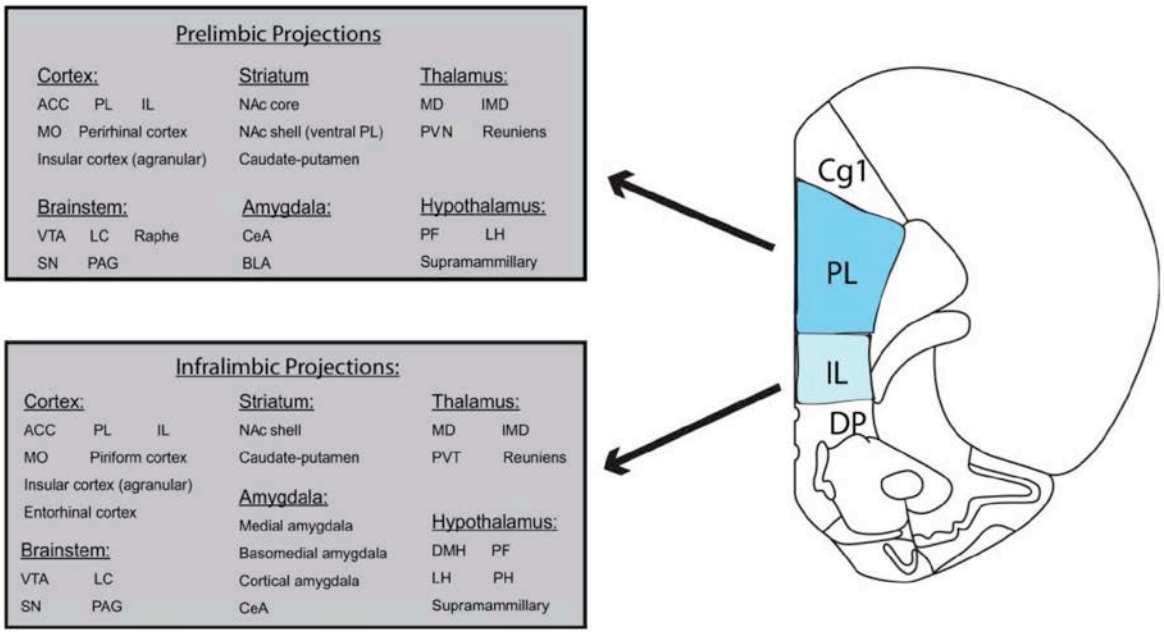

Figure 3. Differential projections of the IL vs PL. Adapted from Moorman et al., 2015.

Chapter 2: VIPergic neurons of the infralimbic and prelimbic cortices control palatable food intake through separate cognitive pathways.

This chapter is a re-print of the JCI Insights article (Newmyer et al., 2019).

2.1 Abstract

The prefrontal cortex controls food reward seeking and ingestion, playing important roles in directing attention, regulating motivation toward reward pursuit, and assigning reward salience and value. The cell types that mediate these behavioral functions, however, are not well described. We report here that optogenetic activation of vasoactive intestinal peptide–expressing (VIP-expressing) interneurons in both the infralimbic (IL) and prelimbic (PL) divisions of the medial prefrontal cortex in mice is sufficient to reduce acute, binge-like intake of high-calorie palatable food in the absence of any effect on low-calorie rodent chow intake in the sated animal. In addition, we discovered that the behavioral mechanisms associated with these changes in feeding differed between animals that underwent either IL or PL VIPergic stimulation. Although IL VIP neurons showed the ability to reduce palatable food intake, this effect was dependent upon the novelty and relative value of the food source. In addition, IL VIP neuron activation significantly reduced novel object and novel social investigative behavior. Activation of PL VIP neurons, however, produced a reduction in high-calorie palatable food intake that was independent of food novelty. Neither IL nor PL VIP excitation changed motivation to obtain food reward. Our data show how neurochemically defined populations of cortical interneurons can regulate specific aspects of food reward–driven behavior, resulting in a selective reduction in intake of highly valued food.

2.2 Introduction

Excessive palatable food consumption is a significant contributor to the development of obesity. Although the ability of neuronal mechanisms to override the homeostatic control of food

intake during periods of energy abundance can lead to overeating (Johnson and Kenny, 2010, Volkow et al., 2017), the identities of specific cortical cell types that can promote changes in feeding behavior are not well described.

The medial prefrontal cortex (mPFC), encompassing the anterior cingulate, infralimbic (IL), and prelimbic (PL) cortices, has been implicated in the control of a myriad of functions, including the attribution of salience (Liang et al., 2018), the regulation of binge food intake (Corwin et al., 2016, Richard and Berridge, 2013), reward prediction error signaling (Matsumoto et al., 2007, Pi et al., 2013), and the drive to expend effort to obtain reward (Seo et al., 2016, Ventura et al., 2007, Warthen et al., 2007). Prior studies within this region have shown how dopamine (Land et al., 2014) and opioid (Mena et al., 2013, Mena et al., 2011, Blasio et al., 2014) action can regulate feeding on both rodent chow and palatable, energy-dense food. However, little is known of how specific neurochemically defined frontal cortical neuronal populations respond to these and other signals to produce a change in either the consumption of or motivation to obtain food. Furthermore, although prior studies have shown how the IL and PL cortices play complementary roles in the regulation of behavioral expression (Moorman and Aston Jones, 2015, Peters et al., 2008, Martin-Garcia et al., 2014), the importance of defined subtypes of neurons in either the IL or PL cortex in the control of food intake has yet to be investigated.

In both the IL and PL subdivisions of the mPFC, GABAergic/vasoactive intestinal peptide–expressing (VIPergic) interneurons are well positioned to regulate feeding behavior. Serving as a convergence point for extracortical glutamatergic (Wall et al., 2016), serotonergic (Rudy et al., 2011), and cholinergic (Rudy et al., 2011, Bourgeois et al., 2012, Alitto and Dan, 2012) inputs that have previously been implicated in the control of food intake, VIP cells become active following reward presentation (Pinto and Dan, 2015), which suggests they act as a feedback signal that conveys a reward prediction error (Pi et al., 2013).

To investigate the sufficiency of VIPergic interneurons in the regulation of food intake, we used a stabilized step-function opsin (SSFO) (Yizhar et al., 2011) to produce VIPergic depolarization and subsequent neuronal activation in either the IL or PL subdivisions of the mouse mPFC. Below, we describe how VIPergic neuronal stimulation in either the IL or PL of sated animals can selectively reduce consumption of palatable food in the absence of any effect on rodent chow consumption or on the drive to work to obtain a palatable food reward. Surprisingly, we also discovered that the ability of IL VIPergic neurons to suppress food intake was likely dependent upon the novelty and relative value of the food source. PL VIPergic neurons, however, modulate feeding behavior of both novel palatable food and familiar food with high perceived value. Thus, our work describes for the first time to our knowledge a neuronal cell type in the cortex capable of selectively reducing the consumption of palatable food while sparing normal chow consumption in sated animals, through the engagement of 2 behavioral mechanisms.

2.3 Results

2.3.1 Selective activation of the IL and PL cortices by SSFO expression in VIPergic neurons.

Because VIP neurons show both burst firing and regular firing properties in response to depolarization (Kawaguchi and Kubota, 1996), we reasoned that to stimulate VIP cells at a specific firing frequency might not reproduce the most physiologically relevant activation of this cell type. Thus, we chose to use an SSFO to produce neuronal depolarization in VIP neurons without dictating a specific firing frequency. After injecting a Cre recombinase–dependent SSFO into either the IL (IL SSFO, Figure 1A) or PL (PL SSFO, Figure 1B) of heterozygous mice expressing Cre recombinase from the VIP locus, optical fibers were unilaterally inserted to allow for light-driven neuronal activation. Following a 5-second light pulse, in IL SSFO mice we observed significant neuronal activation by c-Fos immunohistochemistry in the IL (65.5 ± 7.6 c-Fos+ cells in controls, 108.3 ± 13.8 in IL SSFO mice, $P < 0.05$, quantified in Figure 2A,

visualized in Figure 2, B and C for IL controls and SSFO mice, respectively) but not in the PL (126.2 ± 17.7 c-Fos+ cells in controls, 146 ± 23 in IL SSFO mice, P = 0.51, quantified in Figure 2D, visualized in Figure 2, E and F for IL controls and SSFO mice, respectively). Similarly, following a 5-second light pulse in PL SSFO mice, we observed significant neuronal activation by c-Fos immunohistochemistry in the PL (131 ± 7 c-Fos+ cells in controls, 181.6 ± 14.5 in PL SSFO mice, P < 0.05, Figure 3D, visualized in Figure 3, B and C for controls and PL SSFO mice, respectively) but not the IL (98.9 ± 7.7 c-Fos+ cells in controls, 78.6 ± 7 in PL SSFO mice, P = 0.08, Figure 3A, visualized in Figure 3, E and F for controls and PL SSFO mice, respectively).

Although we did not directly test whether VIPergic neurons showed activation following light exposure, prior studies have validated both the Cre-dependent expression of the SSFO vector (Yizhar et al., 2011) and the selective expression of Cre recombinase in VIPergic neurons of the VIP-IRES-Cre mouse line (Pi et al., 2013). Thus, we subsequently used enhanced yellow fluorescent protein (EYFP) expression from the SSFO vector as a proxy for VIP expression in our work.

Importantly, when we stimulated with SSFO in the IL, the degree of presumptive VIP neuron activation was significantly greater in the IL than when SSFO stimulation occurred in the PL brain region (after light stimulation, 81.8% ± 3.9% total EYFP+ cells also c-Fos+ in the IL of IL SSFO mice, 35.7% ± 6.6% in the IL of PL SSFO mice, P < 0.001, Figure 4, A–C). Results were similar when we targeted the PL, with lower activation of presumptive VIPergic neurons in the neighboring IL brain region being observed (after light stimulation, 78.5% ± 4% total EYFP+ cells also c-Fos+ in the PL of PL SSFO mice, 51.4% ± 4.6% in the PL of IL SSFO mice, P < 0.001, Figure 4, D–F).

These data demonstrate both our ability to selectively target either the IL or PL as well as how VIP neuron stimulation in either brain region can produce spatially localized neuronal excitation. Our data also agree with prior work that showed an increase in c-Fos expression following VIPergic activation in the cortex (Pi et al., 2013) and suggest that the result of VIPergic excitation is indeed neuronal disinhibition. In addition to investigating the actions of SSFO in vivo, we performed slice electrophysiology on brain sections expressing SSFO and a yellow fluorescent protein (YFP) reporter in VIPergic neurons. Following a 5-second light pulse, VIP neurons showed a significant increase in resting membrane potential in the current clamp, confirming the excitatory actions of SSFO in this cell type (Figure 4G, representative trace. Mean change in depolarization 4.467 ± 1.500 mV, n = 3 neurons).

2.3.2 Activation of both IL and PL VIP subpopulations decreases intake of highly valued food but has no effect on motivation to obtain palatable food.

To elucidate roles for IL and PL VIP neurons in the binge-like, acute overconsumption of food, we stimulated IL or PL VIPergic neurons with a 5-second light pulse train, then, in 2 experiments, allowed mice free access to either standard chow or to a highly palatable high-calorie diet (HCD1). Although neither IL nor PL VIPergic stimulation affected standard chow intake at the start of the animal's light cycle, circadian time 0 (CT0, Figure 5A), both IL and PL VIPergic stimulation were sufficient to reduce intake of the energy-dense HCD1 at 30 minutes after stimulation (3.02 ± 0.3 kcal for IL SSFO controls, 1.9 ± 0.26 kcal for IL SSFO, $P < 0.01$; 4.3 ± 0.16 kcal for PL SSFO controls, 3.3 ± 0.34 kcal for PL SSFO, $P < 0.05$, Figure 5C) relative to sham-stimulated littermate controls. We hypothesized that the low value of standard chow in sated mice at CT0 (Warthen et al., 2016) may have masked the ability of VIPergic stimulation to reduce feeding. Thus, we subsequently repeated our chow intake study at the onset of subjective night (CT12), when mice show an enhanced drive to feed, and again at CT0 following an 18-hour overnight fast. Although we found that control mice consumed more food at CT12

than CT0, again neither IL nor PL VIP stimulation affected standard rodent chow intake (Figure 5B). However, following a fast to further increase the relative value of chow, stimulation of both PL and IL VIPergic neurons reduced chow intake (2.199 ± 0.11 kcal for IL SSFO controls, 1.80 ± 0.091 kcal for IL SSFO, $P < 0.05$; 2.129 ± 0.068 kcal for PL SSFO controls, 1.64 ± 0.145 kcal for PL SSFO, $P < 0.05$, Figure 5D), suggesting that this cell type can regulate feeding when the value of the food source changes.

In addition to the regulation of food intake, the frontal cortex has also been shown to regulate the motivation to obtain food reward (Seo et al., 2016, Warthen et al., 2016, Richard and Berridge, 2013). Thus, we investigated whether VIPergic stimulation could also affect the drive to work for food reward using a progressive-ratio operant conditioning paradigm. Unlike the observed effect on palatable food intake, no changes in progressive-ratio operant breakpoint or time to completion of the initial fixed ratios (FRs) in the progressive-ratio paradigm were observed following either PL or IL VIPergic stimulation (Figure 5, E–G). For PL (in seconds): FR5 control 46.57 ± 12.31, FR5 SSFO 114 ± 23.3, $P = 0.54$; FR10 control 45.85 ± 10.21, FR10 SSFO 55.66 ± 11.69, $P = 0.92$; FR20 control 179.71 ± 69.01, FR20 SSFO 82 ± 15.58, $P = 0.35$; FR30 control 192.43 ± 82.75, FR30 SSFO 334 ± 114, $P = 0.56$. For IL (in seconds): FR5 control 47.6 ± 16.82, FR5 SSFO 168 ± 63.34, $P = 0.159$; FR10 control 59.33 ± 15.2, FR10 SSFO 58.16 ± 8.0, $P = 0.94$; FR20 control 53.5 ± 11.59, FR20 SSFO 74.83 ± 10.6, $P = 0.22$; FR30 control 76.5 ± 11, FR30 SSFO 114.7 ± 37.86, $P = 0.39$.

Taken together, these results demonstrate that both IL and PL VIPergic neurons are sufficient to drive a reduction in high-value food intake while sparing effects on the motivation to obtain food reward.

2.3.3 The ability of IL but not PL VIP neuron activation to reduce palatable food intake depends on food novelty.

Novelty and salience are both important factors driving pursuit of both natural and drug rewards (Beckmann et al., 2011, Hansson et al., 2012, Panaro and Cone, 2013). In fact, the availability of a wide variety of energy-dense foods has been suggested to play an important role in driving overeating, preventing the development of sensory-specific satiety (Rolls et al., 1986, Reichelt et al., 2014). To examine whether the observed ability of mPFC VIPergic neurons to reduce food intake was dependent upon the novelty of the food stimulus, we performed an experiment in which mice that underwent our initial food intake evaluation (Figure 5C) were retested using the same diet (HCD1) after either IL or PL VIP stimulation (Figure 6, A and C, for IL and PL, respectively). Interestingly, while IL VIP stimulation failed to affect palatable food intake following the animal's second exposure to the food (2-way repeated measures ANOVA, $F_{1,9} = 9.434$, $P = 0.0133$, 2.84 ± 0.3 kcal for IL SSFO control during second exposure, 2.42 ± 0.6 kcal for IL SSFO second exposure; $P = 0.19$). PL VIP stimulation significantly reduced HCD1 consumption during both the initial and second exposures (2-way repeated measures ANOVA, $F_{1,14} = 8.785$, $P = 0.0103$, 4.08 ± 0.23 kcal for PL SSFO control during second exposure, 3.25 ± 0.26 kcal for PL SSFO second exposure; $P < 0.05$) (Figure 6C). We reasoned that we should be able to rescue the ability of IL VIPergic neurons to reduce food intake if animals were subsequently given a novel palatable diet that was different in nutrient composition and texture (HCD2) from the initial diet (HCD1) used in testing. As predicted, IL VIPergic stimulation produced a reduction in palatable food intake following the first but not the second exposure to HCD2 (2-way repeated measures ANOVA, $F_{1,11} = 6.8$, $P = 0.0244$. First HCD2 exposure: 2.34 ± 0.19 kcal for IL SSFO control, 1.73 ± 0.12 kcal for IL SSFO, $P < 0.05$. Second HCD2 exposure: 2.46 ± 0.1 kcal for IL SSFO control, 2 ± 0.2 kcal for IL SSFO, $P = 0.125$) (Figure 6B). PL VIPergic stimulation produced a reduction in palatable food intake during the first exposure, an effect that was also maintained during the second exposure (2-way repeated measures

ANOVA, $F_{1,12} = 20.11$, $P = 0.0007$. First HCD2 exposure: 4 ± 0.24 kcal for PL SSFO control, 3.05 ± 0.29 kcal for PL SSFO, $P < 0.05$. Second HCD2 exposure: 3.56 ± 0.2 kcal for PL SSFO control, 2.52 ± 0.33 kcal for PL SSFO, $P < 0.05$) (Figure 6D).

Although these experiments demonstrate the role of food valuation in driving food intake, our studies using HCD1 and HCD2 also demonstrate how the initial stimulation paradigm and food intake experiment conducted with HCD1 did not simply produce an irreversible change in neuron function that blunted the ability of IL VIPergic stimulation to affect food intake during the second exposure to HCD1. Furthermore, our experiments examining chow food intake in fasted animals suggests that the effect of VIPergic neuron stimulation was not dependent upon disruption of sensory processing; our stimulation affected chow intake only when the perceived value of this food was high.

We next investigated whether our observations could be extended beyond the 30-minute testing period and conducted a chronic palatable food intake experiment (using HCD2) that lasted for 24 hours. Based on our acute food intake data, we hypothesized that chronic PL VIPergic stimulation would produce a substantial, prolonged reduction in food intake, while IL VIPergic stimulation would be expected to produce minimal effect because animals had been previously exposed to the diet. Indeed, cumulative 24-hour consumption of HCD2 was significantly reduced following continuous PL but not IL VIPergic stimulation, measured at 30-minute intervals (13.9 ± 0.75 kcal for PL SSFO controls, 10.81 ± 1 kcal for PL SSFO, $P < 0.05$, Figure 6G). Interestingly, we determined that the rate of food intake over the 24-hour period was significantly different between SSFO- and control-treated animals following either IL VIPergic stimulation (CT0–12, average difference 0.482 kcal/h with $P = 0.0112$; CT13–24, average difference 0.755 kcal/h with $P = 0.0308$, Figure 6E) or PL VIPergic stimulation (CT0–12, average difference 1.048 kcal/h with $P = 5.74e\text{-}09$; CT13–24 average difference 2.527 kcal/h with $P = 5.12e\text{-}14$, Figure 6F). However, because only PL stimulation produced a statistically

significant reduction in cumulative 24-hour food consumption, this suggests that chronic IL VIP stimulation could produce a small change in food intake that might be measurable at some time point beyond our 24-hour test period. Summarily, these data suggest that IL and PL VIP neurons affect palatable food intake through behaviorally separate pathways.

2.3.4 Activation of IL but not PL VIP neurons suppresses interest in other natural novel stimuli not associated with food intake.

The selective effect of IL VIPergic neuron stimulation on the intake of a highly valued, novel food suggested that IL VIPergic neurons might also control novel social– and novel object–driven investigatory behavior. Thus, we tested whether interaction with a novel object or novel mouse was altered following VIPergic activation. In agreement with our observations on food intake, mice that underwent VIPergic stimulation in the IL exhibited decreased time spent investigating a novel object in an open field with respect to nonstimulated control counterparts. For IL SSFO controls: 115.1 ± 13.7 seconds spent in center with no object, 207.7 ± 21.9 seconds spent in center with novel object present, $P < 0.001$. For IL SSFO: 150 ± 16 seconds spent in center with no object, 158.5 ± 32.8 seconds spent in center with novel object present, $P = 0.82$ (Figure 7A). PL VIPergic stimulation had no effect on novel object investigation. For PL SSFO controls: 115.7 ± 10.7 seconds spent in center with no object, 221 ± 25.7 seconds spent in center with novel object present, $P < 0.01$. For PL SSFO: 126.7 ± 13.3 seconds spent in center with no object, 230.8 ± 51.4 seconds time in center with novel object present, $P < 0.05$ (Figure 7B). Similarly, IL VIPergic stimulation decreased interest in investigating a novel mouse in an open field (43.46 ± 6.6 seconds for IL SSFO control, 8.35 ± 4 seconds for IL SSFO, $P < 0.001$, Figure 7C) while PL VIPergic stimulation was not associated with any changes in social interaction (63.98 ± 6.09 seconds for PL SSFO control, 50.51 ± 11.41 seconds for PL SSFO, Figure 7C). Taken together, these results suggest that IL VIP stimulation may act to decrease the salience or value of both novel food and other natural stimuli.

2.3.5 Neither IL nor PL VIP activation induces anxiety-like behavior.

Although we observed that mPFC VIPergic activation reduced the value of food and other rewarding stimuli, it is also possible that the observed effects may have resulted from a confounding change in other behaviors that the frontal cortex regulates. Although the lack of effect of either VIPergic IL or PL manipulation on motivation (Figure 5D) suggests that no increase in a depression-like or high-stress state occurred (Hershenberg et al., 2016, Bryce and Floresco, 2016, Bergammi et al., 2016), it is possible, based on prior work conducted in the rodent mPFC (Vialou et al., 2014, Bi et al., 2013), that anxiety-like behavior may have been increased following our stimulation paradigm. To test this possibility, mice expressing SSFO in either IL or PL VIPergic neurons were both subjected to an open field assay and tested using an elevated plus maze to elucidate changes in anxiety-like behavior. No effect of either stimulation on time spent in the center of an open field (Figure 8A) or time spent in open arms of an elevated plus maze (Figure 8C) was observed, suggesting that mPFC VIP stimulation does not alter anxiety behavior. Interestingly, both IL and PL VIP stimulation decreased total distance traveled in an open field (5430 ± 431 cm for IL SSFO controls, 4208 ± 336 cm for IL SSFO, $P < 0.05$; 5393 ± 300 cm for PL SSFO controls, 4087 ± 509 cm for PL SSFO, $P < 0.05$, Figure 8B), a result that demonstrates the complexity of VIPergic regulation of IL and PL function. Although VIP neurons act through different mechanisms to reduce food intake in the IL and PL, they appear to act in both areas of the mPFC to reduce exploratory behavior in a novel environment.

2.3.6 IL and PL VIPergic activation produces distinct changes in subcortical neuronal activation.

Because our data indicate that VIP neurons of the IL and PL can produce a reduction in palatable food intake that is differentially sensitive to the novelty of the food source, we examined how VIP stimulation altered neuron activation in subcortical brain areas, hypothesizing that the c-Fos expression patterns from IL or PL VIP-stimulated neurons would differ significantly. Indeed, only the dorsomedial hypothalamic nucleus (DM) was shown to

exhibit a change in c-Fos expression that was similar between the IL and PL stimulation paradigms; both stimulations significantly increased c-Fos expression in this area (Table 1, $P < 0.01$ for IL; $P < 0.05$ for PL). Although IL VIPergic activation significantly increased c-Fos expression in the core of the AcbC and the CeM, no changes in c-Fos expression in these brain structures were observed following PL VIPergic activation. Interestingly, PL activation produced a significant increase in the expression of c-Fos in the PVN while decreasing c-Fos expression in the ARC. Again, IL VIPergic stimulation did not change c-Fos expression in either of these structures. These data demonstrate how manipulations of IL and PL VIPergic neurons produce distinctive changes in subcortical neuronal activation that likely explain observed differences in behavior.

2.4 Discussion

Our data represent the first description to our knowledge of an interneuronal cell type in the cortex that is capable of regulating food intake. To our knowledge, this is also the first description of a cellular pathway capable of selectively modulating palatable food intake while having no effect on standard chow consumption in sated animals. Although prior published reports have described the role of the frontal cortex in controlling feeding, no studies to our knowledge in humans or in animal models have shown how activation of a defined cortical interneuron cell type could alter ingestive behavior. Our studies provide an explanation at the cellular level of how aspects of reward behavior can be regulated by a defined neuronal cell type; mPFC VIPergic neuron stimulation can selectively reduce the intake of a highly valued food while having no effect on the motivation to work for food reward.

Prior studies have shown how VIPergic neuronal activity in both the frontal and auditory cortices is elevated following receipt of either reward or punishment (Pi et al., 2013, Pinto and Dan, 2015); these neurons respond following action outcome, suggesting that they act to relay a feedback signal. In this way, VIPergic activation would be expected to modulate the positive

reward prediction signal associated with the presentation of a novel food or other stimulus, updating the perceived value of the stimulus. Furthermore, this action as a reward prediction error signal would not be expected to affect motivation because any such signal would likely become attenuated over multiple cycles of reward consumption. Indeed, our data partly agree with this hypothesis: VIP neurons in the IL likely regulate high-value food intake through mediating the strength of a reward prediction signal error that would likely result from the consumption of a novel food or a food that undergoes an alteration in perceived value, while having no effect on the motivation to obtain food reward. In the absence of the generation of this hypothetical reward prediction error signal, for example when the same diet is presented multiple times, VIP depolarization in the IL would be expected to exert little effect on feeding.

This interpretation of the function of IL VIP neurons is also in agreement with our observation that these cells, when activated, can also reduce the intake of chow in a fasted animal. In this case, the effect of VIP neuron stimulation can be seen only when chow value is increased through fasting, potentially altering the predicted value of this food, while in the fed state, IL VIP stimulation has no effect on food intake. It has yet to be determined, however, whether IL VIP neuron stimulation amplifies a hypothetical error prediction signal that might result from the elevation in value of chow food that is ingested in the fasted state.

Meanwhile, the reduced palatable food intake we examined after PL VIPergic activation (Figure 5C and Figure 6, C and D) is consistent with the action of these neurons to reduce food intake through modulation of the salience of, value of, or attention to the food source. Although further studies are required to determine which of these processes engaged by reward presentation are altered by changes in PL VIPergic neuron activity, we can conclude from our data that PL VIPergic reduction in palatable food intake is not novelty dependent. This suggests that our stimulation in the PL does not modulate a reward prediction error signal. Interestingly, although the novelty value of palatable food does not appear to be the principal driver of a

reduction in intake by the PL VIP neurons, these cells can act to reduce exploratory locomotion in a novel environment, as we have also observed with IL VIPergic stimulation. Thus, our data demonstrate how mPFC VIP cells can regulate the response to select novel stimuli, an effect that is likely dependent upon the behavioral selectivity of the IL and PL brain regions.

Our c-Fos expression data provide an explanation of how manipulations of IL and PL VIPergic neurons produce differential effects on food intake and novelty-driven behaviors. PL VIPergic stimulation was shown to reduce c-Fos expression in the ARC, while PVN c-Fos expression was increased, with both areas having been implicated in the control of food intake (Elmquist et al., 2005, Krashes et al., 2011, Liu et al., 2017). Although direct activation of these target sites is unlikely, an indirect projection such as that from the PFC to the bed nucleus of the stria terminalis (BNST) (Radley et al., 2009) and subsequently from the BNST to the PVN could mediate the observed increase in c-Fos expression. IL VIPergic activation resulted in significant increases in c-Fos expression in the CeM and AcbC, areas that have been implicated in the regulation of reward valuation and novelty-driven behavior (Murugan et al., 2017, Mannella et al., 2013, Munuera et al., 2018), in addition to food intake (Land et al., 2014, Mena et al., 2013, Maldonado-Irizarry et al., 1995). Although a systematic investigation of PL and IL projections has not been attempted in the mouse, prior work in rats has shown how these brain regions differentially innervate, either directly or indirectly, subcortical structures that include the amygdala and nucleus accumbens (Vertes 2004, Gabbott et al., 2005), observations that could explain our described differences in c-Fos expression and animal behavior. The activation of the DM following stimulation of either IL or PL VIPergic neurons might also contribute significantly to the control of food intake because prior studies have shown how activation of select DM neurons can regulate autonomic outflow (Zhang et al., 2011) and food intake (Jeong et al., 2017) in addition to affecting reward-seeking behavior (Marchant et al., 2010). Neither IL nor PL stimulation produced a change in LH c-Fos levels, which was unexpected given the described

importance of mPFC projections to the LH in the control of feeding behavior (Mena et al., 2013). This result may be due to a lack of activation of this projection or may instead be due to a technical issue. Because mPFC VIPergic activation may be acting to suppress LH activity (Mena et al., 2013), this effect would be difficult to observe in neurons that, under resting conditions, are quiescent.

Finally, although our studies have focused on describing the role of VIPergic neurons in the control of food intake, it is likely that the activity of other interneuronal cell types can also influence aspects of reward valuation or motivation to obtain food. Because one of the main targets of the VIPergic neurons are other GABAergic interneurons that co-express somatostatin (SST) (Walker et al., 2016, Karnani et al., 2016), it is quite likely that activation of this cell type would produce an opposite effect on feeding behavior, enhancing intake. However, because VIPergic neurons also innervate pyramidal neurons directly (Zhou et al., 2017), producing a complex effect on circuit activity, SST activation may not produce a reciprocal change in behavior. Indeed, our observations regarding VIPergic function contrast with those data describing the role of another VIPergic neuronal target, the parvalbumin-expressing (PV) interneurons, suggesting that some of the behavioral consequences of VIPergic activation may be unique to this cell type. Although effects on food intake have yet to be investigated, activation of PV interneurons in the PFC enhances attentional performance (Kim et al., 2016) while manipulation of this cell type in isolation shows no effect on social interaction (Yizhar et al., 2011). These differences between the actions of PV neurons of the frontal cortex and our reported data concerning mPFC VIPergic neurons suggest that our manipulations have revealed an unappreciated behavioral selectivity of this cell type. This selectivity also suggests that our manipulation is not producing a nonspecific effect on network activity but instead produces a specific, behaviorally relevant effect on pyramidal cell output.

When considering potential caveats within the interpretation of our data, it is possible that our manipulation of VIP neuron activity producing a change in behavior did so through a synergy with isoflurane, which was administered in all animals before laser coupling to the ferrule. Although we were careful to begin behavioral testing only 5 minutes following recovery from and washout of isoflurane, it is possible that this induction of anesthesia may have affected behavior. It is also possible that other environmental effects in addition to isoflurane affected the outcome of our feeding experiments in particular, because our control populations appeared to show differences in consumption when tested sequentially. When we subsequently tested another group of PL and IL controls concurrently, however, we were unable to recapitulate the differences in food intake seen between the 2 control populations reported in manuscript (data not shown). Thus, it is quite likely that the observed differences in food intake between PL and IL control groups may have been due to environmental differences present upon testing and likely not due to the surgical manipulation or other aspects of the paradigm.

In conclusion, our studies have identified a potentially unique role for IL and PL VIPergic neurons in the control of palatable food intake. Our work is the first, we believe, to describe the ability of a cortical neuron subtype to selectively reduce intake of highly valued food in the absence of an effect on nonfasted chow intake. In addition, these data demonstrate how novelty-dependent and -independent mechanisms are likely involved in the frontocortical control of feeding behavior.

2.5 Methods

Experimental animals. We purchased 12-week-old adult male VIP-IRES-Cre–transgenic mice (stock 010908) from The Jackson Laboratory and housed them in the Pinn Hall vivarium at the University of Virginia on a 12-hour light/12-hour dark cycle (lights off at 2100 hours) with ad libitum access to food and standard chow (Teklad 2013, 4% fat, 17% protein, 48% carbohydrate, no sucrose, 2.9 kcal/g) unless otherwise noted. The Cre-expressing line was

backcrossed to C57BL/6J animals (Jackson Laboratory) for at least 7 generations. Heterozygous males were used for all described experiments and were generated by crossing VIP Cre–expressing males to C57BL/6J females. Animals were genotyped using the following primer pairs: mutant forward: 5′-CCCCCTGAACCTGAAACATA-3′; common: 5′-GGACACAGTAAGGGCACACA-3′; WT forward: 5′-TCCTTGGAACATTCCTCAGC-3′. We used 6–9 mice per treatment group for each experiment that we conducted.

Adeno-associated viral vector and stereotaxic viral injections. VIP neurons were stimulated using a Cre-dependent SSFO virus, AAV5-EF1a-DIO-ChR2 (C128S/D156A)-EYFP (23), sourced from the University of North Carolina Gene Therapy Core Facility. We injected 100 nl of virus bilaterally into either the PL or IL of 8-week-old male VIP-Cre mice using coordinates based on Frankin and Paxinos (Vogt and Paxinos, 2014, Xiong et al., 2017) (PL: +1.8 mm from bregma, ±0.4 mm lateral of midline, and 1.4 mm ventral of the dura; IL: +1.8 mm from bregma, ±0.4 mm lateral of midline, and 1.8 mm ventral of the dura). We next installed a fiber optic ferrule (FT200EMT, Thor Labs) at the dorsal boundary of the PL (+1.3 mm ventral of the dura) or IL (+1.7 mm ventral of the dura) following viral injection. The ferrule was attached to the skull and held in place using dental adhesive. Animals were allotted 6 weeks to recover from surgery before behavioral experiments were conducted.

SSFO stimulation protocol. Before each experiment, mice were briefly anesthetized with isoflurane, then fiber optically coupled to a diode-pumped, 473-nm blue laser (CrystaLaser model BC-473-060-M) controlled by a function generator (Grass Instruments), which delivered one 5-second train of 20-Hz pulses, 5-ms pulse width, with power output of 10 mW. Following stimulation, the laser was uncoupled, and after a period of 5 minutes to recover from handling, mice underwent all experimentation in the absence of tethering. To control for stress associated with handling, mice were acclimated to this stimulation procedure in the absence of actual

stimulation once daily for 1 week before any experimentation. Control animals were subjected to this tethering procedure for each experiment, minus laser stimulation.

Free feeding assays. All behavioral testing for palatable chow and standard chow feeding assays occurred in the home cage in the home room, except the 24-hour feeding assay (described below). For the 30-minute free feeding on standard chow, mice had their food removed at lights on and were tethered to the laser as described above; then laser stimulation was either applied or withheld depending on treatment condition. After 5 minutes, mice received a novel piece of preweighed standard chow, and food intake was quantified at 30 minutes, after which food was removed and mice resumed ad lib chow feeding. For feeding during the dark cycle, procedures were identical, except the experiment began at CT12 as opposed to CT0.

Measurement of palatable food intake was performed as previously described (Gaykema et al., 2014). On the night before testing, mice received a small (<0.1 g) sample of the HCD of interest (HCD1: Teklad TD.88137, 21% fat, 17.3% protein, 48.5% carbohydrates, 4.5 kcal/g; HCD2: Research Diets Inc., D12331, 58% fat, 17% protein, 25% carbohydrates, 5.56 kcal/g) to reduce aversion. At CT0 all food was removed, and mice were tethered to the laser; then laser stimulation was either applied or withheld depending on treatment condition. After 5 minutes, mice were challenged with approximately 3 g of preweighed HCD and allowed to consume. After 30 minutes, food was removed and weighed; then mice were returned to ad lib chow feeding. Mice were assigned randomly to the treatment or control conditions. Mice were given 4 days to recover from the binge before subsequent HCD exposure. For mice to serve as their own controls when comparing HCD consumption across multiple exposures, animal treatments remained consistent across days.

Measurement of 24-hour food intake. Mice were stimulated with one 5-second train of 20-Hz pulses, 5-ms pulse width, with power output of 10 mW, once every 30 minutes throughout the

23-hour duration of this study. To minimize disturbing the mice during stimulation, mice remained tethered to the laser via a fiber optic cable coupled to an optical commutator for the duration of the study. Mice were placed in cages modified for this setup in a separate room used for behavioral studies for this study, and they were acclimated to the cages 24 hours before testing. At lights on, mice were tethered to commutators, then given free access to the HFD of interest after 1 hour. Laser stimulation occurred at the onset of diet presentation, then every subsequent 30 minutes for 23 hours. Food intake was quantified every hour, and body weight was quantified every 6 hours; mice remained tethered during body weight quantification.

Operant responding for palatable food reward. Behavioral testing for the operant conditioning assay occurred in a dedicated behavior room, separate from the home room, conducted as we described previously (Warthen et al., 2016). Unlike testing during the other described behavioral experiments, mice remained tethered for the duration of the training sessions and the experiment, receiving laser stimulation during the latter at 15-minute intervals. Testing was performed in sound-attenuated boxes (Med-Associates). Each box was equipped with 3 nose poke holes arranged in a line on one side of the chamber and a food magazine on the opposite side. Each nose poke hole, as well as the magazine, was equipped with an infrared beam break detector. Three days before training, mice were placed on food restriction, with access to regular chow for 3 h/day, such that they were maintained at 80% original body weight. Mice were trained for 1 h/day, every day. Before any training, mice initially underwent extinction training to extinguish any innate preferences for any of the nose poke holes. In this phase, a nose poke did not result in any reward delivery. After passing extinction (fewer than 10 pokes in any hole in a given session), mice were passed on to FR training. FR training proceeded in 3 stages: FR1, FR3, and FR5. In FR1, a single nose poke in the center hole resulted in delivery of a palatable food reward (Bio-Serv, F05301, 5.6% fat, 18.7% protein, 59.1% carbohydrates, 3.6 kcal/g) to the magazine. In FR3, 3 nose pokes were required for a reward, and in FR5 5 nose

pokes were required. A mouse was considered to have passed a stage when it attained 30 rewards in a single session. Mice were moved from FR1 to FR3 after passing FR1 1 time, moved from FR3 to FR5 after passing FR3 twice, and moved from FR5 to progressive ratio (PR) testing after passing FR5 3 times. In PR testing, the number of nose pokes required for a reward increased progressively during a session, on the following schedule: 5 pokes for the first reward, then 10, 20, 30, 50, 70, 100, 130, 170, 210, 260, 310, and finally 370. PR testing lasted for a maximum of 2 hours and could terminate early if the mouse did not complete any given stage in 30 minutes or less. Total nose pokes recorded until this point were reported as "breakpoint." Mice underwent 2 days of PR testing on food restriction alternating laser/control treatment, with half receiving the laser stimulation on the first day and half receiving no stimulation, such that each animal underwent PR testing on each treatment. The chambers were cleaned between each trial with Minncare disinfectant to remove residual odors.

Open field. The open field assay was conducted as previously described (Warthen et al., 2016). The lights in the behavioral room were turned down, and mice were allowed to acclimate for at least 1 hour before testing. Five minutes after laser stimulation, mice were placed into the open field chamber and allowed to explore for 15 minutes while movement was recorded using EthoVision XT tracking software (Noldus). The open field chamber was cleaned between each mouse with Minncare disinfectant to remove residual odors. During testing, the lights in the room remained turned down, providing a dim light environment. All mice underwent this experiment before any other experiments in this open field arena so that arena novelty did not exist as a confounding variable during social interaction and novel object assays.

Social interaction. The social interaction task was performed in our open field chamber, as previously described (Golden et al., 2011). Before the social interaction test, all mice were brought to the behavior room and allowed to acclimate for at least 1 hour. Mice received laser stimulation 5 minutes before testing. In brief, the chamber was prepared with an empty

restrainer in the interaction zone, against the wall. The test mouse was placed in the chamber adjacent to the wall opposite the restrainer (as in the open field assay) and allowed to explore for 150 seconds. The test mouse was then removed to the home cage for 30 seconds, while the empty restrainer was replaced with a new, clean restrainer. A novel mouse (129/SJL, Jackson Laboratory) was placed in the new restrainer, and the test mouse was returned to the chamber and allowed to explore for 150 seconds. Behavior and motion were recorded using EthoVision. The chamber was cleaned between each mouse with Minncare disinfectant to remove residual odors.

Novel object interaction. The novel object interaction assay was also performed in our open field chamber, described above. Before the novel object test, all mice were brought to the behavior room and allowed to acclimate for at least 1 hour. Mice received laser stimulation 5 minutes before testing. In brief, following an initial 15 minutes of exposure to the chamber, mice were reintroduced to the chamber that then contained a novel piece of copper piping. Exploration of the piping, placed in the center of the arena, was recorded using EthoVision.

Elevated plus maze. Anxiety-like behavior was measured using an elevated plus maze apparatus according to our prior published procedure (Scott et al., 2011). The 12 cm × 50 cm maze was elevated 55 cm from the floor in a low-light environment. Time in the open arm was measured during a 5-minute period. Scoring was done automatically using EthoVision.

Brain tissue preparation and immunohistochemistry. Immunohistochemistry was performed as previously described (Gaykema et al., 2014). Mice received either laser stimulation or nothing (controls) in the absence of food 90 minutes before sacrifice by transcardial perfusion fixation. After receiving anesthesia, mice were briefly flushed with buffered saline, followed by perfusion with 4% paraformaldehyde in 0.1-M phosphate buffer. Brains were dissected and sectioned at 40-μm thickness on a vibratome (Leica Biosystems). Immunoperoxidase staining was used to

visualize c-Fos expression. All primary and secondary antibody solutions were made in 0.01 M PBS containing 0.5% Triton X-100, 1% normal goat serum, and 0.1% sodium azide with the following dilutions: rabbit anti-Fos (Ab-5, 1:5000, MilliporeSigma, PC38), goat anti–rabbit IgG (1:1000, Jackson ImmunoResearch Laboratories Inc.). After 48 hours of incubation in primary antibody, sections were washed in PBS and incubated in goat anti–rabbit IgG secondary antibody overnight at 4° C. Following a subsequent series of washes in PBS, sections were incubated for 3 hours in avidin-biotin-peroxidasa complex diluted in PBS with 0.1% Triton x-100 (ABC Elite kit, 1:1000, Vector Labs). After a final series of washes, sections were visualized with nickel-enhanced DAB tablets (SIGMAFAST, Sigma-Aldrich) to yield a black color. For fluorescent immunohistochemistry, sections were incubated in a mix of chicken anti-GFP (Aves Labs catalog GFP-1020, 1:2000) and rabbit anti-Fos (Ab-5, 1:5000, MilliporeSigma, catalog PC38) polyclonal antibodies for 24 hours, followed by Alexa Fluor 488–conjugated goat anti-chicken and Cy3-conjugated goat anti–rabbit IgG (Jackson ImmunoResearch Laboratories Inc.; 1:1000) overnight in a light-protected container. Sections from each were then mounted in sequential order, air-dried, dehydrated, cleared, and coverslipped in Vectashield hard-set mounting medium (Vector Laboratories). During the entire process the slides were protected from light exposure.

Quantitative analysis of c-Fos immunoreactivity. In the series stained for only c-Fos, numbers of stained cell nuclei in the mPFC were counted using the ImageJ (NIH). The mPFC area analyzed corresponded closely with the coronal diagram at 1.78 mm anterior to the bregma (Karnani et al., 2016). Quantitation was done in the NIH's ImageJ, where images were equalized in brightness (background subtraction), the threshold was set for binary conversion, and the number of particles (corresponded to labeled nuclei) was counted and recorded. Similarly, c-Fos expression was assessed in the AcbC (bregma +1.34 mm), PVN and LH (bregma –0.58 mm),

BLA and CeM (bregma –1.22 mm), DM and ARC (bregma –1.58 mm), and VTA (bregma –3.08 mm).

Quantitative analysis of fluorescent double-labeled cells. The series of sections fluorescently double-labeled for c-Fos and YFP reporter immunofluorescence was evaluated using Neurolucida 2017 (MBF Bioscience) by capturing pairs of images with a ×20 objective with the excitation/emission filters alternating between Cy4 and Alexa 488 fluorophores. Then the sections were quantified for double-labeling manually by a blinded technician.

Electrophysiology. In vitro slice preparation and intracellular recordings were performed as described previously (Klein et al., 2018) with some modifications. Briefly, VIP-Cre mice were stereotactically injected with AAV5-EF1a-DIO-ChR2 (C128S/D156A)-EYFP into the mPFC. Animals were allowed to recover for 2 weeks and were then injected with pentobarbital and transcardially perfused with an ice-cold solution of (in mM) 92 NMDG, 26 $NaHCO_3$, 25 glucose, 20 HEPES, 10 $MgSO_4$, 5 sodium ascorbate, 3 sodium pyruvate, 2.5 KCl, 2 thiourea, 1.25 NaH_2PO_4, and 0.5 $CaCl_2$ titrated to pH 7.4. Coronal sections were obtained using a VT1200 vibratome (Leica Biosystems), incubated in aCSF (in mM: 126 NaCl, 26 $NaHCO_3$, 10 glucose, 2.5 KCl, 2 $CaCl_2$, 1.25 NaH_2PO_4, and 1 $MgSO_4$), held at room temperature, and equilibrated with 95% O_2/5% CO_2. Intracellular recordings were obtained from tissue slices submerged in a chamber perfused with 31°C to 33°C aCSF. VIPergic neurons expressing the SSFO were identified first by green fluorescent reporter expression and DIC optics using a Zeiss Axio Examiner.A1 microscope and scientific CMOS camera (ORCA-Flash 4.0, Hamamatsu). Recording pipettes were made from borosilicate pipettes pulled using a Sutter P1000 puller. The internal solution was composed of (in mM) 130 KCl, 1 $MgCl_2$, 0.07 $CaCl_2$, 10 HEPES, and 0.1 EGTA, pH 7.3, osmolarity 300 mOsm. Pipettes used tip resistances of 3–4 M. Neurons were stimulated using a diode-pumped, 473-nm blue laser (CrystaLaser model BC-473-060-M), with light delivered through the camera port, controlled by a function generator (Grass Instruments),

which delivered one 5-second train of 20-Hz pulses, 5-ms pulse width, with power output of 10 mW. Data were acquired using pClamp software (Molecular Devices) using a Multiclamp 700B amplifier. Data were low-pass filtered at 2 kHz and digitized at 10 kHz using a Digidata 1440A (Molecular Devices). Analysis of the effect of laser stimulation on membrane potential was performed using a custom MATLAB script (MathWorks).

Statistics. All data were subjected to statistical analysis in GraphPad Prism version 7. IL and PL groups were separate cohorts, and thus controls were not pooled; IL controls were compared to IL SSFO, while PL controls were compared to PL SSFO. When SSFO-stimulated VIP mice were compared to nonstimulated controls, 2-tailed, unpaired t tests were performed (Figures 1–4). For multiple HFD exposure assays, mice received the same treatments across multiple exposures, and data were analyzed with 2-way repeated measures ANOVA and Tukey's post hoc comparisons with treatment and time points as independent variables (Figure 5, A–D). Mice served as their own controls in the operant responding experiment, and thus a 2-way repeated measures ANOVA was used (Figure 4D). For the 24-hour HCD2 consumption study, linear regression models were created with time and treatment group as fixed effects to determine whether differences between control and experimental animals were statistically significant. Separate models were created for light hours (0–12) and dark hours (13–24) (Figure 6, E and F). Data from once-performed behavioral tests (open field, elevated plus maze, novel object, social interaction) were analyzed with unpaired, 2-tailed t tests (Figure 7 and Figure 8). All Data are expressed as mean ±SEM. Statistical significance was considered when P values were less than 0.05. For the comparison between FR completion times, we used multiple t tests with correction for multiple testing, using the Holm-Šídák method with $\alpha = 5\%$. For the c-Fos analysis, cell numbers and percentages of double-labeled cells were analyzed using 2-tailed, unpaired t tests. In all bar graphs and tables, all grouped values are expressed as means and SEM.

Study approval. All experimental procedures were conducted in accordance with NIH guidelines and approved by the University of Virginia's Animal Care and Usage Committee (Charlottesville, Virginia, USA).

2.6 Figures and Tables

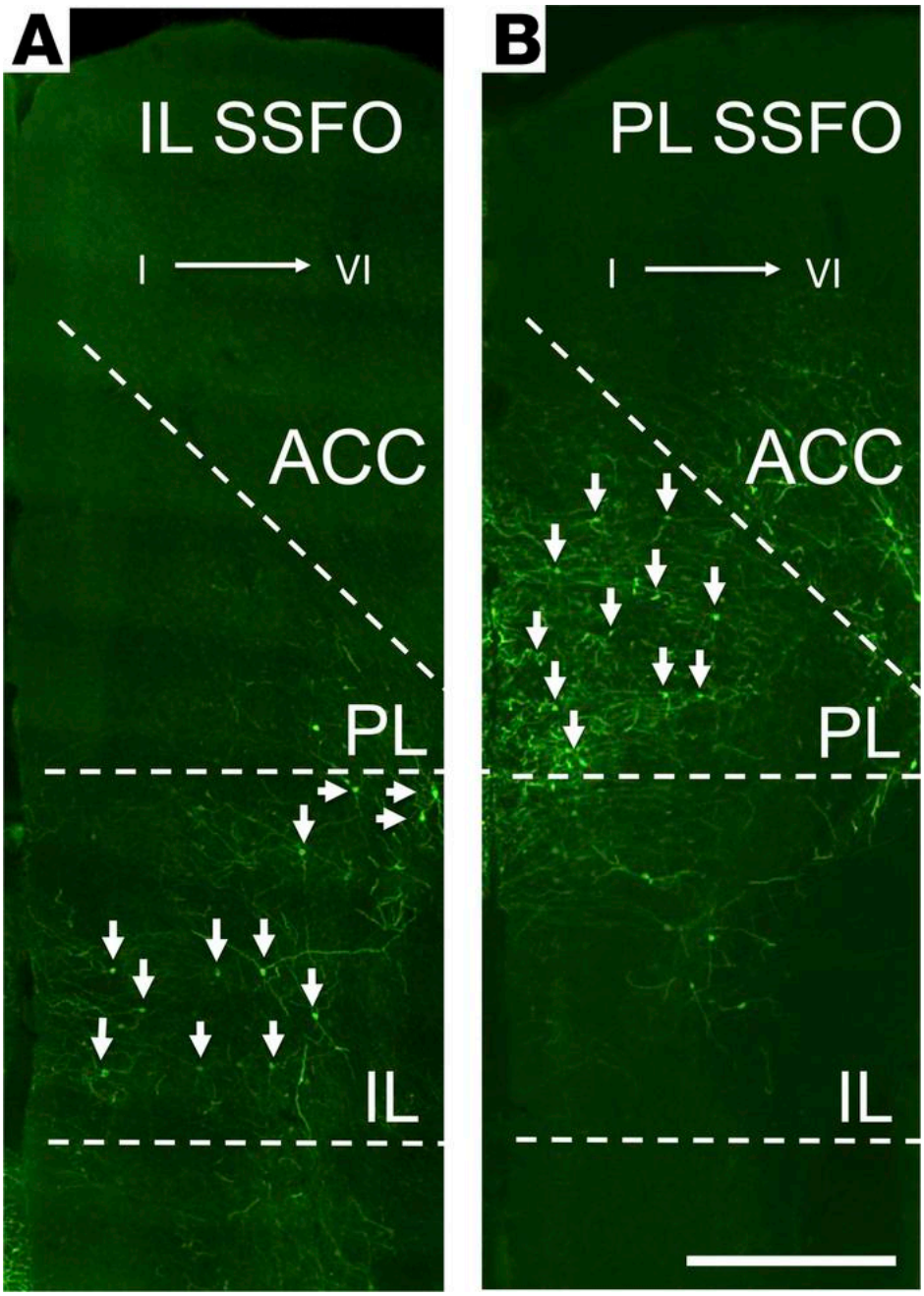

Figure 1. SSFO Expression in the PL and IL. AAV-driven expression of SSFO was selective for the IL (A) and PL (B). Arrowheads indicate SSFO-expressing neurons in representative images of animals with AAV injections targeted to either the IL or PL cortex. Expression of SSFO was observed in all study animals between +1.7 mm and +1.98 mm rostral of the bregma, corresponding to panels 17 to 19 in Paxinos and Franklin (2004). Relative position of cortical layers I → VI indicates orientation of the coronal slice. Scale bar: 500 μm.

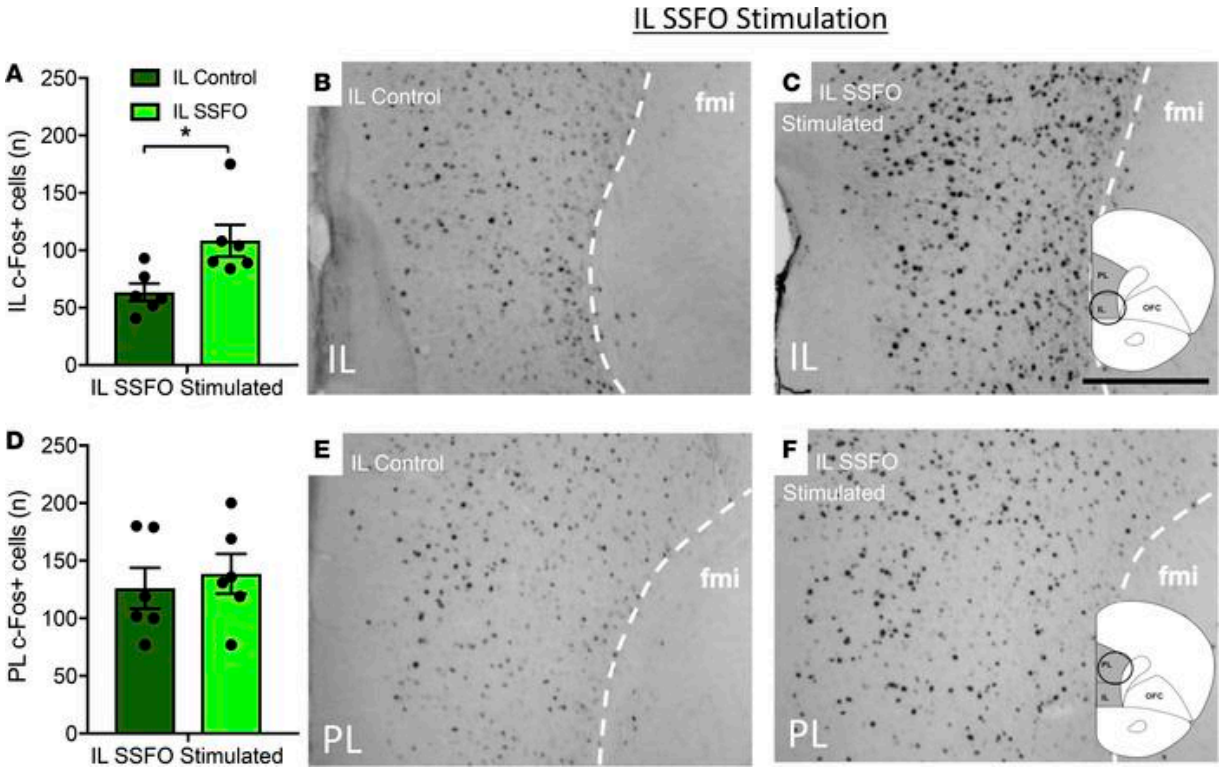

Figure 2. SSFO stimulation of IL VIPergic neurons produces a selective increase in c-Fos expression throughout the IL. IL SSFO stimulation results in an increase in c-Fos expression (C) when compared with controls (B) quantified in (A). IL SSFO stimulation does not result in an increase in c-Fos expression in the PL, when stimulated animals (F) are compared with controls (E) quantified in (D). Scale bar: 200 μm. Fmi, forceps minor corpus callosum. *P < 0.05, unpaired 2-tailed t test. 6 IL control and 6 IL SSFO mice (A and D) were used for analysis.

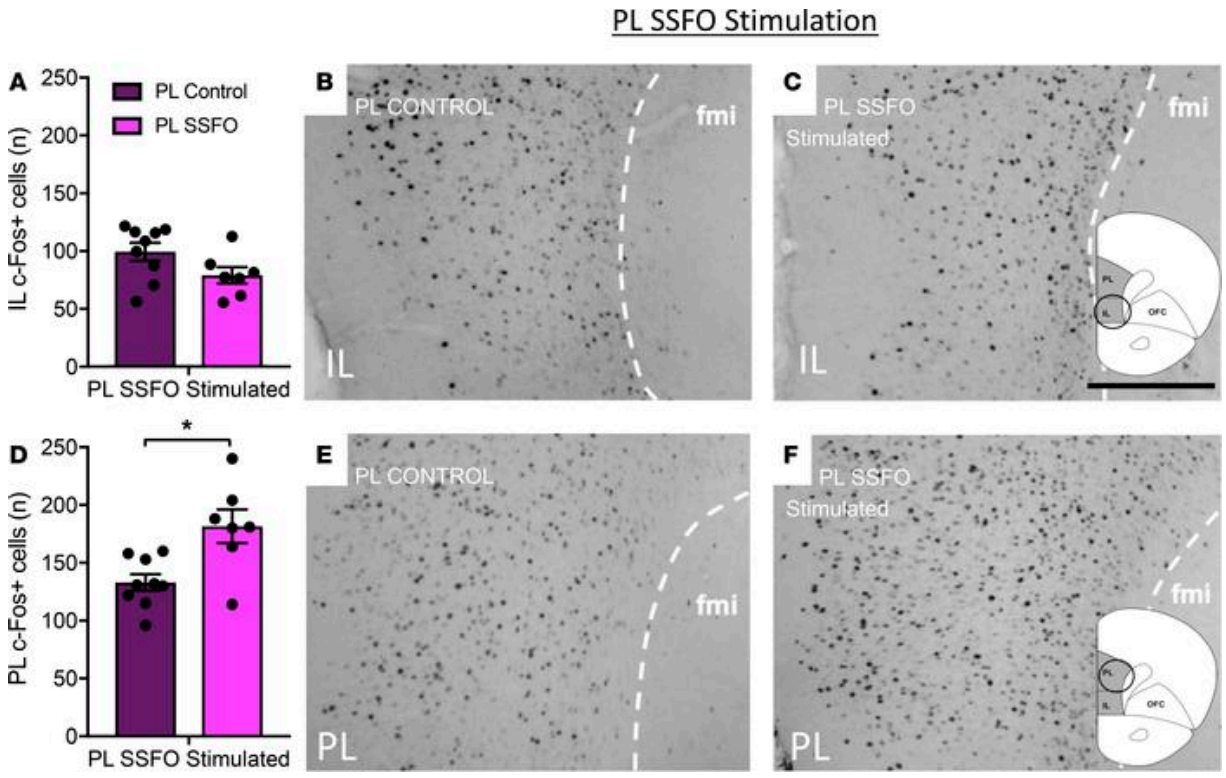

Figure 3. SSFO stimulation of PL VIPergic neurons produces a selective increase in c-Fos expression throughout the PL. PL SSFO stimulation results in an increase in c-Fos expression (F) when compared with controls (E) quantified in (D). PL SSFO stimulation does not result in an increase in c-Fos expression in the IL, when stimulated animals (C) are compared with controls (B) quantified in (A). Scale bar: 200 μm. Fmi, forceps minor corpus callosum. *P < 0.055, unpaired t test. 10 PL control and 7 PL SSFO mice (A and D) were used for analysis.

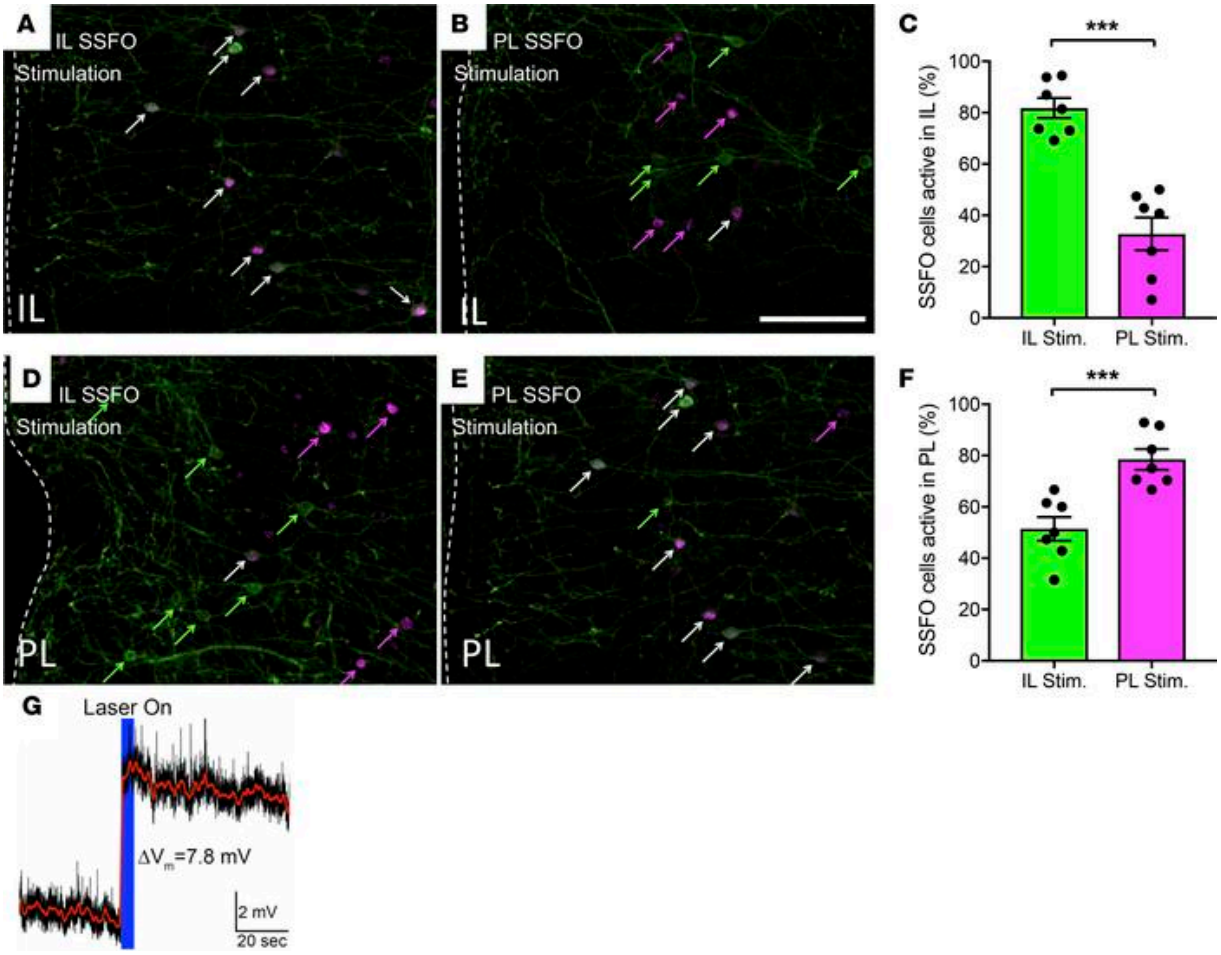

Figure 4. Selective stimulation of IL and PL VIPergic neurons of the mPFC. Activation of an SSFO-YFP driven by 473-nm laser in the IL significantly enhances c-Fos expression in VIPergic neurons of the IL (A) when compared with when SSFO stimulation occurs in the PL (B) as quantified in (C). Similarly, activation of the SSFO in the PL significantly increases VIPergic c-Fos expression in the PL (E) compared with when SSFO stimulation occurs in the IL (D) as quantified in (F). Green arrows denote YFP+ cells, magenta arrows denote c-Fos+ cells, and white arrows denote double-labeled cells. Scale bar: 200 μm. (G) Representative trace showing SSFO-driven VIP neuronal depolarization. ***P < 0.0015, by unpaired t test. 7 IL SSFO and 7 PL SSFO mice (A and D) were used for analysis.

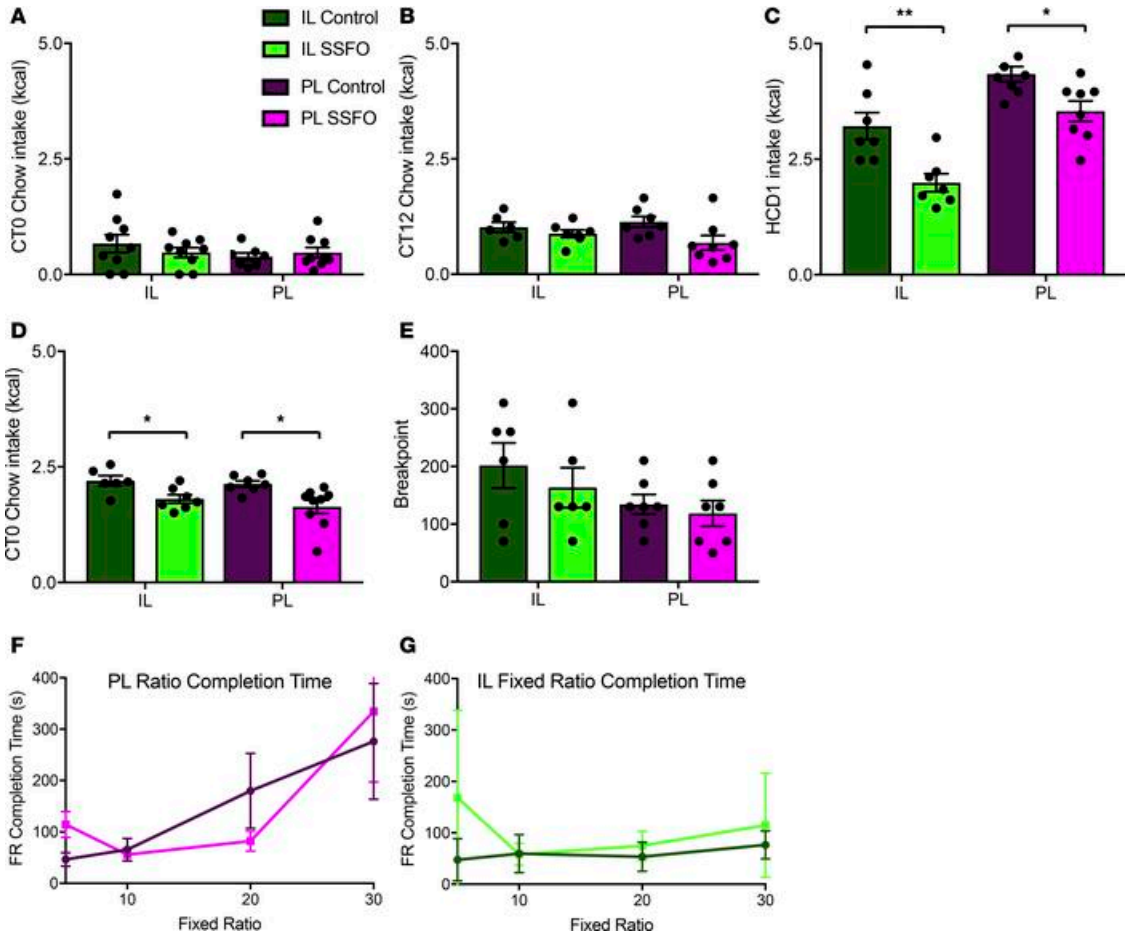

Figure 5. VIPergic stimulation in the IL and PL reduces HCD intake while having no effect on low-calorie rodent chow consumption or on the motivation to obtain food reward. Intake of low-calorie rodent chow at either CT0 (A) or CT12 (B) was unaffected by either IL or PL VIPergic stimulation. Both IL and PL VIPergic stimulation reduced the intake of HCD1 over a period of 30 minutes at CT0 when compared with control-stimulated mice (C). Similarly, both IL and PL VIP stimulation reduced chow intake following an 18-hour fast (D). Progressive ratio responding for chocolate-flavored pellets was unchanged following either IL or PL VIPergic stimulation, as measured by ratio breakpoint (E) or as time to ratio completion (F and G). *P < 0.05; **P < 0.015, by 2-way repeated-measures ANOVA with Tukey's post hoc comparison, with treatment and time points as independent variables. 6-9 IL control, 6-9 IL SSFO, 7 PL control, and 7-9 PL SSFO mice were used for analysis.

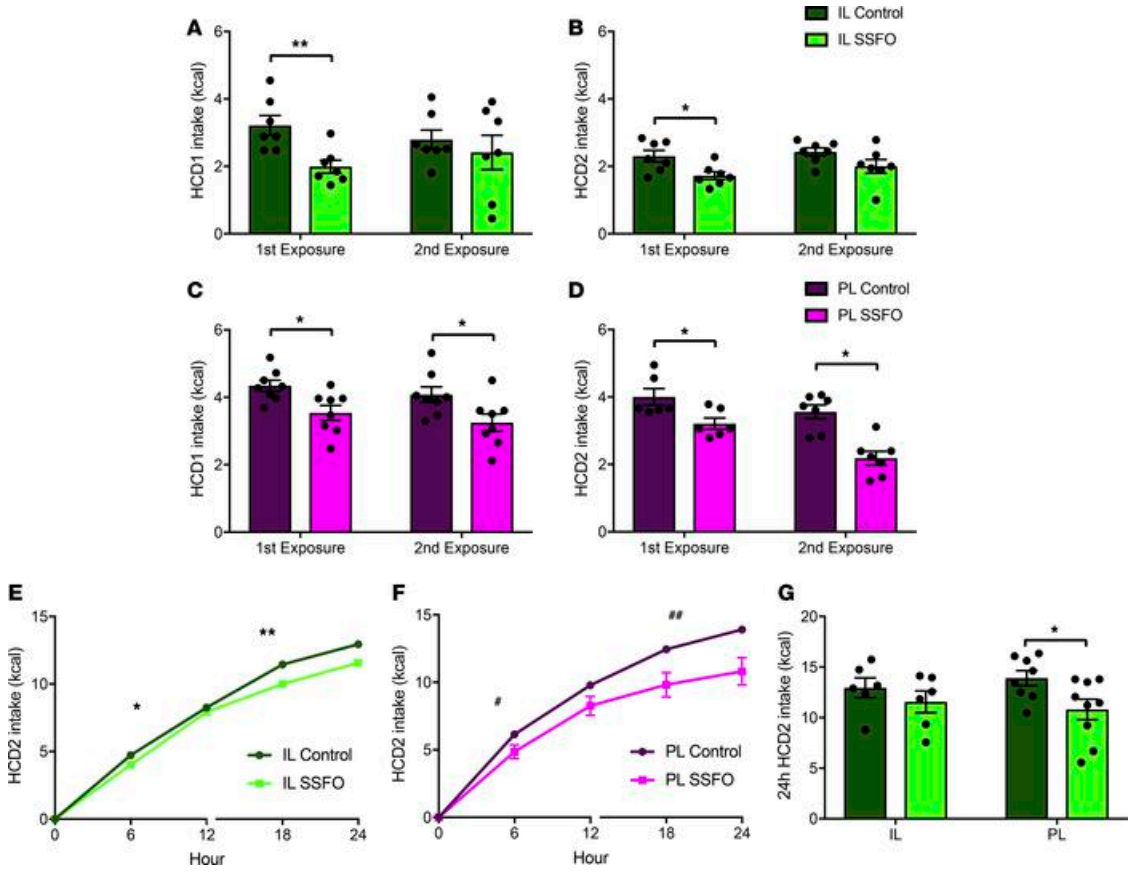
A
HCD1 intake (kcal)
1st Exposure
2nd Exposure
B
IL Control
IL SSFO
HCD2 intake (kcal)
C
PL Control
PL SSFO
D
E
HCD2 intake (kcal)
Hour
F
G
24h HCD2 intake (kcal)
IL
PL

Figure 6. IL but not PL VIPergic stimulation-driven reduction in HCD intake is dependent upon food novelty while showing little effect on 24-hour food intake. Although stimulation of IL VIPergic neurons produced a reduction in food intake of HCD1 during initial testing, these neurons produced no change in feeding when retested using the same diet (A). The effect of IL VIPergic stimulation to reduce food intake can be rescued, however, when animals are subsequently tested using a novel HCD (HCD2) (B, left). Again, when animals were retested using this same diet, IL VIPergic stimulation had no effect on food intake (B, right). PL VIPergic stimulation produced a reduction in HCD intake regardless of whether the diet was novel, when tested using either HCD1 (C) or HCD2 (D). IL VIPergic stimulation for 24 hours exerted a minimal effect on food intake (E and G, left) while PL VIPergic stimulation produced a significant reduction in consumption (F and G, right). *$P < 0.05$; **$P < 0.01$; #$P < 10–8$; ##$P < 10–13$ by 2-way repeated-measures ANOVA with Tukey's post hoc comparison, with treatment and time points as independent variables (A–D), linear regression models were created with time and treatment group as fixed effects (separate models were created for light hours [0–12] and dark hours [13–24]) (E and F), or unpaired 2-tailed t test (G). 7 IL control, 7 IL SSFO, 8 PL control, and 7 PL SSFO mice were available for analysis.

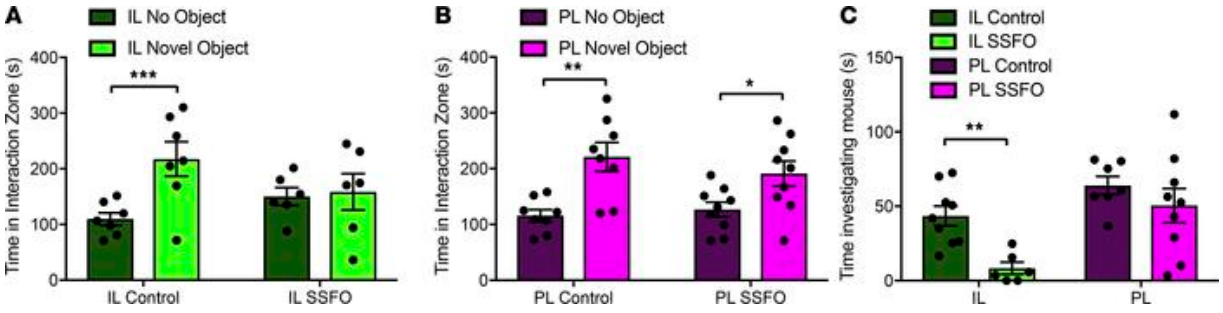

Figure 7. IL but not PL VIPergic stimulation reduces novel object and novel social investigatory behavior. SSFO-driven stimulation of IL VIPergic neurons reduced novel object investigation when compared with controls (A). PL VIPergic stimulation had no effect on novel object investigatory behavior (B). IL VIPergic stimulation reduced time spent investigating a novel conspecific animal while PL VIPergic stimulation exhibited no effect (C). *P < 0.05; **P < 0.01; ***P < 0.0015 by unpaired 2-tailed t test. 9 IL control, 6 IL SSFO, 8 PL control, and 9 PL SSFO mice were available for analysis.

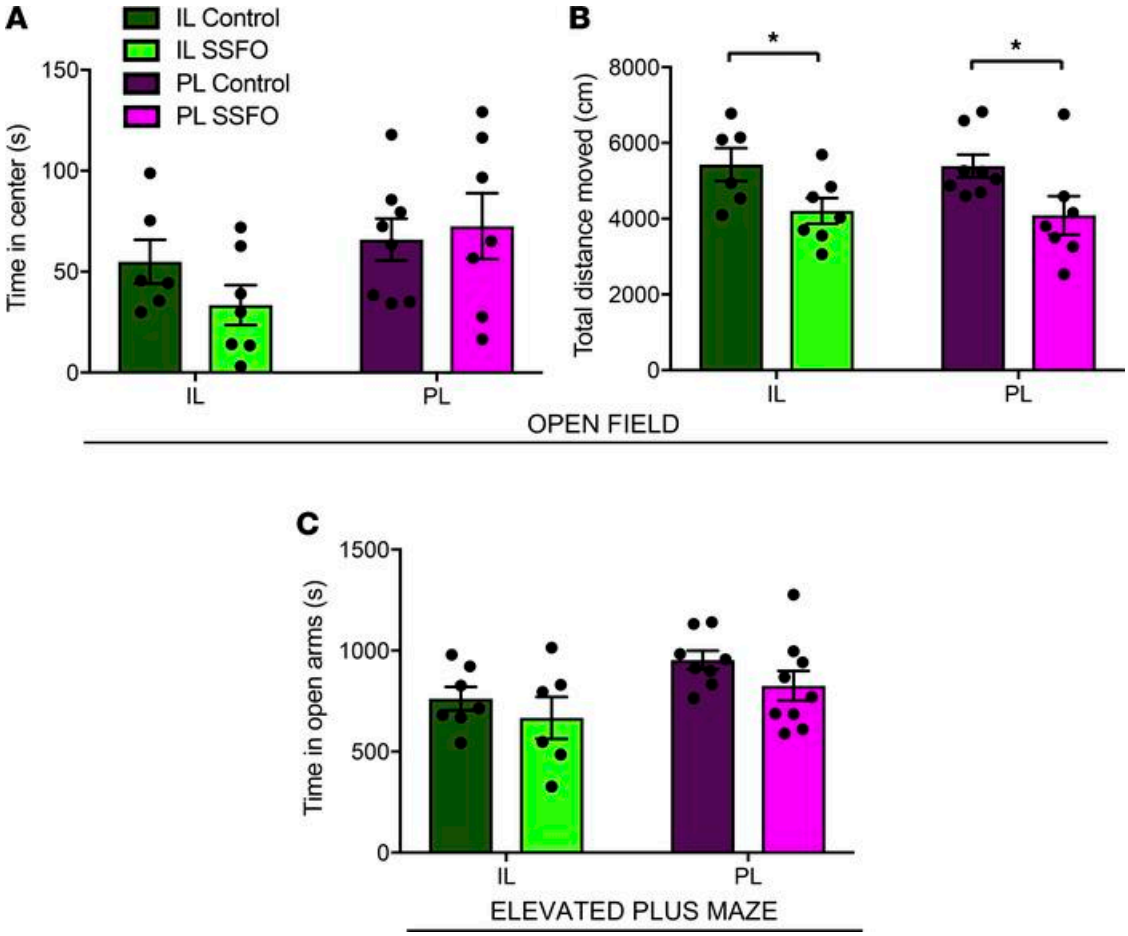

Figure 8. Neither IL nor PL VIPergic stimulation affects the expression of anxiety-like behavior. No effect of IL or PL VIPergic stimulation was seen on time spent in the center of an open field arena (A) or in time spent in the open arms of an elevated plus maze (C). However, both IL and PL VIPergic activation reduced novel environment–driven exploratory behavior in the open field arena (B). *P < 0.05 by unpaired 2-tailed t test. 6 IL control, 7 IL SSFO, 8 PL control, and 9 PL SSFO mice were available for analysis.

Table 1. Distinct patterns of c-Fos expression are observed throughout the brain following SSFO-driven stimulation of IL and PL VIPergic neurons

	Contralateral IL		Ipsilateral IL		Contralateral PL		Ipsilateral PL	
	SSFO	Control	SSFO	Control	SSFO	Control	SSFO	Control
PVN	161 ± 41	218.2 ± 29	162 ± 40	204 ± 26	127 ± 16	216 ± 20[A]	152 ± 25	210 ± 23
DM	52 ± 10	71.2 ± 4	44 ± 5	74.2 ± 7[B]	55 ± 8	73.6 ± 9	50.5 ± 5	73.8 ± 10[B]
Rostral LH	127 ± 28	116 ± 14	129 ± 15	117 ± 15	112 ± 18	99 ± 17	112 ± 12	100 ± 24
ARC	48 ± 10	53 ± 15	62 ± 9	56 ± 7	51 ± 4	40 ± 4	60 ± 3	47 ± 5[B]
BLA	37 ± 3	44 ± 9	27 ± 4	37 ± 6	36 ± 8	26 ± 5	36 ± 6	37 ± 8
CeM	80 ± 13	107 ± 25	52 ± 7	112 ± 13[A]	88 ± 11	106 ± 20	96 ± 20	130 ± 23
VTA	49 ± 14	35 ± 7	52 ± 11	31 ± 9	34 ± 6	39 ± 7	37 ± 7	39 ± 3
AcbC	237 ± 40	353 ± 57	167 ± 32	314 ± 41[B]	223 ± 19	230 ± 41	212 ± 18	296 ± 37

IL VIPergic stimulation enhanced c-Fos expression in the dorsomedial hypothalamus (DM), the central nucleus of the amygdala (CeM), and nucleus accumbens core (AcbC). PL VIPergic stimulation enhanced c-Fos expression in the paraventricular hypothalamic nucleus (PVN) and in the DM, while reducing c-Fos expression in the arcuate nucleus of the hypothalamus (ARC). [A]$P < 0.01$, unpaired 2-tailed t test; [B]$P < 0.05$, unpaired 2-tailed t test. Neither treatment affected c-Fos expression in the lateral hypothalamus (LH), basolateral amygdala (BLA), or ventral tegmental area (VTA).

Table 1. Distinct patterns of c-Fos expression are observed throughout the brain following SSFO-driven stimulation of IL and PL VIPergic neurons.

Chapter 3: Deletion of mPFC VIP neurons in both the IL and PL increases palatable food- while sparing normal chow intake

In order to further strengthen our data demonstrating behavioral roles for mPFC VIP neurons, we have recently begun to investigate whether deletion of these cells in both the IL and the PL could be necessary as well as sufficient (as previously demonstrated in our SSFO studies) for the regulation of appetitive and select non-appetitive behaviors.

3.1 Methods

Experimental Animals

We purchased 12-week-old adult male VIP-IRES-Cre–transgenic mice (stock 010908) from The Jackson Laboratory and housed them in the Pinn Hall vivarium at the University of Virginia on a 12-hour light/12-hour dark cycle (lights off at 2100 hours) with ad libitum access to food and standard chow (Teklad 2013, 4% fat, 17% protein, 48% carbohydrate, no sucrose, 2.9 kcal/g) unless otherwise noted. The Cre-expressing line was backcrossed to C57BL/6J animals (Jackson Laboratory) for at least 7 generations. Heterozygous males were used for all described experiments and were generated by crossing VIP Cre–expressing males to C57BL/6J females. Animals were genotyped using the following primer pairs: mutant forward: 5'-CCCCCTGAACCTGAAACATA-3'; common: 5'-GGACACAGTAAGGGCACACA-3'; WT forward: 5'-TCCTTGGAACATTCCTCAGC-3'. We used 6–9 mice per treatment group for each experiment that we conducted.

Cell-specific deletion protocol

To ablate interneurons of the PL and IL, we performed bilateral injections of an AAV that expressed an activated form of caspase 3 in a Cre-dependent manner (Yang et al., 2013). In order to silence large areas of the PL or IL, we reasoned that it would not be practical to use

laser light, as VIP and SST neurons are present through several cortical layers that would make uniform, bilateral silencing difficult. One additional hurdle to using SSFO was the bilateral nature of the deletion; SSFO stimulation was performed unilaterally, as positioning two ferrules in the proximity required to bilaterally stimulating the mPFC in a 20g mouse is technically difficult. Quantifying silencing would also be a problem using such tools such as Archaerhodopsin, unlike the use of the caspase approach.

In the preliminary work presented here, we first investigated whether deleting VIP neurons throughout the entire mPFC could affect appetitive behaviors as well as both novel- and social interaction. Thus, we injected into VIP-Cre mice a large volume (200nl/side) of AAV caspase uniformly throughout the IL and PL (1.4 to 1.8mm ventral of the dura, based on coordinates from Paxinos and Franklin, 2004). After surgery, mice were allowed 4 weeks to recover from surgery and for sufficient virally-mediated neuronal deletion to occur before behavioral experiments were conducted. For control animals, an equivalent volume of sterile saline was bilaterally injected into the mPFC.

Behavioral Experiments

Nine control and 10 caspase-treated mice were available for behavioral analyses. We performed several of the same behavioral experiments as described in Chapter 2, section 2.5, using the same methodologies. Specifically, we conducted:

- Free feeding assays using both normal chow and HCD1 (page 45)
- Operant responding for palatable food reward (page 46)
- Social interaction (page 47)
- Novel object interaction (page 48)
- Open field as measure of anxiety (page 47).

In all experiments, no stimulation protocol was required, as neuronal deletion had already occurred. Thus, mice could be tested without any additional manipulation.

3.2 Results

3.2.1 Deletion of mPFC VIP neurons

To determine the requirement of mPFC VIP neurons in the regulation of behaviors detailed above, we bilaterally injected a Cre-dependent AAV that encoded caspase-3 into both the IL and PL of VIP Cre mice. To determine the efficiency and specificity of neuron deletion using this technique, we use RNAscope to quantify both VIP and SST (a subpopulation that should not have been affected by injection) neuron subpopulations in the mPFC after caspase-3 injection (Figure 1). VIP neurons were selectively deleted (Figure 1 A-C, Control=162±13 cells, Caspase=62±14 cells, $p<0.0001$), while SST neurons were unaffected (Figure 1A-C, 305±28 cells, 238±30 cells, $p=0.1202$). As a control for the spread of the viral injection, we also quantified VIP and SST cells in the adjacent AAC, an area where no deletion should have occurred. Indeed, we found that both VIP and SST subpopulations were unaffected in animals injected with caspase-3 in the ACC (Figure 1D, Control= 98±10, Caspase=78±12 cells, $p=0.23$). These data indicate both site- and cell-specific neuronal deletion.

3.2.2 mPFC VIP ablation increases palatable food intake

We demonstrated in Chapter 2 that mPFC VIP neuron stimulation decreased palatable food consumption while sparing effects on standard chow consumption in sated mice. To determine the necessity of these neurons in this behavior, we allowed caspase-3-injected VIP mice and their control counterparts free access to either standard chow or to a highly palatable high calorie diet (HCD1). We found that mPFC VIP neuron deletion was associated with increased binge-like consumption of HCD1 (Figure 2A, Control=2.87± 0.132g Caspase=3.497± 0.237g, $p=0.0375$), while standard chow intake was again unaffected (Figure 2B,

Control=0.4785± 0.175g, Caspase=0.493± 0.101, p=0.94g). Similar to results observed using SSFOs, we observed that deleting mPFC VIP neurons had no effect on effort to obtain palatable food reward, as measured using a progressive-ratio operant conditioning paradigm (Figure 2C, Control=471.3± 109.1 nosepokes, Caspase=500± 136.5 nosepokes, p=0.3883). These results collectively demonstrate that VIP neurons spanning the entirety of the mPFC (both IL and PL subdivisions) are required to regulate palatable food intake consumption, while sparing effects on motivation to obtain food reward.

3.2.3 VIP deletion in the mPFC does not affect anxiety, novel object- or social investigation

Although we observed reduction in both novel object- and social investigation behavior when stimulating VIP neurons in the IL, we observed no changes in either of these behaviors after deleting VIP neurons in both the IL and the PL (Figure 3A and B). Similar to what we observed in our SSFO study (Section 2.3.5), we saw no effect on anxiety-like behavior as measured by an open field assay (Figure 3C).

3.3 Discussion / Future Work

To our knowledge, these data are the first to demonstrate the necessity of mPFC VIP neurons in the regulation of palatable food intake. We demonstrated in Chapter 2 that VIP neurons of the IL and PL regulate palatable food intake through different mechanisms; PL VIP neuron stimulation significantly decreased consumption of palatable food over multiple exposures through a mechanism that likely involves modulating the salience or reward value of the food source, while the ability of IL VIP neurons to decrease palatable food intake was dependent upon the novelty of the food source. While our caspase data demonstrates the necessity of both of these populations combined in the suppression of excess palatable food consumption, it is unclear through which mechanism this change in food intake is being mediated. Further work will address this concern by targeting either the IL or the PL for VIP neuron deletion, in a similar design as our SSFO work.

Our preliminary work presented here also agrees with our previous hypothesis that VIP neurons modulate food intake only when the perceived value of the food is high, in that only palatable food intake was affected by mPFC VIP neuron deletion. Future work can test this hypothesis further by increasing the value of standard chow through fasting and observing effects of both IL and PL VIP deletion on standard chow intake. Because the ability of IL VIP neurons to reduce palatable food intake was dependent upon the novelty of the food (2.3.3), testing whether the effect on food intake in VIP-caspase animals across multiple exposures to multiple palatable diets is also a logical next step for future work.

Stimulating IL VIP cells was associated with a decrease in both social- and novel object investigatory behavior (Section 2.3.4). However, deleting VIP neurons in both the IL and the PL was not associated with any changes in novel object- or social investigation, which was consistent with our findings when we stimulated VIP cells in the PL with SSFO. Because we saw an opposite effect on palatable food intake when deleting (increased consumption) vs stimulating (decreased consumption) VIP cells, one might also expect to observe similar trends in novelty-driven investigatory behaviors, had our caspase injection been targeted exclusively to the IL. Disrupting circuitries in both the IL and PL simultaneously appears to have overridden any changes in interest in natural novel stimuli that may have been modulated by IL VIP neurons exclusively. Alternatively, like we observed in our PFC-Acb deletion study, this projection may not be important in the regulation of social novelty investigatory behavior, but may have an effect on social-spatial coding, as described recently (Murugan et al., 2017).Again, performing these experiments in mice with selective IL and PL VIP deletion will clarify these results. That our caspase deletion was not indicative of anxiety as indexed by time spent in the center of an open field suggests that the effects we observed when manipulating mPFC VIP neurons were not secondary to increased stress.

3.4 Figures

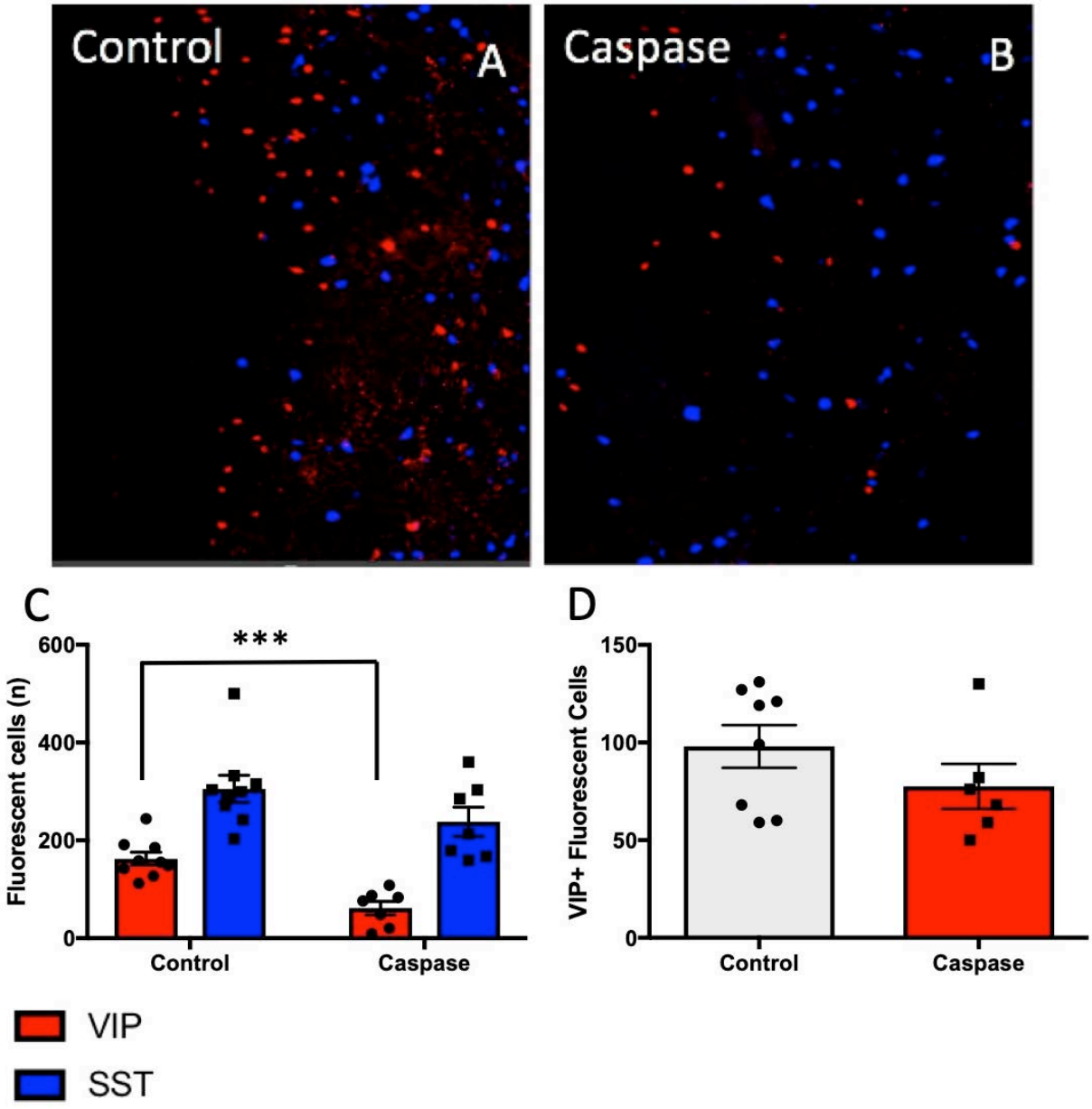
Control
A
Caspase
B
C
***
600
400
200
0
Fluorescent cells (n)
Control
Caspase
VIP
SST
D
150
100
50
0
VIP+ Fluorescent Cells
Control
Caspase

Figure 1. Selective deletion of VIP neurons from the IL and PL, extending from +1.7mm to +1.98mm rostral of Bregma (RNAscope (ACD, California) conducted as per manufacturer's instructions. VIP probe 415961-C2 (red), somatostatin (SST) probe 404631-C3 (blue)). Representative images at the injection site demonstrate VIP cell-specific deletion (A). While significant loss of VIP neurons was observed (A-C, Control=162±13 cells, Caspase=62±14 cells, $p<0.0001$), no significant loss of SST neurons was seen (A-C, 305±28 cells, 238±30 cells, $p=0.1202$). (D) No loss of VIP neurons was observed in adjacent cortical areas, such as the more dorsal anterior cingulate cortex (ACC) Control= 98±10, Caspase=78±12 cells, p=0.

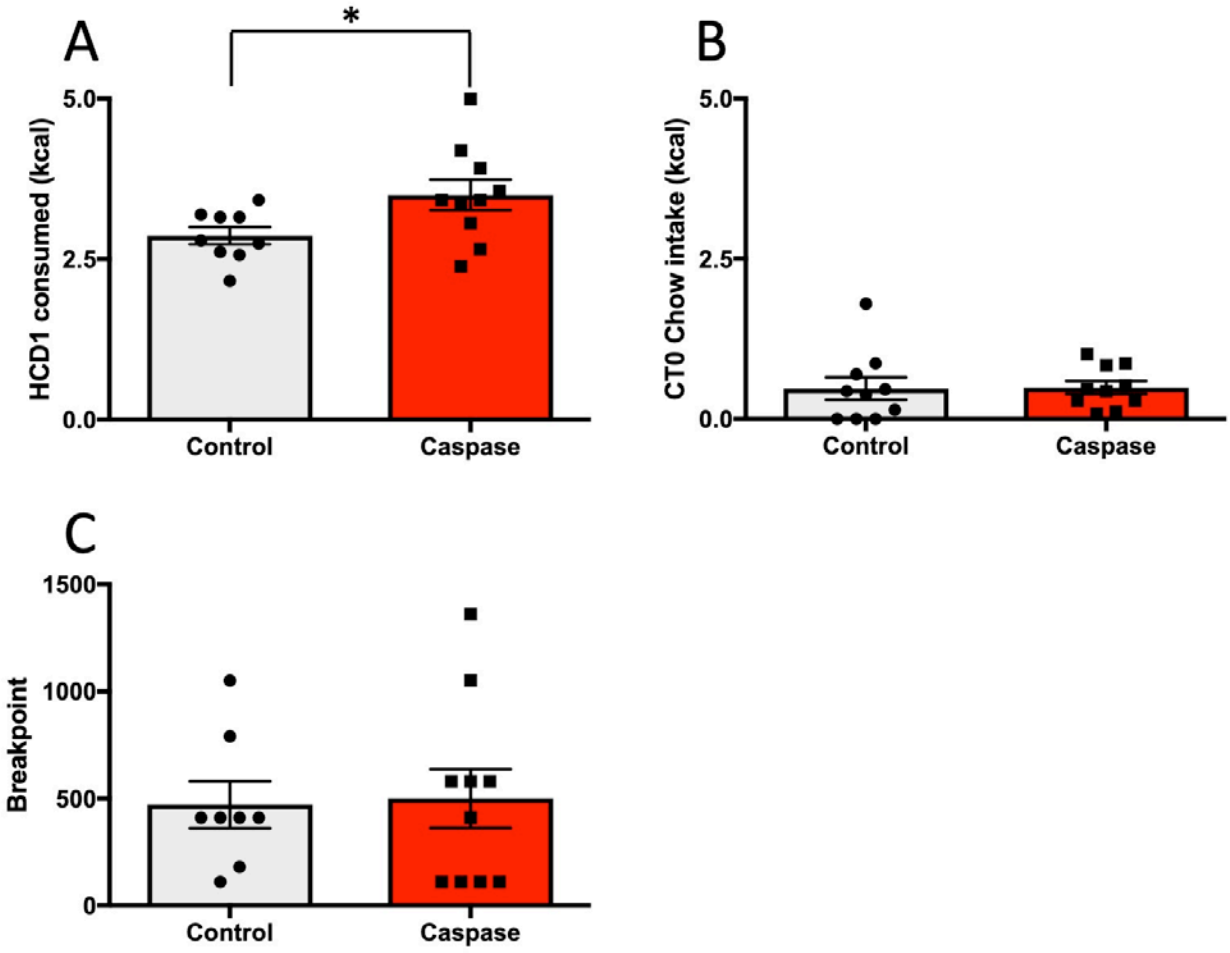

Figure 2. Selective deletion of mPFC VIP neurons increases palatable food consumption while sparing standard chow intake and effort to obtain palatable food reward. (A) Deletion of VIP neurons in the PL and IL results in an increase in HCD1 intake over 30 minutes (Control=2.87± 0.132g Caspase=3.497± 0.237g, p=0.0375). (B) No change in chow intake was observed when animals were retested using the same paradigm (Control=0.4785± 0.175g, Caspase=0.493± 0.101, p=0.94g). (C) No change in operant responding for palatable food reward, as measured by breakpoint, were detected (Control=471.3± 109.1 nosepokes, Caspase=500± 136.5 nosepokes, p=0.3883).

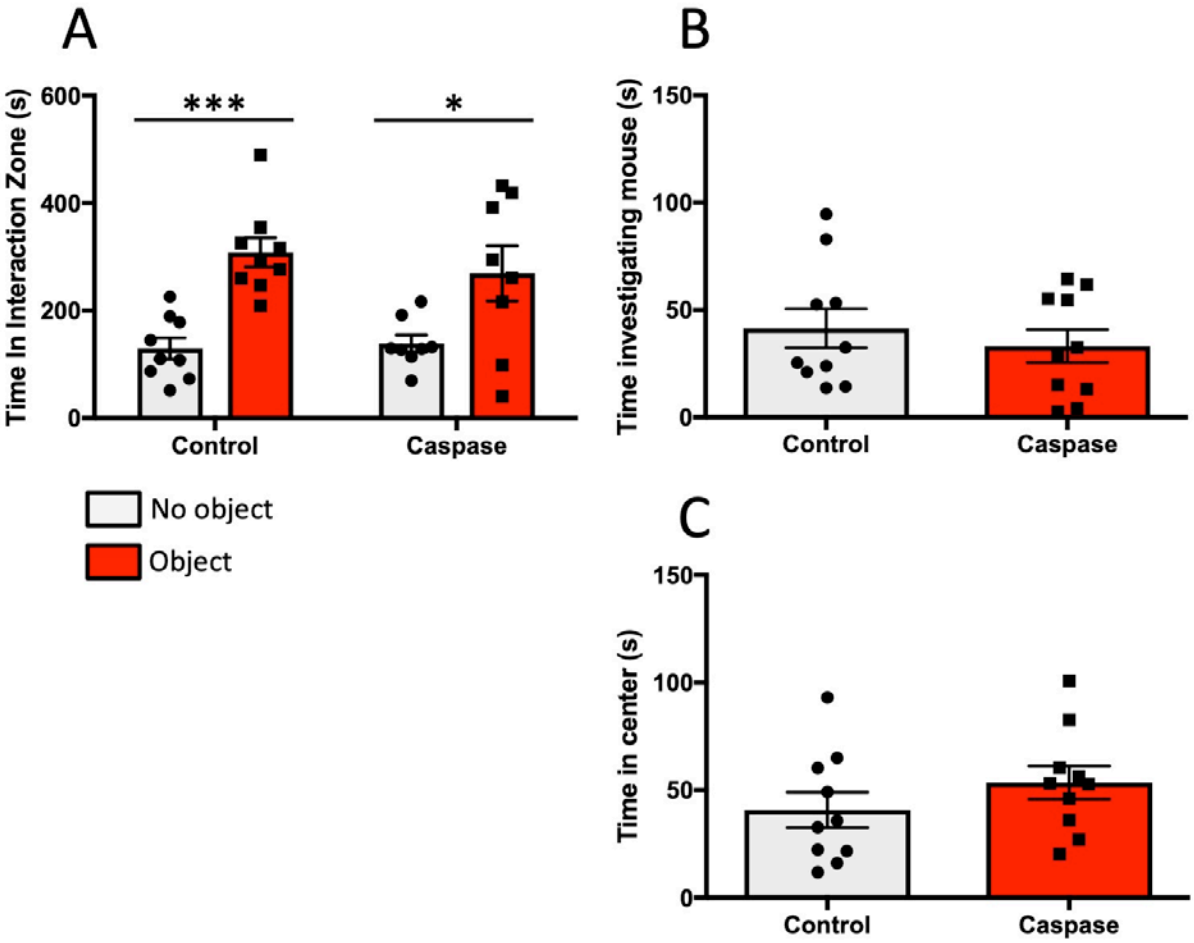

Figure 3. Deletion of mPFC VIP neurons did not affect social interaction, novel object investigation, or locomotion in an open field. (A) Both controls and mice treated with AAV-caspase spent significantly more time in an interaction zone in an open field when a novel object was present (Control without object=129.8± 19.47 seconds, Control with object= 308.4±26.93 seconds, $p<0.0001$, Caspase without object=138.8 ±16.14 seconds, Caspase with object=269.3 ±51.54 seconds, $p=0.0299$). Deletion of mPFC VIP neurons did not affect social interaction behavior (B, Control=41.45± 9.057 seconds interacting with novel mouse, Caspase=33.21± 7.663 seconds, $p=0.4958$), or time spent in the center of an open field (C, Control=40.79± 8.173 seconds, Caspase=53.53± 7.674 seconds, $p=0.2707$).

Chapter 4: The prefrontal cortical projection to the nucleus accumbens is required for novel object and novel environment driven investigatory behavior in the mouse

This chapter is a re-print of the eNeuro article (Newmyer et al., 2019C, in re-submission).

4.1 Abstract

The detection and evaluation of novel stimuli determine the drive to investigate both drug and natural reward. While both the prefrontal cortex (PFC) and the nucleus accumbens (Acb) have been implicated in controlling novelty-dependent investigatory behavior, the necessity of the direct projection between these structures in the regulation of novel social- and object-driven investigatory behavior is unknown. Through the genetic lesioning of the PFC-Acb pathway, we discovered that loss of this projection produces a large increase in both novel object investigatory behavior and locomotion driven by exposure to a novel environment, while no change was observed in either social investigatory behavior or binge-like consumption of a palatable food source. These data significantly increase our understanding of how PFC-Acb projections regulate the drive to investigate a specific subset of novel stimuli.

Significance Statement

Reward novelty influences the pursuit of both drug and food reward and involves both the prefrontal cortex (PFC) and nucleus accumbens (Acb), but the necessity of projections between these two regions in novelty seeking behavior has not been extensively investigated. In this study, we used genetic lesioning in mice to demonstrate that deleting projections from the PFC to the Acb increased time spent investigating a novel object or exploring a novel environment, while time spent investigating a novel mouse was unaffected. Thus, our results demonstrate that PFC-Acb projections are selectively required for some novelty-associated exploratory behaviors while sparing others.

4.2 Introduction

The desire to pursue both drug and natural reward is significantly influenced by reward novelty. While a high correlation between sensation seeking and cocaine use has been previously documented in humans (Ersche et al., 2013), rats with high novelty preference show elevated motivation to work for cocaine and are predisposed to developing compulsive cocaine intake (Belin et al., 2011). Likewise, alteration in dopamine signaling as a result of polymorphisms in Drd4 type dopamine receptors is associated with high levels of novelty seeking and alcohol consumption (Laucht et al., 2007). Drd4 null mice show a similar phenotype, exhibiting higher alcohol consumption and elevated exploratory behavior in a novel environment (Thanos et al., 2015). With respect to natural reward, a similar positive correlation between sensation seeking and binge feeding is suggested, as people that have diseases of disordered feeding and exhibit binge feeding often show elevations in novelty seeking behavior (Rotella et al., 2018).

Both the frontal cortex and striatum have been implicated in driving the exploration of novel objects while also supporting aspects of novel social investigatory behavior, suggesting that projections between these structures may be required for the appropriate regulation of novelty seeking behavior. Deletion of neurons from the medial prefrontal cortex (mPFC) in rats significantly enhanced novelty driven locomotion (Dalley et al., 1999), while stimulation of the mPFC was shown to decrease social investigation in mice (Yizhar et al., 2011, Murugan et al., 2017) with ensembles of neurons within this brain region being either activated or inhibited as a result of social exploration (Liang et al., 2018). Within the ventral striatum, altered dopamine and peptidergic neurotransmission has been suggested to lead to a change in novelty seeking behavior. In rats, dopamine efflux is increased selectively in the nucleus accumbens (Acb) shell in response to the investigation of a novel environment (Rebec et al., 1997), while changes in

both prodynorphin expression (Egervari et al., 2016) and oxytocin signaling (Smith et al., 2017) within the Acb have also been shown to regulate novelty-driven investigatory behavior.

Consequently, it is quite likely that the direct connection between the frontal cortex and Acb, two brain areas that exert significant control over novelty seeking behavior, is crucial to driving the appropriate pursuit of rewarding stimuli. Although a recent report demonstrated that the projection from the prelimbic subdivision of the prefrontal cortex to the Acb is required for spatially-dependent social investigation (Murugan et al., 2017), it is unclear whether novel environment- or object driven investigatory behavior requires a functional projection from the mPFC to Acb.

To address this question, we genetically lesioned mPFC-Acb projections and investigated whether loss of this pathway affected novel social-, novel object-, and novel environment-driven investigatory behavior. In agreement with previous data (Yizhar et al., 2011, Smith et al., 2017), we found that the deletion had no effect on social investigatory behavior. However, we also observed a large increase in novel object investigatory behavior in addition to an increase in novel environment-stimulated locomotion.

4.3 Methods

Experimental Animals: For all behavioral experiments, nine-week-old male C57BL/6J mice were purchased from Jackson Laboratory (Bar Harbor, ME, USA). Mice were housed on a 12h light:12h dark cycle (lights off at 21:00) with ad libitum access to food and standard chow (Teklad #2013, 4% fat, 17% protein, 48% carbohydrate (no sucrose), 2.9kcal/g). Prior to experimentation the animals were separated and subsequently individually housed for at least another week. All testing was performed during the light portion of the light:dark cycle. For viral targeting validation experiments, nine-week old male Ai14 mice were purchased from Jackson Laboratory (Stock 007914). All experiments were performed in accordance with the Association

for Assessment of Laboratory Animal Care policies and approved by the University Animal Care and Use Committee. For all experiments, C57bl/6j animals were randomly assigned to receive either control or caspase expressing viral injections. Seven control and 11 caspase-treated animals were used for analysis. Six animals were used for the determination of caspase deletion efficiency.

Adeno-associated Viral Vectors and Stereotaxic Viral Injections: Projections from the mPFC to Acb were targeted using a combinatorial strategy where an adeno-associated virus encoding a Cre recombinase-dependent caspase 3 protein (AAV5-flex-taCasP3-TEV (Yang et al., 2013)), sourced from UNC Gene Therapy Core Facility) was bilaterally injected into the mPFC (from Bregma, +2.05 mm anterior, ±0.35 mm lateral, and −1.50 mm ventral of dura, 100nl of virus per side) and a canine adenovirus expressing Cre recombinase (CAV2-Cre, synthesis previously described in (Carter et al., 2013)) was injected into the Acb (from Bregma, ±1mm anterior, 1.0mm lateral, -4.0mm ventral of dura, 300 nl of virus per side). Animals were allotted 4 weeks to recover from surgery before behavioral experiments were conducted. Control mice were injected with Cav-Cre in the Acb and AAV5-CamKII-mCherry into the prefrontal cortex, using the same volumes and identical stereotaxic coordinates.

The behavioral experiments described below are listed in their order of performance:

Open Field: The Open Field assay was conducted as previously described (Warthen et al., 2016). The lights in the behavioral room were dimmed and mice were allowed to acclimate for at least 1 h prior to testing. Mice were placed into the open field chamber and allowed to explore for 5 min while movement was recorded using EthoVision XT tracking Software (Noldus, Leesburg, VA, USA). The open field chamber was cleaned between each mouse with Minncare disinfectant to remove residual odors. During testing, the lights in the room remained dimmed. All mice underwent this experiment prior to any other experiments in this open field arena, so

that arena novelty did not exist as a confounding variable during social interaction and novel object assays.

Novel Object Interaction: The novel object interaction assay was also performed in our open field chamber, described above. Prior to the novel object test, all mice were brought to the behavior room and allowed to acclimate for at least 1 h. In brief, mice were placed in the open field area for an initial 10 min period in the absence of a novel object. As this assay was performed following open field testing in the same arena, we determined the distance travelled during the 10 min period and reported this as measure of locomotor activity in a familiar environment. Following this initial 10 min period, a novel piece of copper piping was introduced to the arena. Exploration of the piping, placed in the center of the arena, was recorded using Ethovision for 10 min.

Novel Social Interaction: The Social Interaction task was performed in our open field chamber, as previously described (Golden et al., 2011). Prior to the social interaction test, all mice were brought to the behavior room and allowed to acclimate for at least 1 h. In brief, the chamber was prepared with an empty restrainer in the interaction zone (IZ), against the wall. The test mouse was placed in the chamber adjacent to the wall opposite the restrainer (as in the open field assay), and allowed to explore for 150 s. The test mouse was then removed to the home cage for 30 s, while the empty restrainer was replaced with a new, clean restrainer. A novel mouse (129/SJL) was placed in the new restrainer, and the test mouse was returned to the chamber and allowed to explore for 150 s. Behavior and motion were recorded using Ethovision. The chamber was cleaned between each mouse with Minncare disinfectant to remove residual odors.

Binge Feeding Assay: The binge feeding assay was conducted in the home cage and home housing room of the mouse. Measurement of palatable food intake was performed as previously

described (Gaykema et al., 2014). On the night before testing, mice received a small (<0.1 g) sample of HCD (Teklad TD.88137, 21% fat, 17.3% protein, 48.5% carbohydrates, 4.5kcal/g) in order to reduce aversion. At CT0 mice were challenged with ~3 g of pre-weighed HCD and allowed to consume. Food intake was quantified at 15, 30 and 60 minutes.

Confirmation of cell- and site-specific deletion: Ai14 mice have a loxP-flanked Neomycin encoding cassette preventing transcription of a CAG promotor-driven red fluorescent reporter, tdTomato, inserted into the Gt(ROSA)26Sor locus; thus, tdTomato is only expressed in the presence of Cre Recombinase. Cav2-Cre was injected bilaterally into the Acb as described above. Additionally, into the right hemisphere of the mPFC, AAV5-flex-taCasP3-TEV was injected, while Cre-dependent GFP reporter expressing virus AAV5-CAG-Flex-GFPsm_myc-WPRE-SV40 was injected into the left hemisphere of the mPFC.

Brain Tissue Preparation and Immunohistochemistry: Immunohistochemistry was performed as previously described (Gaykema et al., 2014). Mice were sacrificed by transcardial perfusion. After anesthesia, mice were briefly flushed with buffered saline, followed by perfusion with 4% paraformaldehyde in 0.1 M phosphate buffer. Brains were dissected and sectioned at 40 μm on a Vibratome. For fluorescent immunohistochemistry, sections were incubated in anti-GFP (Aves Labs catalog GFP-1020, 1:2000) for 24h, followed by Alexa Fluor 488-conjugated goat anti-chicken (Jackson ImmunoResearch; 1:1000) overnight in a light-protected container. Sections from each were then mounted in sequential order, air-dried, and coverslipped in Vectashield hard-set mounting medium with DAPI (Vector Labs). During the entire process, the slides were protected from light exposure.

Statistics: All data were graphed and analyzed using Graphpad Prism (ver.6) and are presented as Mean+/-SEM. Unpaired t-tests were used to compare groups in Figure 2A -D and F while a repeated measures 2-way ANOVA was used to analyze data in Figure 2E.

4.4 Results

4.4.1 Deletion of mPFC-Acb projection neurons

To determine the requirement of the mPFC-Acb projection in the regulation of novel object and novel social interaction, we injected a CAV2 virus expressing Cre recombinase into the rostral Acb and a Cre recombinase dependent, caspase-expressing virus into the infralimbic and prelimbic cortices, two subdivisions comprising the mPFC. To determine the efficiency of neuron deletion using this technique, we examined the percentage of mPFC-Acb projecting neurons ablated unilaterally compared to the contralateral, control virus-injected side. We determined that greater than 85% of all neurons expressing Cre recombinase and projecting from the mPFC to the Nac were deleted (Figure 1A and B, 85.96% ±5.3) when the number of tdTomato reporter-expressing neurons were compared between control and caspase-injected hemispheres. No significant difference in DAPI expression between hemispheres suggests that the deletion was selective for the Cre-expressing population of neurons (Figure 1D). When we investigated the location of the neurons within the mPFC that were targeted, cells in both the prelimbic and infralimbic cortices (Figure 1C and D) expressed GFP reporter following AAV-smGFP injection into both of these regions of the mPFC, in addition to Cav-Cre injection into both the shell and core of the Acb.

4.4.2 mPFC-NAc neuronal ablation increases interest in novel objects while sparing changes in social novelty behavior

To determine the necessity of mPFC-Acb projections in behaviors associated with novelty, we observed differences between caspase-injected mice and their control counterparts in interaction time spent with a novel object or a novel mouse. We found that selective mPFC-Acb neuronal ablation was associated with increased time spent investigating a novel object (Control 146.7±28.2 s vs Caspase 256.1±9.738 s time spent in center with novel object present, $p=0.0005$, Figure 2A, Table 1A). In addition, we observed that novel environment-driven

exploratory behavior was also increased (Control 4.61±0.3548 m/s vs Caspase 6.029±0.3016 m/s Figure 2B, Table 1B, p=0.0061). When re-tested in the same environment, control mice and mice with the selective loss of mPFC-Acb projections exhibited identical levels of locomotion (Control 0.3859±0.287 m/s vs. Caspase 0.4223±0.0313 m/s, p=0.436 Figure 2C, Table 1C).

To further test the selectivity of the mPFC-Acb pathway in the control of novel object- and environmentally-driven exploratory behavior, we investigated whether pathway deletion affected novel social-driven interaction. While stimulation of this pathway has been shown to affect social interaction behavior (Yizhar et al., 2011, Murugan et al., 2017), neuronal silencing of the projection failed to alter interaction time between the test and target novel mouse (Murugan et al., 2017). In agreement with this data, deletion of the mPFC-Acb projection failed to affect novelty-driven social investigatory behavior (Control 64.90±9.59 s vs Caspase 77.32±6.55 s, p=0.282 Figure 2D, Table 1D). Taken together, these data suggest that social- and novel object interaction may require signaling through different mPFC projection neurons.

4.4.3 mPFC-NAc neuronal ablation does not alter binge-like food intake

Our data support the premise that mPFC-Acb projections can affect the drive to interact with a select subset of rewarding stimuli in the absence of an effect on novelty-driven social interaction. We subsequently hypothesized that, given the ability of both the Acb and mPFC to regulate food reward seeking and ingestion, that deletion of the mPFC-Acb pathway may affect other naturally rewarding behavior, specifically palatable food consumption.

We allowed sated mice free access to highly palatable high-calorie diet (HCD) and quantified food intake at 15, 30 and 60 min. Interestingly, unlike the effect on novel object or environment interaction, mPFC-Acb ablation did not affect HCD consumption at any time point (Repeated Measures ANOVA, Effect of Treatment $F_{1,9}=1.981$, $p=0.1929$, Effect of Time $F_{2,18}=75.73$,

p<0.0.0001, Figure 2E, Table 1E), further demonstrating the selectivity of the projection in regulating interaction with rewarding stimuli.

4.4.4 mPFC-NAc neuronal ablation does not alter anxiety-like behavior

Finally, it is possible that the enhanced environment- and object driven investigatory behavior may be due to an anxiolytic effect caused by mPFC-Acb pathway deletion (Vialou et al., 2014). To examine this possibility, we investigated behavior of mPFC-Acb projection-deleted mice in an open field arena. Unlike the effect on novel object exploration, neuron deletion did not affect time spent in the center of an open field (Time Spent in Center, Control 28.01±5.04 vs Caspase 35.02±3.698, p=0.266, Time Spent in Periphery, Control 271.9±5.04 vs Caspase 264.8±3.71, p=0.258, Figure 2F, Table 1F,G), suggesting that no change in anxiety levels of the animal occurred as a result of our manipulation.

4.5 Discussion

In the current report, we describe for the first time how the projection from the mPFC to the Acb is selectively required for the expression of appropriate novel object- and novel environment-driven exploratory behavior, while being dispensable for driving social interaction. Deletion of this projection was associated with an elevation in time spent investigating a novel object and distance travelled in a novel environment. No change in familiar environment investigatory behavior was observed. Similar to data reported previously, no change in time spent investigating a novel mouse was observed, while additionally no change in palatable food intake or anxiety-like behavior occurred. Our data therefore suggest that the PFC-Acb pathway is required in the mouse to regulate the drive to investigate a subset of rewarding stimuli.

Although we did not investigate whether our loss of function manipulation could produce an effect on novel object- or novel social investigatory behavior that was dependent upon the spatial localization of the rewarding stimuli, our work demonstrates the complexity of the PFC-

Acb projection with respect to the control of novelty driven investigatory behavior. Indeed, our data extends our understanding of how the mPFC-Acb pathway functions to regulate reward pursuit and is in agreement with studies published previously in both rats and mice. For example, our work suggests that loss of the mPFC-Acb projection could be primarily responsible for the observed effect of mPFC lesioning enhancing novelty seeking behavior (Dalley et al., 1999). Our data also agrees with the observation that either silencing mPFC neurons (Yizhar et al., 2011) or more selectively, their projections to the Acb (Liang et al., 2018), does not affect social investigatory behavior.

Finally, our reported lack of an effect on palatable food intake agrees with prior data generated in rats (Mena et al., 2013), further illustrating the selective role of the mPFC-Acb projection in the control of the drive to interact with rewarding stimuli.

While our data suggests that mPFC-Acb projections are required for the regulation of investigatory behavior in response to natural rewards, it is also likely that this pathway could affect the pursuit of drug reward as well. In addition our studies pave the way for future work that focuses on describing whether the projection neurons that mediate the effects on novelty described in this report can also encode spatial information during social interaction (Murugan et al., 2017). While prior data illustrated the role of the projection of the PL subdivision of the mPFC to the Acb in social spatial coding, our manipulations targeted both the PL and IL mPFC subdivisions (Figure 1B). Thus, it is possible that different subsets of mPFC projection neurons are required for social spatial coding and for controlling novel object and novel environment driven exploratory behavior.

In conclusion, our work expands our knowledge of how specific neuronal pathways are involved in the control of reward pursuit and suggests that the mPFC-Acb pathway is required to

regulate both spatial coding (based on prior reports (Murugan et al., 2017)) and the drive to interact with novel stimuli.

4.6 Figures

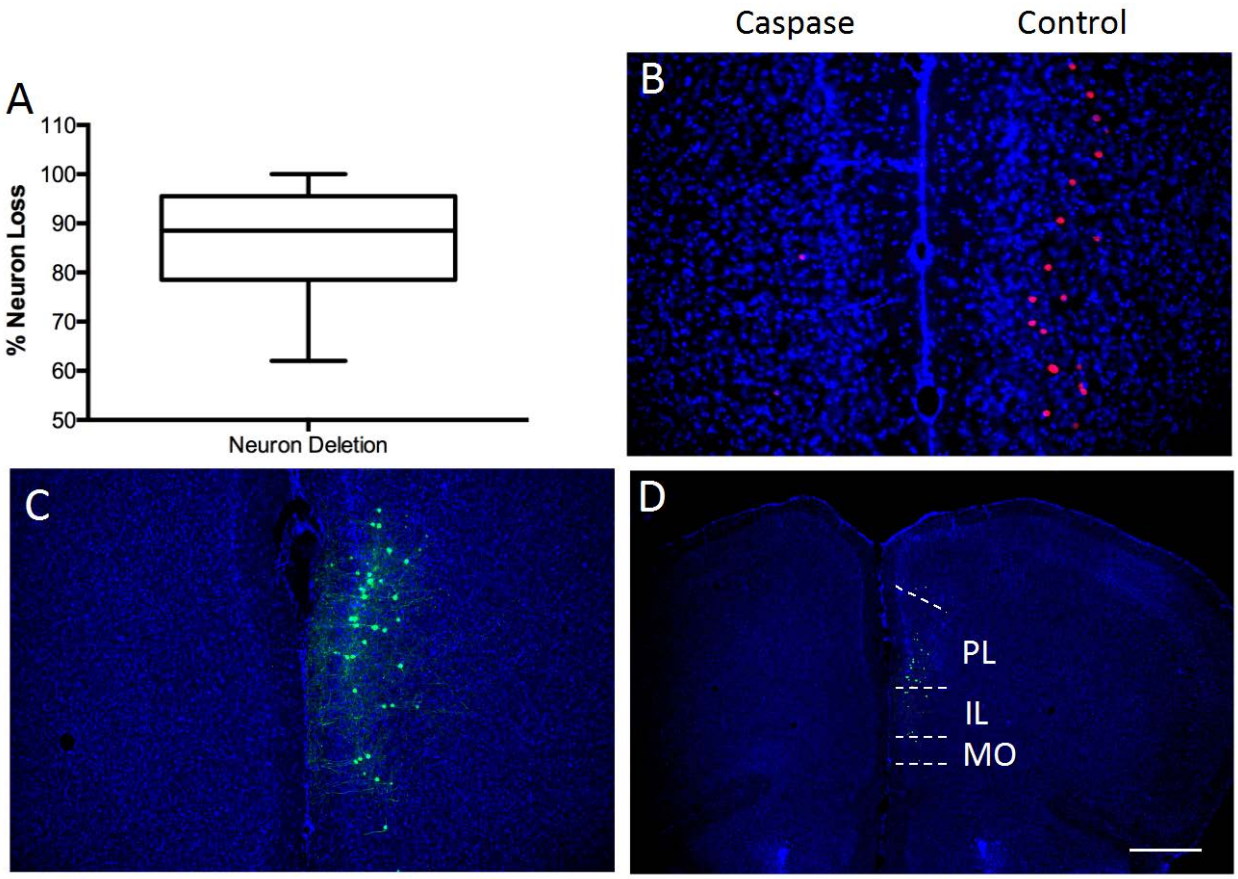
Caspase
Control
A
110
100
90
80
70
60
50
% Neuron Loss
Neuron Deletion
B
C
D
PL
IL
MO

Figure 1. Caspase expression in the mPFC produces neuronal deletion. AAV5-flex-taCasP3-TEV injection into the mPFC in conjunction with CAV2-Cre injection into the Acb resulted in an 85% cell loss (A) of cells expressing Cre recombinase and projecting to the Acb. B. While significant tdTomato reporter expression is observed in the mPFC in tdtTomato reporter animals injected with CAV2-Cre into the Acb and control AAV5-CAG-Flex-GFPsm_myc-WPRE-SV40 virus into the mPFC, minimal tdTomato expression is observed following caspase expression in the opposite hemisphere and CAV2-Cre expression in the Acb. C, D. When investigating the location of neurons within the mPFC that were targeted for deletion, injection of AAV5-CAG-Flex-GFPsm_myc-WPRE-SV40 into the mPFC and Cav2-Cre injection into the Acb showed neurons of both the PL and IL that would likely exhibit caspase expression and subsequent ablation. Scale Bar = B=50µm, C=100µm, D=250µm

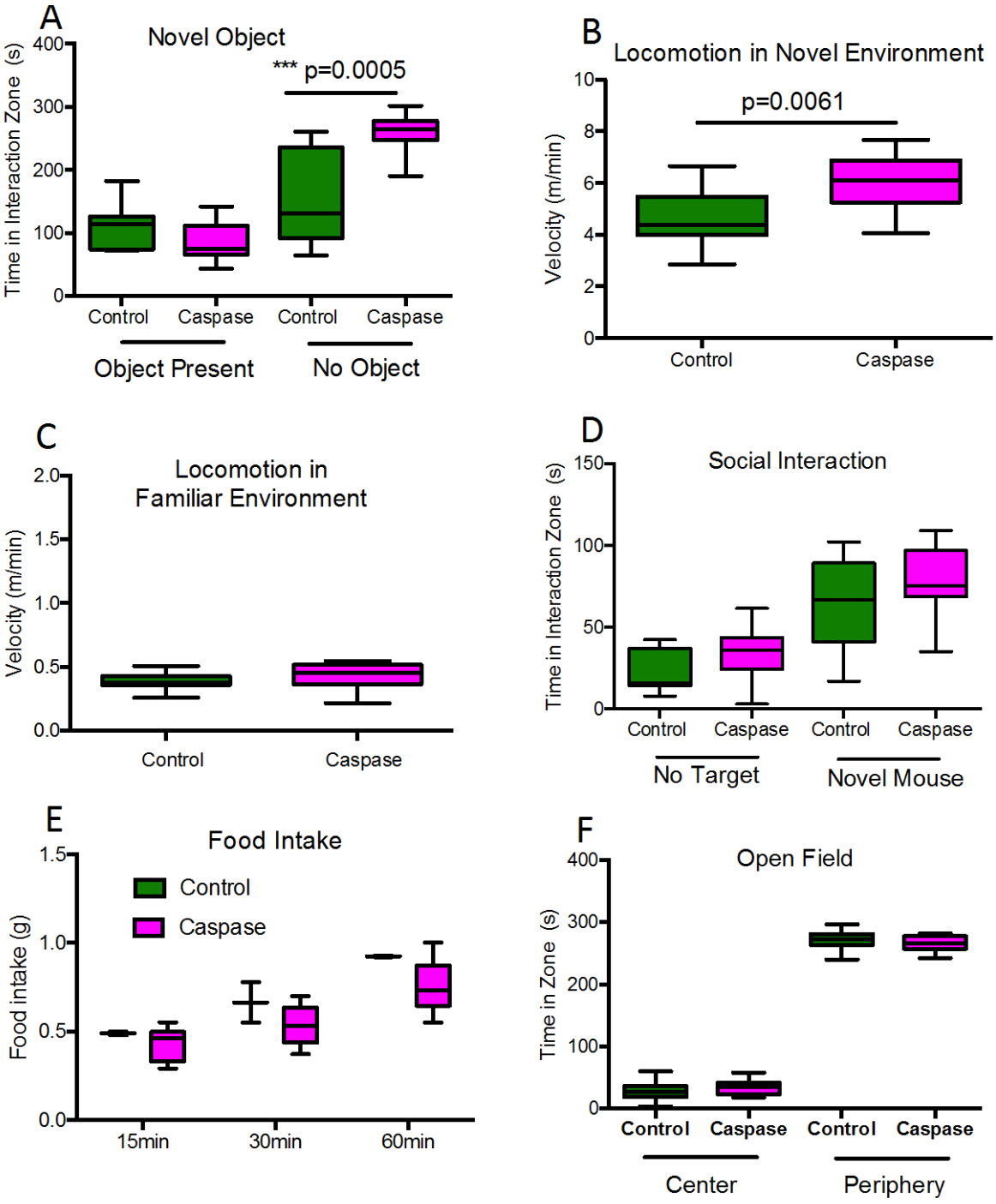
A
Novel Object
*** p=0.0005
Time in Interaction Zone (s)
400
300
200
100
0
Control
Caspase
Control
Caspase
Object Present
No Object
B
Locomotion in Novel Environment
p=0.0061
Velocity (m/min)
10
8
6
4
2
0
Control
Caspase
C
Locomotion in
Familiar Environment
Velocity (m/min)
2.0
1.5
1.0
0.5
0.0
Control
Caspase
D
Social Interaction
Time in Interaction Zone (s)
150
100
50
0
Control
Caspase
Control
Caspase
No Target
Novel Mouse
E
Food Intake
Control
Caspase
Food intake (g)
1.5
1.0
0.5
0.0
15min
30min
60min
F
Open Field
Time in Zone (s)
400
300
200
100
0
Control
Caspase
Control
Caspase
Center
Periphery

Figure 2. Deletion of mPFC-Acb projections produces a selective increase in novel object- and novel environment-driven exploratory behavior. A. Deletion of mPFC-Acb projections resulted in a significant increase in novel object-driven investigatory behavior when compared to control animals. B. In addition, mPFC-Acb pathway deletion significantly enhanced locomotion in a novel environment but failed to affect locomotion in a familiar environment (C). No effect of mPFC-Acb pathway deletion was observed on investigatory behavior directed towards a novel mouse (D) or on the consumption of a highly-valued high calorie diet (E). No change in anxiety-like behavior was observed when measured using an open field assay (F).

	Data Structure	Type of Test	Confidence Interval
A	Normal Distribution	Unpaired t-test	55.83 to 163.1
B	Normal Distribution	Unpaired t-test	-2.384 to -0.454
C	Normal Distribution	Unpaired t-test	-0.1332 to 0.06021
D	Normal Distribution	Unpaired t-test	-35.88 to 11.06
E	Normal Distribution	Repeated Measures 2-way ANOVA	15 min -0.2954 to 0.1776 30min -0.3649 to 0.1082 60min -0.4115 to 0.6152
F	Normal Distribution	Unpaired t-test	-19.79 to 5.769
G	Normal Distribution	Unpaired t-test	-5.650 to 19.93

Table 1. Statistical tests used in analyses, as referenced in Results.

Chapter 5: Genetic variation affects binge feeding behavior in female inbred mouse strains.

This chapter is a re-print of the Scientific Reports article (Newmyer et al., 2019B, in review).

5.1 Abstract

Identifying genetic variants that regulate binge eating (BE) is critical for understanding the factors that control this behavior and for the development of pharmacological treatment strategies. Although several studies have revealed specific genes capable of affecting BE behavior, less is known about how genetic variation modulates BE. Thus, through a paradigm that promoted binge-like food intake through intermittent access to HCD, we quantified food-intake in four inbred mouse strains: C57Bl/6J (B6), NOD/LtJ (NOD), 129S1/SvlmJ (S1), and A/J (AJ). We report that genetic variation likely influences the short-term regulation of both food intake driven by homeostatic demand and binge-like consumption of a palatable, high calorie diet (HCD): AJ mice consumed more of both standard chow and HCD than the other three strains tested when both diets were available ad libitum, while S1 mice consumed significantly less HCD than other strains during intermittent HCD access. Behavioral differences were also associated with differential changes in c-Fos immunohistochemistry in brain regions traditionally associated with appetite regulation. Our results identify 129S1/SvlmJ as a strain that exhibits low levels of binge feeding behavior and highlights a potential role for this strain in the investigation of the influence of genetic variation in the control of binge feeding.

5.2 Introduction

Binge eating (BE) is characterized as compulsive and unrestrained consumption of a large amount of food, typically highly palatable and calorically dense, within a brief time period (Wolfe et al., 2018). While Binge Eating Disorder is recognized as a psychiatric condition in its

own right, BE is also often observed in diseases of disordered feeding such as bulimia (Donnelly et al., 2018, Rotella et al., 2018) and in subsets of patients with obesity (Lavagnino et al., 2016, Hsu et al., 2002). Identifying genetic variants that regulate BE is critical to both understanding the mechanisms driving this behavior and for the development of pharmacological strategies to combat this condition.

Several gene deletion studies in mice have elucidated specific genes capable of affecting BE behavior: heterozygous cytoplasmic FMR1-interacting protein 2 knockout reduces binge eating of palatable food but not chow consumption in C57BL/6NJ mice (Kirkpatrick et al., 2017), while growth-hormone secretagogue receptor 1A (GHSR) knockout decreased intermittent high fat diet intake in CD-1 mice (King et al., 2016). Although these and other studies utilizing genetic mouse models have revealed how select factors influence BE, considerably less is known pertaining to what extent natural genetic variation can affect BE behavior. Even though differences in binge food intake between C57bl/6J and N lines (Kirkpatrick et al., 2017), in addition to DBA mice (Babbs et al., 2018), have been described, these mouse populations all exhibit high levels of binge food intake. No data describing a mouse strain that shows reduced binge feeding, and may therefore possess genetic variants that act to reduce binge food intake, has been reported.

Thus, using a paradigm that involved allowing mice intermittent access to a palatable, high-calorie diet (HCD) (Czyzyk et al., 2010), female mice from four inbred lines that form part of the Collaborative Cross population (Churchill et al., 2004) (C57Bl/6J (B6), NOD/LtJ (NOD), 129S1/SvlmJ (S1), and A/J (AJ)) were tested for BE behavior. When given ad libitum access to either chow or HCD in two separate experiments, little variation was observed between strains, with only AJ mice consuming significantly more of both diets relative to the other strains tested. Interestingly, during intermittent access to HCD, the four strains showed significantly more variation in binge food intake. NOD, S1, and AJ mice all consumed less HCD than the B6 mice

during a 3h HCD binge, while S1 mice ate significantly less HCD than NOD, and AJ mice. In addition, significant variation in neuronal activation was observed between strains in select brain nuclei shown to modulate feeding behavior, suggesting that gene expression differences within circuits involving these neuronal populations may control binge food intake.

5.3 Methods

Animals: Female mice that comprise the four founder strains of the Collaborative Cross (Churchill et al., 2004) population were obtained from The Jackson Laboratory. 8 week old C57Bl/6J (B6), NOD/LtJ (NOD), 129S1/SvlmJ (S1), and A/J (AJ) female mice were acclimated (single- housed) for 1 week upon arrival. 6-7 animals were used from each line in the food intake experiments and in the cFos analysis. Animal use was in accordance with guidelines approved by the University of Virginia Animal Care and Use Committee.

Measurement of Food Intake and Binge Feeding Behavior: Our food intake paradigm was performed as described by Czyzyk et al (2010), avoiding the use of animal stress or food restriction to produce the binge like intake of food. Briefly, intake of regular chow (Teklad #2014, 4% fat, 17% protein and 48% carbohydrate (no sucrose), 2.9 kcal/g) or HCD (Teklad TD.88137, 21% fat, 48% sucrose, 17% protein 4.5kcal/g) in the continual, ad libitum access groups was weighed daily following a 1- week acclimation period, then averaged over a 7 day period to obtain daily food intake values. In the intermittent food exposure group, mice initially received 48-hour continuous access to both chow and HCD. This initial access period was important to reduce neophobia and novelty for the HCD; parameters that would affect food intake. After 48hr, the HCD was removed for 5 days while the chow diet was still available ad libitum. HCD then was reintroduced in addition to chow, starting 2 hours following the onset of the dark cycle. Chow and HCD were separated by a divider that was part of the metal rack top of the animal's home cage. Position of the HCD and chow in the metal rack was varied to avoid position effects. Intake was monitored for 3 hours and then 24 hours, following initial HCD presentation. Data are

presented from the first binge feeding episode. Food intake was normalized to body weight, as described by Czyzyk et al (2010). Estrous cycle was not determined during testing.

c-Fos Immunohistochemistry: Animals that were naïve for intermittent or constant HCD exposure were presented with 0.1g of HCD and sacrificed 90 minutes following the onset of consumption. Importantly, all mice showed complete consumption of the small sample of HCD within 30 minutes of presentation. Mice were anesthetized i.p. with euthanasia solution (0.1 ml euthasol) and underwent trans-cardiac perfusion with buffered saline followed by fixative solution (4% paraformaldehyde in 0.1 M phosphate buffer, pH 7.4, containing 15% saturated picric acid). Each mouse was perfused with 50 ml fixative over a 5 min time period. Following perfusion, brains were dissected and post-fixed in the same fixative solution overnight, after which they were transferred to 0.1 M phosphate buffer. Brains were blocked coronally into three equally sized sections using a mouse brain mold. The brain parts were blotted, dried and arranged into standard cryomolds (Tissue Tek, #4557) with brain sections from four to six different mice in each cryomold. The molds were then filled with warmed 10% gelatin solution, allowed to cool to solidify, and post-fixed in 4% paraformaldehyde solution at 4◦C overnight. The blocks were then removed from molds, trimmed, glued on polystyrene dishes, and cut into coronal sections (40 µm thick) using a vibratome (Leica). The sections were collected serially in six-well tissue culture plates such that each well contained a representative series with every 6th section present (distance between adjacent sections in each well was therefore 240µm). Sections were stored at 4◦C in 0.1 M phosphate buffer containing 0.1% sodium azide as a preservative prior to immunohistochemical procedures. Sections were stained for c-Fos immunoreactivity using peroxidase staining(Gaykema et al., 2014, Gaykema et al., 2017). Phosphate-buffered saline (PBS) was used for all rinses, whereas all antibody solutions were made in PBS containing 0.5% Triton X-100, 0.1% sodium azide, and 2% normal goat serum. First, sections were pretreated with sodium borohydride (0.1%) in PBS for 20 min followed by

immersion into 0.3% hydrogen peroxide and 0.1% sodium azide in PBS (30 min) to quench endogenous peroxidase activity. Next, the sections were immersed in blocking solution containing 2% normal goat serum and Fab' fragments of goat anti-mouse IgG (1:1000) for 4 h at room temperature. Sections were then incubated in anti-c-Fos (Ab5, EMD Millipore, #PC38, 1:50,000) for 72 h followed by overnight incubation in biotinylated goat anti-rabbit IgG (Jackson ImmunoResearch, 1:1000) with antibodies diluted in PBS containing 0.5% Triton X-100 and 0.1% sodium azide. Subsequently the sections were immersed in avidin– biotin–peroxidase complex diluted in PBS with 0.1% Triton X-100 (ABC Elite kit, Vector; 1:1000, 4 h). Staining was completed using nickel-enhanced 3,3' -diaminobenzidine (DAB, 0.02%, nickelous ammonium sulfate 0.15%) in Tris–HCl (0.05 M, pH 7.6) yielding a black reaction product.

Microscopy: The sections were examined with an Olympus BX51 microscope using 10, 20, and 40× objectives and digital images were captured using a Magnafire digital camera (Optronics, Goleta, CA, USA) and stored images in TIFF format or loaded into NIH Image (version 1.61) for counting cell nuclei stained for c-Fos immunoreactivity.

Counting of Fos+ cells: Quantitation of c-Fos expression was done using NIH Image (v.1.61). Images were first processed by equalizing brightness (background subtraction), and were then thresholded for binary conversion. The number of particles (which corresponded to labeled nuclei) were then counted and recorded. For each brain area investigated, we chose two sections that showed well defined nuclei prominently present, and the number of c-Fos-labeled cells were counted bilaterally in each section and summated to yield the total number. We performed cell counts from nuclei centered on the following stereotaxic coordinates relative to mouse Bregma, as determined from the atlas of Paxinos and Franklin (13). Medial (MO), ventral (VO) orbitofrontal cortex +3.08mm, prelimbic (PL) and infralimbic (IL) cortex (combined to form the PFC cell counts) +1.8mm, granular gustatory (Gran) cortex +1.8mm, rostral accumbens (Acb) +1.54mm, lateral hypothalamus (LH), arcuate nucleus (Arc), paraventricular nucleus

(PVN) - 0.82mm, central nucleus of the amygdala (CeA) -1.22mm, medial parabrachial nucleus (PB) -2.92mm, nucleus of the solitary tract (NTS) -7.2mm.

Statistical Analysis: The amount of food intake consumed was analyzed using a one-way ANOVA with Tukey's multiple comparisons test in GraphPad Prism (ver.6). Correlations between the intake of chow, HCD intake during continual exposure and HCD intake during intermittent exposure were performed in Graphpad Prism (ver.6). Analysis of c-Fos expression differences between genotypes were analyzed using multiple ANOVAs followed by Benjamini-Hochberg p-value correction for multiple comparisons, performed in R (ver. 3.5.3). All grouped values in the bar graphs are expressed as means and standard error of the mean (SEM). Differences with $p < 0.05$ were considered statistically significant. Graphs were prepared in Graphpad Prism (ver.6).

5.4 Results

We investigated whether four inbred strains of female mice showed differences with respect to the ingestion of chow or HCD under constant or intermittent access conditions. While the S1, NOD and B6 strains all showed similar levels of chow and HCD consumption, AJ female mice showed an elevation in intake of both diets (Fig.1 A,B and D (ANOVA, $F_{3,21}=21.54$, $p<0.001$, Table 1), E (ANOVA $F_{3,21}=35.30$, $p<0.0001$, Table 1) when ad libitum fed. Interestingly, when mouse strains had intermittent access to HCD, the resulting binge-like, elevated intake of HCD did not occur to the same extent across all strains (Fig.1C). While all inbred strains showed an average intake during the 3 hour binge intake that was less than that of the B6 strain, the S1 animals consumed less than all other strains, showing a significant reduction in binge food intake (Fig.1G, ANOVA, $F_{3,25}=25.05$, $p<0.0001$ Table 1). In addition, the rank order with respect to the amount of ingested food varied between the 3 hour and 24 hour measurement periods (Fig. 1F and G). These data suggest that the NOD, AJ and particularly the S1 mouse lines show greater restraint with respect to acute binge food intake,

when compared to the B6 animals and also suggests that genetic variation between the strains significantly affects binge feeding behavior. We then wanted to determine whether the regulation of ad libitum food intake in these inbred strains correlated with intermittent food intake, as prior studies suggest that the neuronal mechanisms that regulate food intake differ between these two behavioral paradigms (Czyzyk et al., 2010). As expected, intake in the ad libitum fed chow and HCD groups was highly correlated (Fig. 2A, r =0.97, p=0.0298, suggesting that similar neuronal systems may be involved in determining intake based on the caloric content of food. However, neither HCD nor chow intake correlated with the food intake of intermittent HCD exposed animals, either at 3hr (Fig 2B r =-0.03, p=0.969, Fig. 2C r =0.19, p=0.806) or 24hr (Fig 2D r =0.3385, p=0.338, Fig. 2E r=0.235, p=0.235) time points. Thus, our work suggests that binge food intake and the regulation of food intake based on caloric value may be regulated by separate mechanisms that are affected by the genetic variation observed between the S1, NOD, B6 and AJ inbred mouse strains.

To begin to characterize whether neuronal activation within brain regions shown to regulate feeding is dependent upon strain genotype, we examined c-Fos expression following the ingestion of a small quantity (0.1g) of HCD in naïve animals. Several brain areas exhibited genotype-dependent expression of c-Fos. The lateral hypothalamus (ANOVA, $F_{3,24} =13.55$, $p=1.23\times10^{-4}$) , medial- (ANOVA, $F_{3,23} =14.46$, $p=1.23\times10^{-4}$) and ventral orbitofrontal cortices (ANOVA, $F_{3,23} =4.028$, $p=0.0379$), medial prefrontal cortex (ANOVA, $F_{3,25} =11.75$, $p=1.98\times10^{-4}$), ventral tegmental area (ANOVA, $F_{3,22} =3.992$, $p=0.0379$), and parabrachial nucleus (ANOVA, $F_{3,23} =6.856$, $p=0.00502$) all showed significant differences in c-Fos expression across genotype (Figure 3). However, several brain areas that have been demonstrated to regulate food intake exhibited no differences in c-Fos expression across the genotypes tested (Figure 3): the arcuate nucleus (ANOVA, $F_{3,25} =1.017$, $p=0.468$), nucleus accumbens (ANOVA, $F_{3,24} =2.978$, $p=0.07189$) central nucleus of the amygdala (ANOVA,

F3,25 =2.947, p=0.07189), granular cortex (ANOVA, F3,18 = 0.9769, p=0.468) and caudal nucleus of the solitary tract (ANOVA, F3,25 =0.3978, p=0.756). Differences in c-Fos expression can be readily observed in images presented from the S1, NOD, AJ and B6 strains, of sections from medial orbitofrontal cortex and parabrachial nucleus (Fig. 4 A and B). Little difference in expression can be seen across genotype within the arcuate nucleus (Fig 4. C).

5.5 Discussion

Our data suggest that genetic variation likely influences the regulation of excessive food intake over short periods of time. Minimal variation in food intake (either of chow or palatable diet) during constant, ad libitum access was observed between strains, with only the A/J strain showing increased consumption relative to other mice. However, the four strains tested showed markedly larger differences in levels of binge food intake of HCD, exhibiting a two-fold variation in HCD consumption when given intermittent access. Indeed, while chow- and HCD intake between mouse strains showed a high level of correlation, no correlation was observed between intermittent, binge-like intake and the levels of total food intake during ad libitum access conditions. In addition, these data also suggest that the differences in binge intake were not due simply to differences in perception of food palatability or nutrient concentration (based on the observed correlation between chow and HCD intake) but were a result of the behavioral reaction to intermittent feeding.

The identification of inbred mouse strains that show significant variation in binge food intake under an intermittent exposure paradigm will be extremely useful in the investigation of genetic variants that influence excessive reward-seeking behavior. While mouse strains such as DBA and C57Bl/6J exhibit high levels of binge food intake(8), our data describes how inbred lines, most notably the 129S1/SvlmJ line, exhibit significantly reduced binge food intake, relative to these other commonly used strains. Consequently, the description of mouse strains that show

both excessive and constrained binge feeding could significantly increase our ability to identify the genetic networks that drive aberrant food- and possibly drug intake behavior.

Interestingly, significant variation between 129 substrains and the C57Bl/6j strain have been reported in prior work investigating both reward seeking and reward potency. For example, food and cocaine reinforcement in addition to place preference for cocaine was reduced in 129X1/SvJ animals compared to C57bl/6J mice (Thomsen and Caine 2006, 2011). Morphine, however, was significantly more potent in producing analgesia in 129 substrains compared to C57Bl/6 mice (Mogil and Wilson, 1997). DBA animals, meanwhile, were shown to lack any sensitivity towards the rewarding effects of morphine unlike that observed with C57Bl/6j mice (Dockstader and van der Kooy, 2001). This variation in response to morphine is especially relevant, given that prior work has demonstrated the importance of the μ-opioid receptor in driving binge feeding behavior (Blasio et al., 2013, Mena et al., 2013). Our study therefore demonstrates that in addition to exhibiting significantly different responses to drugs of abuse, these strains also exhibit differences in binge-like consumption of natural rewards.

The diversity outbred (DO) (Churchill et al., 2012) and collaborative cross (CC) (Churchill et al., 2004) populations both include the founder strains investigated here, suggesting that these mouse populations should be extremely useful for the study of binge feeding genetics. In addition to the inbred strains, the DO and CC also include wild-derived founder animals. Although we attempted to investigate whether one of these wild derived strains, the Cast/EiJ line (Churchill et al., 2004), exhibits binge food intake, we found it impossible to measure consumption of the TD.88137 diet. Whether as a pellet or in a paste formulation, the Cast/J mice would disperse the food around their cage in small fragments, making measurement of intake imprecise. Future work will focus on investigating how the wild-derived and inbred strains tested in the current report differ with respect to binge food intake, using a modified binge food intake paradigm.

When we examined the brain regions activated following exposure to calorically dense food, significant differences in c-Fos expression were observed in several brain regions involved in food intake regulation based on palatability (Lindgren et al., 2018, Simon et al., 2016, Avena and Bocarsly, 2012). Significantly less of an effect on c-Fos expression was observed in brain regions shown to regulate food intake based on the metabolic requirement of the animal, similar to data reported previously (Bake et al., 2013). Although it is difficult to conclude that our observed c-Fos expression differences reflect changes in the activity of brain areas that drive observed strain-dependent differences in binge food intake, our work is highly suggestive of this possibility, as the rank order of c-Fos expression in many frontal cortical brain areas reflects a similar rank order in levels of HCD intake.

Both the prefrontal and orbitofrontal cortices, brain areas that showed significant differences in c-Fos expression between strains, have previously been shown to play important roles in driving binge feeding behavior. In rodents, μ-opioid receptor activation has been shown to be both necessary and sufficient (Blasio et al., 2013, Mena et al., 2013) in these brain areas to affect binge-like food intake. Optogenetic manipulation of projections from the frontal cortex to the amygdala, meanwhile, has revealed this subcortical projection to be both necessary and sufficient to regulate feeding behavior (Land et al., 2014). Additionally, changes in brain activity in medial prefrontal regions is often observed in fMRI studies in humans with altered food intake behavior. For example, reduced blood flow to fronto-striatal circuits is frequently seen in people exhibiting eating disorders, suggesting that alterations in these brain regions could drive changes in both feeding behavior and impulsive action (Donnelly et al., 2018, Oliva et al., 2019). Furthermore, people who show successful weight loss following the development of obesity demonstrate alterations in the activation of brain areas that regulate sensory processing, reward and impulsivity, when compared to overweight controls (Sweet et al., 2012).

In conclusion, our work demonstrates how genetic variation may directly or indirectly affect the activity of brain regions shown to regulate feeding behavior. We also suggest that the mouse strains tested in the current study could be utilized to map genetic variants that could contribute to the development of disordered feeding.

5.6 Figures and Tables

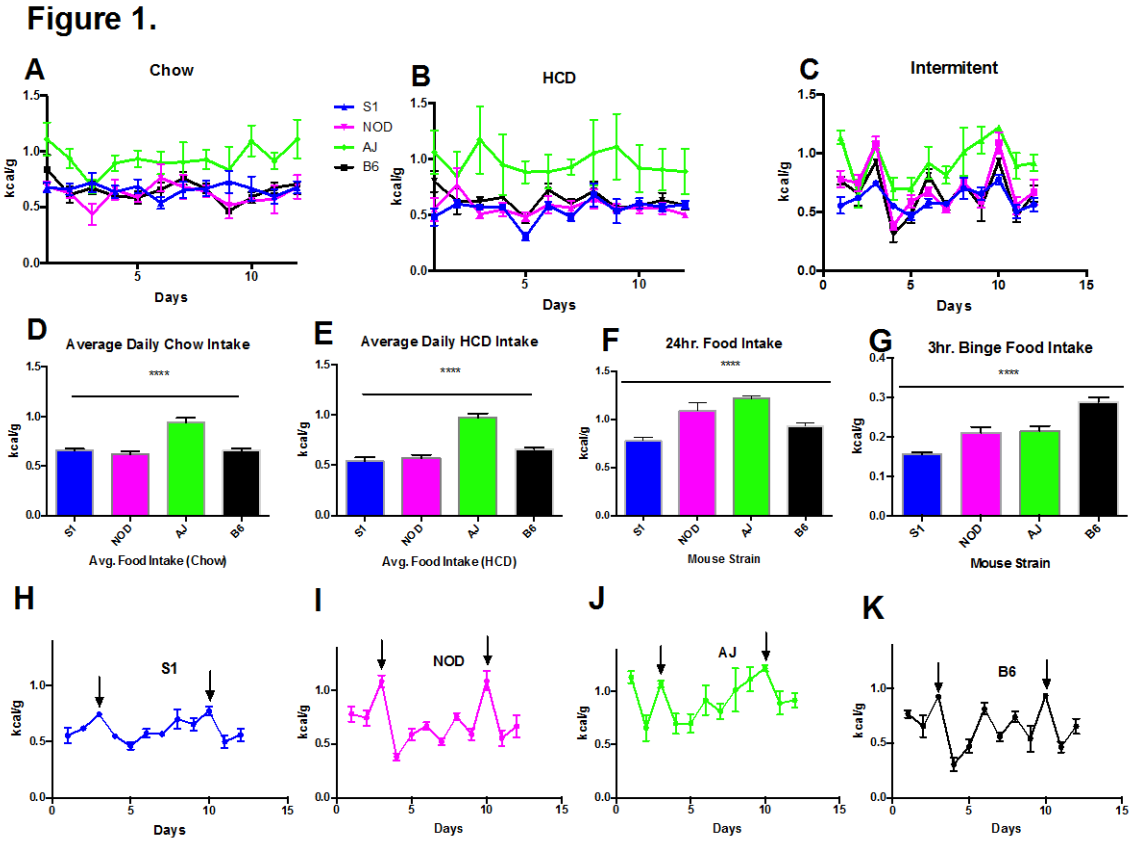

Figure 1. Daily food intake for mouse inbred strains consuming chow (A), HCD (B) and receiving intermittent access to HCD (C). Significant differences in Chow (D) and HCD (E) intake were observed between the AJ strain and the other mouse populations studied (ANOVA $P<0.0001$). Greater variation between strains was observed following binge feeding, observed at 24(F, ANOVA $p<0.0001$) and 3(G, ANOVA, $p<0.0001$) hr. Panels H-K are derived from panel C, demonstrating the timing of the binge feeding episodes (arrows). 6-7 animals from each genotype were used for each treatment

Figure 2.

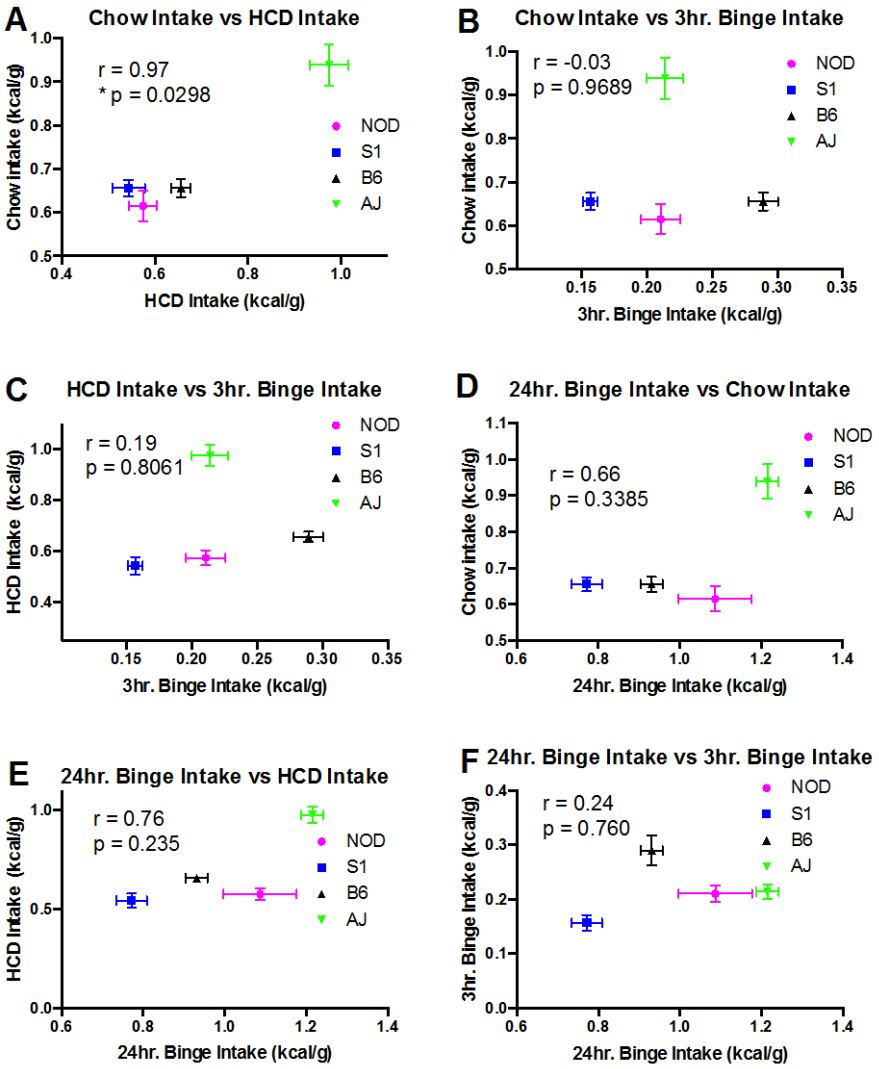

Figure 2. (A) Chow food intake and HCD diet intake show high levels of correlation across mouse strains (r=0.97, p=0.298) Binge food intake shows little correlation with chow intake (B,D) or with HCD intake (C,E). Acute versus chronic feeding in the intermittent exposure group also shows little correlation across mouse strains (F).

Figure 3.

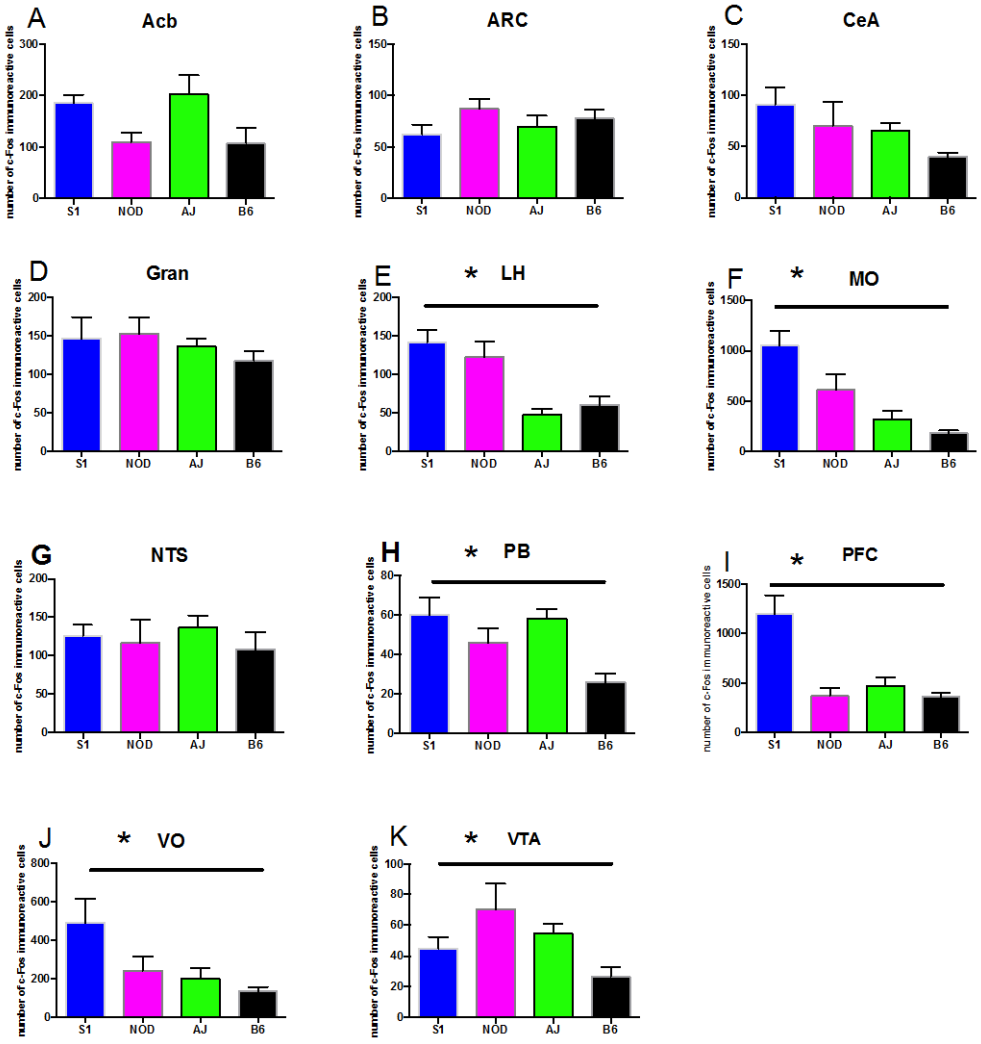

Figure 3. c-Fos expression does not show variation between mouse strains in select brain nuclei (A, Acb, B, Arc, C, CeA, D, Gran and G, NTS). C-Fos expression in the LH (E), MO (F), PB (H), PFC (I), VO (J), VTA (K) all exhibited genotype dependent differences (ANOVA, $p<0.05$, Benjamini-Hochberg p-value correction for multiple comparisons).

Figure 4.

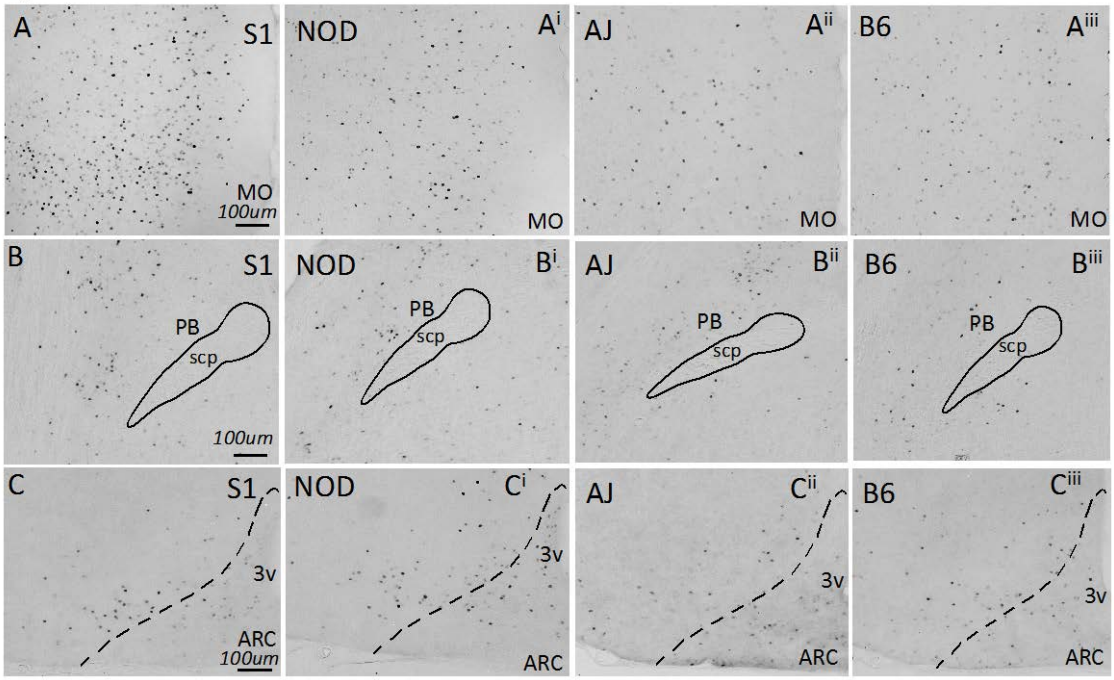

Figure 4. Increased cFos expression was observed in the MO (A) and PB (B) across mouse lines, while little change in cFos expression was observed in the Arc (C).

Figure 1D

ANOVA table	SS	DF	MS	F (DFn, DFd)	P value
Treatment (between columns)	0.4053	3	0.1351	F (3, 21) = 21.54	P < 0.0001
Residual (within columns)	0.1317	21	0.006271		
Total	0.537	24			

Tukey's multiple comparisons test	Mean Diff.	95% CI of diff.	Significant?	Summary
AJ vs. S1	0.283	0.1602 to 0.4058	Yes	****
AJ vs. NOD	0.3232	0.1958 to 0.4506	Yes	****
AJ vs. B6	0.2829	0.1555 to 0.4103	Yes	****
S1 vs. NOD	0.0402	-0.08260 to 0.1630	No	ns
S1 vs. B6	-0.0001	-0.1229 to 0.1227	No	ns
NOD vs. B6	-0.0403	-0.1677 to 0.08713	No	ns

Figure 1E

ANOVA table	SS	DF	MS	F (DFn, DFd)	P value
Treatment (between columns)	0.7181	3	0.2394	F (3, 21) = 35.30	P < 0.0001
Residual (within columns)	0.1424	21	0.006781		
Total	0.8605	24			

Tukey's multiple comparisons test	Mean Diff.	95% CI of diff.	Significant?	Summary
AJ vs. S1	0.4302	0.3025 to 0.5579	Yes	****
AJ vs. NOD	0.3989	0.2664 to 0.5314	Yes	****
AJ vs. B6	0.3187	0.1862 to 0.4512	Yes	****
S1 vs. NOD	-0.0313	-0.1590 to 0.09639	No	ns
S1 vs. B6	-0.1115	-0.2392 to 0.01619	No	ns
NOD vs. B6	-0.0802	-0.2127 to 0.05231	No	ns

Figure 1F

ANOVA table	SS	DF	MS	F (DFn, DFd)	P value
Treatment (between columns)	0.8706	3	0.2902	F (3, 26) = 18.71	P < 0.0001
Residual (within columns)	0.4032	26	0.01551		
Total	1.274	29			

Tukey's multiple comparisons test	Mean Diff.	95% CI of diff.	Significant?	Summary
S1 vs. NOD	-0.3152	-0.4997 to -0.1307	Yes	***
S1 vs. AJ	-0.4435	-0.6143 to -0.2727	Yes	****
S1 vs. B6	-0.1591	-0.3299 to 0.01172	No	ns
NOD vs. AJ	-0.1283	-0.3128 to 0.05622	No	ns
NOD vs. B6	0.1561	-0.02836 to 0.3406	No	ns
AJ vs. B6	0.2844	0.1136 to 0.4552	Yes	***

Figure 1G

ANOVA table	SS	DF	MS	F (DFn, DFd)	P value
Treatment (between columns)	0.07126	3	0.02375	F (3, 25) = 25.05	P < 0.0001
Residual (within columns)	0.0237	25	0.0009482		
Total	0.09496	28			

Tukey's multiple comparisons test	Mean Diff.	95% CI of diff.	Significant?	Summary
S1 vs. NOD	-0.05397	-0.09971 to -0.008228	Yes	*
S1 vs. AJ	-0.05724	-0.1011 to -0.01341	Yes	**
S1 vs. B6	-0.1327	-0.1750 to -0.09033	Yes	****
NOD vs. AJ	-0.003271	-0.05039 to 0.04385	No	ns
NOD vs. B6	-0.07871	-0.1245 to -0.03297	Yes	***
AJ vs. B6	-0.07544	-0.1193 to -0.03160	Yes	***

Table 1. Statistical table describing the multiple comparisons made in Figure 1 panels D-G

Chapter 6: Overview and Conclusions

This dissertation has focused on elucidating roles for specific circuitries within the mPFC in various appetitive behaviors as well as non-appetitive behaviors associated with higher cognitive processing. Our interpretations are based on behavioral experiments in mice following specific neural manipulations via microinjections of various viral constructs. Our work has demonstrated several behavioral roles for mPFC VIP neurons, in addition to probing the necessity of mPFC-Acb projections in the regulation of behaviors that we found to be modulated by VIP neurons. Lastly, we demonstrated that genetic variation can influence excessive binge eating of palatable food, possibly through alterations in frontal cortical function, while sparing normal chow intake.

6.1 mPFC VIP neurons regulate food intake when perceived food value is high

While considerable data exists implicating the mPFC in food intake regulation (reviewed in Section 1.25), no prior work focused on probing roles for specific interneuron populations in this behavior. This is despite that data from several studies, including some of our own work, suggested that mPFC VIP cells are well positioned to regulate feeding (reviewed in Section 1.37). Indeed, VIP cells are the most active of any mPFC interneuron subtype when mice are foraging for palatable food (Gaykema et al., 2014). Additionally, Blasio et al. (2014) demonstrated that antagonization of mPFC μ-opioid receptors decreased effort to obtain palatable food but not standard chow in rats, while 92% of interneurons that express these receptors co-express VIP (Taki et al., 2000). Thus, we first investigated appetitive roles for VIP neurons in both the IL and PL subdivisions of the mPFC (Chapter 2). This work revealed several novel roles for these neurons in behavior.

To our knowledge, our data represents the first description of any cortical interneuronal cell type that is capable of regulating food intake. By utilizing both SSFOs to stimulate- and AAV caspase-3 (Chapter 3) to delete mPFC VIP neurons, we demonstrated these neurons both

sufficient and necessary to regulate palatable food intake while sparing effects on standard chow intake in sated animals. In our SSFO studies, we examined this behavior further by selectively stimulating VIP neurons in both the IL and PL. We found that by increasing the value of standard chow through overnight fasting, we could affect standard chow intake after stimulating PL but not IL VIP cells. Additionally, we found that IL SSFO stimulation only decreased palatable food intake when the food source was novel. Thus we were able to conclude that VIP neurons in the IL and PL regulate food intake through separate cognitive pathways:

- In the IL, VIP neurons likely modulate the positive reward prediction signal associated with a novel food source, i.e. stimulating this subpopulation decreases the novelty-associated value of the food.
- In the PL, VIP neurons regulate food intake by modulation of the salience, value, or attention to food source. Only when the perceived value of the food source was high (palatable food, novel food, or standard chow presented after fasting) were PL VIP neurons able to modulate food intake. Further studies are required to elucidate which of these specific processes are engaged by our stimulation.

6.2 IL VIP neurons modulate the novelty value of non-appetitive natural stimuli

We next demonstrated that SSFO VIP stimulation in the IL but not the PL decreased interest in both a novel object and a novel conspecific mouse. These data reinforced our hypothesis based on our food intake findings that IL VIP neurons selectively modify interest in highly valued, novel stimuli, which can extend beyond food. Changes we observed in c-Fos immunohistochemistry in several brain regions support the absence of any observed effects on these behaviors after PL VIP stimulation; IL VIPergic activation resulted in significant increases in c-Fos expression in several areas implemented in regulation of reward valuation and novelty-

driven behavior, while PL VIPergic activation increased c-Fos expression in several hypothalamic areas associated with food intake regulation.

6.3 mPFC-Acb projections are required for novel object investigatory behavior

The Acb through reciprocal connections with the PFC is integral in goal directed behavior (Mannella et al., 2013) and this region has been implicated in the regulation of motivational salience broadly (reviewed in Section 1.24) in addition to novel investigatory behavior (Smith et al., 2017). While ours and other previous work has illustrated roles for the mPFC in these behaviors, it remained unclear as to whether direct functional projections between the PFC and Acb are required to modulate novelty-driven behaviors. Thus, through genetic lesioning we next investigated whether loss of the PFC-Acb pathway affected novel social-, novel object-, and novel environment-driven investigatory behavior (Chapter 4).

We found that lesioning this pathway increased interest in both a novel object and exploration of a novel environment, while no effect was observed on social investigatory behavior. Additionally, we observed no changes in palatable food consumption. With respect to novel object investigation, stimulating VIP neurons in the IL was associated with the opposite behavioral effect: disinhibition of IL PYR output via SSFO VIP stimulation resulted in decreased interest in a novel object (Section 2.3.4) and increased c-Fos immunoreactivity in the Acb (Section 2.3.6). While these data suggest increased indirect activation of PFC-Acb projections can negatively modulate this behavior, our stimulation paradigm also simultaneously increased activation of other mPFC projections to various cortical and subcortical nuclei. Thus, it is unlikely that the changes in behavior we observed in our SSFO study can be solely attributed to increased activation of one particular projection pathway. Indeed, Vertes (2004) conducted a mPFC projection labeling study in the rat and found that there were very few direct projections from the IL to the Acb, while projections from the PL to the Acb were dense. Therefore, it is more feasible that our IL SSFO stimulation perturbed multiple projection pathways within the

mPFC to affect several behaviors. One of these was likely local projections to the PL, which caused subsequent Acb activation.

This is further supported by data demonstrating that several of the behavioral changes observed after IL VIP stimulation were not affected by deleting PFC-Acb projections, including social investigatory behavior and palatable food consumption. These discrepancies may also be explained by the localization of neuronal deletion that occurred in our studies in Chapter 3; while SSFO activation was specifically targeted to either the IL or PL subdivisions of the mPFC, the entirety of the mPFC was targeted when genetically deleting PFC-Acb projections. Thus, future work will focus on deleting VIP neurons in the IL and PL exclusively and examining subsequent effects on these behaviors.

6.4 Genetic variation affects binge feeding behavior

The work presented in Chapters 2 through 4 focused on elucidating specific neuronal pathways within the mPFC capable of driving several cognitively complex behaviors, including excessive consumption of palatable food in a short period of time, i.e. binge eating. We published our SSFO work with the ultimate goal of our preclinical findings guiding pharmacological treatment strategies to target various diseases of disordered feeding, such as obesity. While researchers have identified several genes that contribute to obese phenotypes by utilizing single gene deletion studies in animal models, human obesity is multifaceted and often polygenic in nature (Hinney et al., 2010). Identifying an animal model with inherently low levels of binge feeding could provide insight into natural genetic variation that influences this complex behavior.

Thus, we investigated binge feeding behavior in four inbred lines of mice that serve as popular models in preclinical research: C57Bl/6J (B6), NOD/LtJ (NOD), 129S1/SvlmJ (S1), and A/J (AJ). We found that these lines showed significant variation in binge food intake and subsequent neuronal activation after consumption, as indexed by c-Fos expression. We

identified S1 mice as a strain that exhibits low levels of binge feeding behavior, highlighting a potential role for this strain in the future investigation of the specific mechanisms of genetic variation that may be responsible for this behavior.

6.5 Conclusions and Future Directions

VIP neurons in both the IL and the PL regulate hedonistic food intake, the intake of highly-valued food, while sparing effects on standard chow consumption driven by homeostatic demand. They accomplish this through separate cognitive pathways; IL VIP neurons likely modulate positive reward prediction signals through interactions with several brain regions associated with reward valuation and novelty exploration, while PL VIP neurons likely modulate the reward value or salience of food through interactions with brain regions traditionally associated with appetite regulation.

Direct communication between the mPFC and the Acb is required to modulate a subset of novel investigatory behaviors. It is likely that VIP neurons increase output of a subset of mPFC PYR cells that directly innervate the Acb, thus supporting the hypothesis that mPFC VIP neurons regulate numerous behaviors associated with motivational salience.

As discussed in detail above (Section 3.6, Figure 3), the IL and PL differ greatly with respect to the regions to which they project. While our work has illustrated novel behavioral roles for mPFC VIP neurons, the specific mPFC PYR projections required to observe changes in behavior after VIP stimulation remain to be elucidated. Thus, a logical next step in our work is to design studies to address this question. Once we have identified downstream projections associated with specific behavioral changes after SSFO stimulation, we can determine the necessity of these projections in the behaviors we observed through genetic deletion techniques similar to those utilized in Chapter 3.

While we have demonstrated changes in transcriptional activation after mPFC VIP stimulation, how selective activation of these neurons shapes neuronal activity in the mPFC, including how the magnitude of activation affects PYR firing synchronicity and output, has yet to be determined. Other groups have previously demonstrated that optogenetically manipulating mPFC interneurons can disrupt PYR cell firing patterns to affect behavior: inhibiting PFC PV cells in freely behaving mice disrupted local theta oscillations, thus synchronizing firing patterns of mPFC PYR cells projecting to the BLA (Courtin et al., 2014). In the future, our laboratory will conduct electrophysiological recordings in awake and behaving animals after SSFO mPFC VIP stimulation to investigate these questions further. Together, these approaches will allow for a greater expansion of our knowledge of how mPFC interneurons modulate PYR cells to regulate complex behaviors.

The findings presented in this dissertation collectively contribute to a greater understanding of frontocortical regulation of feeding, in addition to further illustrating the complexities of central regulation of food intake; a synergism of both homeostatic and hedonistic impulses in various brain regions, integrated within the mPFC and Acb, ultimately drive decision to eat. Our work additionally reveals details of the central processes that regulate motivational salience, a critical component in modulating goal-directed behavior.

References

Abbas AI, Sundiang MJM, Henoch B, Morton MP, Bolkan SS, Park AJ, Harris AZ, Kellendonk C, Gordon JA. (2018). Somatostatin interneurons facilitate hippocampal-prefrontal synchrony and prefrontal spatial encoding. *Neuron* **100**, 926-39.

Ahn S, Phillips AG. (1999). Dopaminergic correlates of sensory-specific satiety in the medial prefrontal cortex and nucleus accumbens of the rat. *J Neurosci* **19**, RC29.

Alitto HJ, and Dan Y. (2012). Cell-type-specific modulation of neocortical activity by basal forebrain input. *Front Syst Neurosci* **6**,79.

Anastasiades PG, Boada C, Carter AG. (2018). Cell-Type-Specific D1 Dopamine Receptor Modulation of Projection Neurons and Interneurons in the Prefrontal Cortex. *Cereb Cortex*, ePub ahead of print.

Avena NM, Bocarsly ME. (2012). Dysregulation of brain reward systems in eating disorders: neurochemical information from animal models of binge eating, bulimia nervosa, and anorexia nervosa. *Neuropharmacology* **63**, 87-96.

Babbs RK, Kelliher JC, Scotellaro JL, Luttik KP, Mulligan MK, Bryant CD. (2018). Genetic differences in the behavioral organization of binge eating, conditioned food reward, and compulsive-like eating in C57BL/6J and DBA/2J strains. *Physiol Behav* **197**, 51-66.

Bake T, Duncan JS, Morgan DG, Mercer JG. (2013). Arcuate nucleus homeostatic systems are not altered immediately prior to the scheduled consumption of large, binge-type meals of palatable solid or liquid diet in rats and Mice. *J Neuroendocrinol* **25**, 357-71.

Baldwin AE, Sadeghian K, Kelly AE. (2002). Appetitive instrumental learning requires coincident activation of NMDA and dopamine D1 receptors within the medial prefrontal cortex. *J Neurosci* **22**, 1063-71.

Barbas H. (1992). Architecture and cortical connections of the prefrontal cortex in the rhesus monkey. *Adv Neurol* **57**, 91-115.

Barbas H. (2000). Proceedings of the human cerebral cortex: from gene to structure and function connections underlying the synthesis of cognition, memory, and emotion in primate prefrontal cortices. *Brain Res Bull* **52**, 319-330.

Barbas H. (2010). Prefrontal Cortex: Structure and Anatomy. In: *Encyclopedia of Neuroscience.* Elsevier Ltd, 909-918.

Batista-Brito R, Vinck M, Ferguson KA, Chang J, Laubender D, Lur G, Mossner JM, Hernandez VG, Ramakrishnan C, Deisseroth K, Higley MJ, Cardin JA. (2017). Developmental dysfunction of VIP interneurons impairs cortical circuits. *Neuron* **95**, 884-895.

Beckmann JS, Marusich JA, Gipson CD, and Bardo MT. (2011). Novelty seeking, incentive salience and acquisition of cocaine self-administration in the rat. *Behav Brain Res* **216**, 159-65.

Belin D, Berson N, Balado E, Piazza PV, Deroche-Gamonet . (2011). High-novelty-preference rats are predisposed to compulsive cocaine self-administration. *Neuropsychopharmacology* **36**, 569-79.

Bergamini G, Cathomas F, Auer S, Sigrist H, Seifritz E, Patterson M, Gabriel C, Pryce CR. (2016). Mouse psychosocial stress reduces motivation and cognitive function in operant reward tests: A model for reward pathology with effects of agomelatine. *Eur Neuropsychopharmacol* **26**, 1448-64.

Bi LL, Wang J, Luo ZY, Chen SP, Geng F, Chen YH, et al. (2013). Enhanced excitability in the infralimbic cortex produces anxiety-like behaviors. *Neuropharmacology* **72**, 148-56.

Blasio A, Steardo L, Sabino V, Cottone P. (2014). Opioid system in the medial prefrontal cortex mediates binge-like eating. *Addict Biol* **19**, 652-662.

Bourgeois JP, Meas-Yeadid V, Lesourd AM, Faure P, Pons S, Maskos U, Changeux JP, Olivo-Marin JC, Granon S. (2012). Modulation of the mouse prefrontal cortex activation by neuronal nicotinic receptors during novelty exploration but not by exploration of a familiar environment. *Cereb Cortex* **22**,1007-15.

Brenhouse HC, Andersen SL. (2008). Delayed extinction and stronger reinstatement of cocaine conditioned place preference in adolescent rats, compared to adults. *Behavioral Neuroscience* **122**, 460-465.

Brown VJ, Bowman EM. (2002). Rodent models of prefrontal cortical function. *Trends in Neuroscience* **25**, 340-343.

Bryce CA, Floresco SB. (2016). Perturbations in Effort-Related DecisionMaking Driven by Acute Stress and Corticotropin-Releasing Factor. *Neuropsychopharmacology* **41**, 2147-59.

Burns SM, Wyss JM. (1985). The involvement of the anterior cingulate cortex in blood pressure control. *Brain Res* **340**, 71-7.

Buzsaki G, Wang X. (2012). Mechanisms of gamma oscillations. *Annu Rev Neurosci* **35**, 203-225.

Camus M, Halelamien N, Plassmann H, Shimojo S, O'Doherty J, Camerer C, Rangel A. (2009). Repetitive transcranial magnetic stimulation over the right dorsolateral prefrontal cortex

decreases valuations during food choices. *European Journal of Neuroscience* **30**, 1980-1988.

Caracheo BF, Emberly E, Hadizadeh S, Hyman JM, Seamans JK. (2013). Abrupt changes in the patterns and complexity of anterior cingulate cortex activity when food is introduced into an environment. *Front Neurosci* **7**, 74.

Cardin JA, Carlén M, Meletis K, et al. (2009). Driving fast-spiking cells induces gamma rhythm and controls sensory responses. *Nature* **459**, 663-7.

Carter ME, Soden ME, Zweifel LS, Palmiter RD. (2013). Genetic identification of a neural circuit that suppresses appetite. *Nature* **503**, 111-4.

Carus-Cadavieco M, Gorbati M, Ye L, Bender F, van der Velt S, Kosse C, Borgers C, Lee SY, Ramakrishnan C, Hu Y, Denisova N, Ramm F, Volitaki E, Brudakov D, Deisseroth K, Ponomarkeno A, Korotkova T. (2017). Gamma oscillations organize top-down signaling to hypothalamus and enable food seeking. *Nature* **542**, 232-236.

Chudasama Y, Passetti F, Rhodes SE, Lopian D, Desai A, Robbins TW. (2003). Dissociable aspects of performance on the 5-choice serial reaction time task following lesions of the dorsal anterior cingulate, infralimbic and orbitofrontal cortex in the rat: differential effects on selectivity, impulsivity and compulsivity. *Behav Brain Res* **146**, 105-19.

Churchill GA, Airey DC, Allayee H, Angel JM, Attie AD, Beatty J, et al. (2004). The Collaborative Cross, a community resource for the genetic analysis of complex traits. *Nat Genet* **36**, 1133-7.

Churchill GA, Gatti DM, Munger SC, Svenson KL. (2012). The Diversity Outbred mouse population. *Mamm Genome* **23**, 713-8.

Cone JJ, Scantlen MD, Histed MH, Maunsell JHR. (2019). Different inhibitory interneuron cell classes make distinct contributions to visual contrast perception. *eNeuro* **6**, .0337-18.2019.

Corwin RL, Wojnicki FH, Zimmer DJ, Babbs RK, McGrath LE, Olivos DR, Mietlicki-Baase EG, Hayes MR. (2016). Binge-type eating disrupts dopaminergic and GABAergic signaling in the prefrontal cortex and ventral tegmental area. *Obesity (Silver Spring)* **24**, 2118-25.

Costa VD, Tran VL, Turchi J, Averbeck BB. (2014). Dopamine modulates novelty seeking behavior during decision making. *Behav Neurosci* **128**, 556-566.

Courtin J, Chaudun F, Rozeske RR, Karalis N, Gonzalez-Campo C, Wurtz H, Abdi A, Baufreton J, Bienvenu TC, Herry C. (2014). Prefrontal parvalbumin interneurons shape neuronal activity to drive fear expression. *Nature* **505**, 92-6.

Cowin RL, Avena NM, Boggiano MM. (2011). Feeding and reward: perspective from three rat models of binge eating. *Physiol Behav* **104**, 87-97.

Czyzyk TA, Sahr AE, Statnick MA. (2010). A model of binge-like eating behavior in mice that does not require food deprivation or stress. *Obesity (Silver Spring)* **18**, 1710-7.

Dalley JW, Thomas KL, Howes SR, Tsai TH, Aparicio-Legarza MI, Reynolds GP, Everitt BJ, Robbins TW. (1999). Effects of excitotoxic lesions of the rat prefrontal cortex on CREB regulation and presynaptic markers of dopamine and amino acid function in the nucleus accumbens*. Eur J Neurosci* **11**, 1265-74.

Del Arco A, Mora F. (2008). Prefrontal cortex-nucleus accumbens interaction: *in vivo* modulation by dopamine and glutamate in the prefrontal cortex. *Pharma Biochem Behav* **90**, 226-235.

Di Pietro NC, Black YD, Kantak KM. (2006). Context-dependent prefrontal cortex regulation of cocaine self-administration and reinstatement behaviors in rats. *Eur J Neurosci* **24**, 3285-98.

Dockstader CL, van der Kooy D. (2001). Mouse strain differences in opiate reward learning are explained by differences in anxiety, not reward or learning. *J Neurosci* **21**, 9077-81.

Donnelly B, Touyz S, Hay P, Burton A, Russell J, Caterson I. (2018). Neuroimaging in bulimia nervosa and binge eating disorder: a systematic review. *J Eat Disord* **6**, 3.

Dulawa SC, Grandy DK, Low MJ, Paulus MP, Geyer MA. (1999). Dopamine D4 receptor-knock-out mice exhibit reduced exploration of novel stimuli. *J Neurosci* **19**, 9550-6.

Duzel E, Bunzeck N, Guitart-Masip M, Duzel S. (2010). Novelty-related motivation of anticipation and exploration by dopamine (NOMAD): implications for heathy aging. *Neuroscience and Biobehavioral Reviews* **34**, 660-669.

Egervari G, Jutras-Aswad D, Landry J, Miller ML, Anderson SA, Michaelides M, Jacobs MM, Peter C, Yiannoulos G, Liu X, Hurd YL. (2016). A Functional 3'UTR Polymorphism (rs2235749) of Prodynorphin Alters microRNA-365 Binding in Ventral Striatonigral Neurons to Influence Novelty Seeking and Positive Reward Traits. *Neuropsychopharmacology* 41, 2512-20.

Elmquist JK, Coppari R, Balthasar N, Ichinose M, Lowell BB. (2005). Identifying hypothalamic pathways controlling food intake, body weight, and glucose homeostasis. *J Comp Neurol* **493**, 63-71.

Ersche KD, Jones PS, Williams GB, Smith DG, Bullmore ET, Robbins TW. Distinctive personality traits and neural correlates associated with stimulant drug use versus familial risk of stimulant dependence. *Biol Psychiatry* **74**, 137-44.

Feenstra MGP, Botterblom MHA. (1996). Rapid sampling of extracellular dopamine in the rat prefrontal cortex during food consumption, handling and exposure to novelty. *Brain Res* **742**, 17-24.

Funahashi S, Bruce CJ, Goldman-Rakic PS. (1993). Dorsolateral prefrontal lesions and oculomotor delayed-response performance: evidence for mnemonic "scotomas". *J Neurosci* **13**, 1479-97.

Gabbott PL, Warner TA, Jays PR, Salway P, Busby SJ. (2005). Prefrontal cortex in the rat: projections to subcortical autonomic, motor, and limbic centers. *J Comp Neurol* **492**, 145-77.

García-López P, García-Marín V, Freire M. (2006). Three-dimensional reconstruction and quantitative study of a pyramidal cell of a Cajal histological preparation. *J Neurosci* **26**, 11249-52.

Gaykema RP, Newmyer BA, Ottolini M, Raje V, Warthen DM, Lambeth PS, Niccum M, Yao T, Huang Y, Schulman IG, Harris TE, Patel MK, Williams KW, Scott MM. (2017). Activation of murine pre-proglucagon-producing neurons reduces food intake and body weight. *J Clin Invest* **127**, 1031-45.

Gaykema RP, Nguyen XT, Boehret JM, Lambeth PS, Joy-Gaba J, Warthen DM, Scott MM. (2014). Characterization of excitatory and inhibitory neuron activation in the mouse medial prefrontal cortex following palatable food ingestion and food driven exploratory behavior. *Front Neuroanat* **8**, 60.

Gentet LJ, Kremer Y, Taniguchi H, Huang ZJ, Staiger JF, Peterson CCH. (2012). Unique functional properties of somatostatin-expressing GABAergic neurons in mouse barrel cortex. *Nat Neurosci* **15**, 607-12.

Ghazizadeh A, Ambroggi F, Odean N, Fields HL. (2012). Prefrontal cortex mediates extinction of responding by two distinct neural mechanisms in accumbens shell. *J Neurosci* **32**, 726-737.

Golden SA, Covington HE, Berton O, Russo SJ. (2011). A standardized protocol for repeated social defeat stress in mice. *Nat Protoc* **6**, 1183-91.

Hallock HL, Wang A, Griffin AL. (2016). Ventral midline thalamus is critical for hippocampal-prefrontal synchrony and spatial working memory. *J Neurosci* **36**, 8372-89.

Hansson C, Shirazi RH, Naslund J, Vogel H, Neuber C, Holm G, Anckarsater H, Dickson SL, Eriksson E, Skibicka KP. (2012). Ghrelin influences novelty seeking behavior in rodents and men. *PLoS One* **7**, e50409.

Hardung S, Epple R, Jackel Z, Eriksson D, Uran Cem, Senn V, Gibor L, Yizhar O, Diester I. (2017). A functional gradient in the rodent prefrontal cortex supports behavioral inhibition. *Current Biology* **27**, 549-555.

Hershenberg R, Satterthwaite TD, Daldal A, Katchmar N, Moore TM, Kable JW, Wolf DH. (2016). Diminished effort on a progressive ratio task in both unipolar and bipolar depression. *J Affect Disord* **196**, 97-100.

Hinney A, Vogel CIG, Hebebrand J. (2010). From monogenic to polygenic obesity: recent advances. *Eur Child Adolesc Psychiatry* **19**, 297-310.

Hioki H, Okamoto S, Konno M, Kameda H, Sohn J, Kuramoto E, Fujiyama F, Kaneko T. (2013). Cell type-specific inhibitory inputs to dendritic and somatic compartments of parvalbumin-expressing neocortical interneuron. *J Neurosci* **33**, 544-55.

Howard MW, Rizzuto DS, Caplan JB, Madsen JR, Lisman J, Aschenbrenner-Scheibe R, Schulze-Bonhage A, Kahana MJ. (2003). Gamma oscillations correlate with working memory load in humans. *Cerebral Cortex* **13**, 1369-1374.

Hsu LK, Mulliken B, McDonagh B, Krupa Das S, Rand W, Fairburn CG, Rolls B, McCrory MA, Saltzman E, Shikora S, Dwyer J, Roberts S. (2002). Binge eating disorder in extreme obesity. *Int J Obes Relat Metab Disord* **26**, 1398-403.

Ishikawa A, Ambroggi F, Nicola SM, Fields HL. (2008). Dorsomedial prefrontal cortex contribution to behavioral and nucleus accumbens neuronal responses to incentive cues. *J Neurosci* **28**, 5088-98.

Jeong JH, Lee DK, Jo YH. (2017). Cholinergic neurons in the dorsomedial hypothalamus regulate food intake. *Molecular metabolism* **6**, 306-12.

Johnson PM, Kenny PJ. (2010). Dopamine D2 receptors in addiction-like reward dysfunction and compulsive eating in obese rats. *Nat Neurosci* **35**, 635-41.

Johnson TN, Rosvold HE, Mishkin M. (1968). Projections from behaviorally-defined sectors of the prefrontal cortex to the basal ganglia, septum, and diencephalon of the monkey. *Experimental Neurology* **21**, 20-34.

Jones MW, Wilson MA. (2005). Theta rhythms coordinate hippocampal-prefrontal interactions in a spatial memory task. *PLOS Biology* **3**, e402.

Kamigaki T, Dan Y. (2017). Delay activity of specific prefrontal interneuron subtypes modulates memory-guided behavior. *Nat Neurosci* **20**, 854-63.

Karnani MM, Jackson J, Ayzenshtat I, Tucciarone J, Manoocheri K, Snider WG, Yuste R. (2016). Cooperative subnetworks of molecularly similar interneurons in mouse neocortex. *Neuron* **90**, 86-100.

Kawaguchi Y, Kondo S. (2003). Parvalbumin, somatostatin and cholecystokinin as chemical markers for specificGABAergic interneuron types in the rat frontal cortex. *J Neurocytol* **31**, 277-87.

Kawaguchi Y, Kubota Y. (1996). Physiological and morphological identification of somatostatin- or vasoactive intestinal polypeptide containing cells among GABAergic cell subtypes in rat frontal cortex. *J Neurosci* **16**, 2701-15.

Keefer SE, Petrovich GD. (2017). Distinct recruitment of basolateral amygdala-medial prefrontal cortex pathways across Pavlovian appetitive conditioning. *Neurobiology of Learning and Memory* **141**, 27-32.

Kim D, Jeong H, Lee J, Ghim J, Her ES, Lee S, Jung MW. (2016b). Distinct roles of parvalbumin- and somatostatin-expressing interneurons in working memory. *Neuron* **92**, 902-915.

Kim H, Ahrlund-Richter S. Wang X. Deisseroth K, Carlen M. (2016). Prefrontal parvalbumin neurons in control of attention. *Cell* **164**, 208-218.

King SJ, Rodrigues T, Watts A, Murray E, Wilson A, Abizaid A. (2016). Investigation of a role for ghrelin signaling in binge-like feeding in mice under limited access to high-fat diet. *Neuroscience* **319**, 233-45.

Kirkpatrick SL, Goldberg LR, Yazdani N, Babbs RK, Wu J, Reed ER, Jenkins DF, Bolgioni AF, Landaverde KI, Luttik KP, Mitchell KS, Kumar V, Johnson WE, Mulligan MK, Cottone P, Bryant CD. (2017). Cytoplasmic FMR1-Interacting Protein 2 Is a Major Genetic Factor Underlying Binge Eating. *Biol Psychiatry* **81**, 757-69.

Klein PM, Lu AC, Harper ME, McKown HM, Morgan JD, Beenhakker MP. (2018). Tenuous Inhibitory GABAergic Signaling in the Reticular Thalamus. *JNeurosci* **38**, 1232-48.

Kolb B, Nonneman AJ. (1975). Prefrontal cortex and the regulation of food intake in the rat. *J Comp Physiol Psychol* **88**, 806-15.

Krashes MJ, Koda S, Ye C, Rogan SC, Adams AC, Cusher DS, Maratos-Flier E, Roth BL, Lowell BB. (2011). Rapid, reversible activation of AgRP neurons drives feeding behavior In mice. *J Clin Invest* **121**, 1424-8.

Krebs RM, Schott BH, Schutze H, Duzel E. (2009). The novelty exploration bonus and its attentional modulation. *Neuropsychologia* **47**, 2272-81.

Kubota Y, Hattori R, Yui Y. (1994). Three distinct subpopulations of GABAergic neurons in rat frontal agranular cortex. *Brain Research* **649**, 159-173.

Kvitsiani D, Ranade S, Hangya B, Taniguchi H, Huang JZ, Kepecs A. (2013). Distinct behavioural and network correlates of two interneuron types in prefrontal cortex. *Nature* **498**, 363-66.

Laberge D, Kasevich R. (2007). The apical dendrite theory of consciousness. *Neural Netw* **20**, 1004-20.

Land BB, Narayanan NS, Liu RJ, Gianessi CA, Brayton CE, Grimaldi DM, Sarhan M, Guarnieri DJ, Deisseroth K, Aghajanian GK, DiLeone RJ. (2014). Medial prefrontal D1 dopamine neurons control food intake. *Nat Neurosci* **17**, 248-53.

Laucht M, Becker K, Blomeyer D, Schmidt MH. (2007). Novelty seeking involved in mediating the association between the dopamine D4 receptor gene exon III polymorphism and heavy drinking in male adolescents: results from a high-risk community sample. *Biol Psychiatry* **61**, 87-92.

Lavagnino L, Arnone D, Cao B, Soares JC, Selvaraj S. (2016). Inhibitory control in obesity and binge eating disorder: A systematic review and meta-analysis of neurocognitive and neuroimaging studies. *Neurosci Biobehav Rev* **68**, 714-26.

Lee AT, Vogt D, Rubenstein JL, Sohal VS. (2014). A class of GABAergic neurons in the prefrontal cortex sends long-range projections to the nucleus accumbens and elicits acute avoidance behavior. *J Neurosci* **35**, 11519-11525.

Lee S, Kruglikov I, Huang ZJ, Fishell G, Rudy B. (2013). A disinhibitory circuit mediates motor integration in the somatosensory cortex. *Nat Neurosci* **16**, 1662-70.

Li F, Li M, Cao W, Xu Y, Luo Y, Zhong X, Zhang J, Dai R, Zhou XF, Li Z, Li C. (2012). Anterior cingulate cortical lesion attenuates food foraging in rats. *Brain Res Bull* **88**, 602-8.

Liang B, Zhang L, Barbera G, Fang W, Zhang J, Chen X, Chen R, Li Y, Lin DT. (2018). Distinct and Dynamic ON and OFF Neural Ensembles in the Prefrontal Cortex Code Social Exploration. *Neuron* **100**, 700-14.

Lindgren E, Gray K, Miller G, Tyler R, Wiers CE, Volkow ND, Wang GJ. Food addiction: A common neurobiological mechanism with drug abuse. *Front Biosci (Landmark Ed)* **23**, 811-36.

Lisman JE, Grace AA. (2005). The hippocampal-VTA loop: controlling the entry of information into long-term memory. *Neuron* **46**, 703-13.

Liu D, Gu X, Zhu J, Zhang X, Han Z, Yan W, Cheng Q, Hao J, Fan H, Hou R, Chen Z, Chen Y, Li CT. (2014). Medial prefrontal activity during delay period contributes to learning of a working memory task. *Science* **346**, 458-63.

Liu J, Conde K, Zhang P, Lilascharoen V, Xu Z, Lim BK, Seeley RJ, Zhu JJ, Scott MM, Pang ZP. (2017). Enhanced AMPA Receptor Trafficking Mediates the Anorexigenic Effect of Endogenous Glucagon-like Peptide-1 in the Paraventricular Hypothalamus. *Neuron* **96**, 897-909.

Logue SF, Gould TJ. (2014). The neural and genetic basis of executive function: Attention, cognitive flexibility, and response inhibition. *Pharmacol Biochem Behav* **123**, 45-54.

Maldonado-Irizarry CS, Swanson CJ, Kelley AE. (1995). Glutamate receptors in the nucleus accumbens shell control feeding behavior via the lateral hypothalamus. *J Neurosci* **15**, 6779-88.

Mannella F, Gurney K, Baldassarre G. (2013). The nucleus accumbens as a nexus between values and goals in goal-directed behavior: a review and a new hypothesis. *Front Behav Neurosci* **7**, 135.

Marchant NJ, Furlong TM, McNally GP. (2010). Medial dorsal hypothalamus mediates the inhibition of reward seeking after extinction. *J Neurosci* **30**, 14102-15.

Marín O. (2012). Interneuron dysfunction in psychiatric disorders. *Nat Rev Neurosci* **13**, 107-20.

Markram H, Toledo-Rodriguez M, Wang Y, Gupta A, Silberberg G, Wu C. (2004). Interneurons of theneocortical inhibitory system. *Nat Rev Neurosci* **5**, 793-807.

Martin-Garcia E, Courtin J, Renault P, Fiancette JF, Wurtz H, Simonnet A, Levet F, Herry C, Deroche-Gamonet V. (2014). Frequency of Cocaine Self-Administration Influences Drug Seeking in the Rat: Optogenetic Evidence for a Role of the Prelimbic Cortex. *Neuropsychopharmacology* **39**, 2317-30.

Matsumoto M, Matsumoto K, Abe H, Tanaka K. (2007). Medial prefrontal cell activity signaling prediction errors of action values. *Nat Neurosci* **10**, 647-56.

Megías M, Emri Z, Freund TF, Gulyás AI. (2001). Total number and distribution of inhibitory and excitatory synapses on hippocampal CA1 pyramidal cells. *Neuroscience* **102**, 527-40.

Mena JD, Sadeghian K, Baldo BA (2011). Induction of Hyperphagia and Carbohydrate Intake by μ-Opioid Receptor Stimulation in Circumscribed Regions of Frontal Cortex. *J Neurosci* **31**, 3249-3260.

Mena JD, Selleck RA, Baldo BA. (2013). Mu-opioid stimulation in rat prefrontal cortex engages hypothalamic orexin/hypocretin-containing neurons, and reveals dissociable roles of nucleus accumbens and hypothalamus in cortically driven feeding. *J Neurosci* **33**, 18540-52.

Miller EK, Freedman DJ, Wallis JD. (2002). The prefrontal cortex: categories, concepts and cognition. *Philos Trans R Soc Lond B Biol Sci.* **357**, 1123-36.

Mogil JS, Wilson SG. (1997). Nociceptive and morphine antinociceptive sensitivity of 129 and C57BL/6 inbred mouse strains: implications for transgenic knock-out studies. *Eur J Pain* **1**, 293-7.

Moorman DE, and Aston-Jones G. (2015). Prefrontal neurons encode context based response execution and inhibition in reward seeking and extinction. *Proc Natl Acad Sci USA* **112**, 9472-7.

Moorman DE, James MH, McGlinchley EM, Aston-Jones G. (2015). Differential roles of medial prefrontal subregions in the regulation of drug seeking. *Brain Res* **1628**, 130-146.

Munuera J, Rigotti M, Salzman CD. (2018). Shared neural coding for social hierarchy and reward value in primate amygdala. *Nat Neurosci* **21**, 415-23.

Murugan M, Jang HJ, Park M, Miller EM, Cox J, Taliaferro JP, Parker NF, Bhave V, Hur H, Liang Y, Nectow AR, Pillow JW, Witten IB. (2017). Combined Social and Spatial Coding in a Descending Projection from the Prefrontal Cortex. *Cell* **171**, 1663-77 e16.

Newmyer BA, Whindleton CM, Klein PM, Beenhakker MP, Jones MK, Scott MM. (2019). VIPergic neurons of the infralimbic and prelimbic cortices control palatable food intake through separate cognitive pathways. *JCI Insight* **2**, 5.

Newmyer BA, Whindleton CM, Srinivasa N, Jones MK, Scott MM. (2019B). Genetic variation affects binge feeding behavior in female inbred mouse strains. *Scientific Reports*, submitted April, 2019.

Newmyer BA, Warthen DM, Rogers NP, Hatter J, Zweifel LS, Scott MM. (2019C). The prefrontal cortical projection to the nucleus accumbens is required for novel object and novel environment driven investigatory behavior in the mouse. *eNeuro*, submitted May, 2019.

O'Driscoll K, Leach JP. (1998). "No longer Gage": an iron bar through the head. Early observations of personality change after injury to the prefrontal cortex. *BMJ* **317**, 1673-4.

Obermayer J, Luchicchi A, de Kloet SF, Terra H, Bruinsma B, Heistek TS, Mnie-Filali O, Kortleven C, Kroon T, Jonker AJ, Khalil AJ, de Haan R, Goriounova NA, van den Berg WDJ, de Kock CPJ, Pattijj T, Mansvelder HD. (2018). Prefrontal cortical ChAT-VIP interneurons provide local excitation by cholinergic synaptic transmission and control attention. *Preprint only*.

Oliva R, Morys F, Horstmann A, Castiello U, Begliomini C. (2019). The impulsive brain: Neural underpinnings of binge eating behavior in normal-weight adults. *Appetite* **136**, 33-49.

Padoa-Schioppa C, Assad JA. (2006). Neurons in the orbitofrontal cortex encode economic value. *Nature* **441**, 223–226.

Panaro BL, Cone RD. (2013). Melanocortin-4 receptor mutations paradoxically reduce preference for palatable foods. *Proc Natl Acad Sci USA* **110**, 7050-5.

Paxinos G, Franklin KBJ. The mouse brain in stereotaxic coordinates. Amsterdam ; Boston: Elsevier Academic Press; 2004.

Pelloux Y, Murray JE, Everitt BJ. (2013). Differential roles of the prefrontal cortical subregions and basolateral amygdala in compulsive cocaine seeking and relapse after voluntary abstinence in rats. *Eur J Neurosci* **38**, 3018-26.

Peters J, LaLumiere RT, Kalivas PW. (2008). Infralimbic prefrontal cortex is responsible for inhibiting cocaine seeking in extinguished rats. *J Neurosci* **28**, 6046-53.

Petrovich GD, Holland PC, Gallagher M. (2005). Amygdalar and prefrontal pathways to the lateral hypothalamus are activated by a learned cue that stimulates eating. *J Neurosci* **25**, 8295-302.

Petrovich GD, Ross CA, Holland PC, Gallagher M. (2007). Medial Prefrontal Cortex Is Necessary for an Appetitive Contextual Conditioned Stimulus to Promote Eating in Sated Rats*. J Neurosci* **27**, 6436-6441.

Pfeffer CK, Xue M, He M, Huang ZJ, Scanziani M. (2013). Inhibition of inhibition in visual cortex: the logic of connections between molecularly distinct interneurons. *Nat Neurosci* **16**, 1068-76.

Pfeffer CK. (2014). Inhibitory neurons: VIP cells hit the brake on inhibition. *Current Biology* **24**, R18-R20.

Pi H, Hangya B, Kvitsiani D, Sanders JI, Huang ZJ, Kepecs A. (2013). Cortical interneurons that specialize in disinhibitory control. *Nature* **503**, 521-524.

Pinto L, Dan Y. (2015). Cell type-specific activity in the prefrontal cortex during goal-directed behavior. *Neuron* **87**, 437-450.

Puglisi-Allegra S, Ventura R. (2012). Prefrontal/accumbal catecholamine system processes high motivational salience. *Front Behav Neurosci* **6**, 31.

Radley JJ, Gosselink KL, Sawchenko PE. (2009). A discrete GABAergic relay mediates medial prefrontal cortical inhibition of the neuroendocrine stress response. *J Neurosci* **29**, 7330-40.

Rebec GV, Christensen JR, Guerra C, Bardo MT. (1997). Regional and temporal differences in real-time dopamine efflux in the nucleus accumbens during free-choice novelty. *Brain Res* **776**, 61-7.

Reed P, Mitchell C, Nokes T. (1996). Intrinsic reinforcing properties of putatively neutral stimuli in an instrumental two-lever discrimination task. *Animal Learning and Behavior* **24**, 38-45.

Reichelt AC, Morris MJ, Westbrook RF. (2014). Cafeteria diet impairs expression of sensory-specific satiety and stimulus-outcome learning. *Front Psychol* **5**, 852.

Reppucci CJ, Petrovich GD. (2012). Learned food-cue stimulates persistent feeding in sated rats. *Appetite* **59**, 437-447.

Richard JM, Berridge KC. (2013). Prefrontal cortex modulates desire and dread generated by nucleus accumbens glutamate disruption. *Biol Psychiatry* **73**, 360-70.

Rolls ET, Murzi E, Yaxley S, Thorpe SJ, Simpson SJ. (1986). Sensory specific satiety: food-specific reduction in responsiveness of ventral forebrain neurons after feeding in the monkey. *Brain Res* **368**, 79-86.

Rose JE, Woolsey CN. (1948). The orbitofrontal cortex and its connections with the mediodorsal nucleus in rabbit, sheep and cat. *Res Publ Assoc Res Nerv Ment Dis.* **27**, 210-32.

Rotella F, Mannucci E, Gemignani S, Lazzeretti L, Fioravanti G, Ricca V. Emotional eating and temperamental traits in Eating Disorders: A dimensional approach. *Psychiatry Res* **264**, 1-8.

Rudebeck PH, Walton ME, Smyth AN, Bannerman DM, Rushworth MFS. (2006). Separate neural pathways process different decision costs. *Nat Neurosci* **9**, 1161-8.

Rudy B, Fishell G, Lee S, Hjerling-Leffler J. (2011). Three groups of interneurons account for nearly 100% of neocortical GABAergic neurons. *Dev Neurobiol* **71**, 45-61.

Sanchez CJ, Bailie TM, Wu WR, Li N, Sorg BA. (2003). Manipulation of dopamine d1-like receptor activation in the rat medial prefrontal cortex alters stress- and cocaine-induced reinstatement of conditioned place preference behavior. *Neuroscience* **119**, 497-505.

Schultz W. (1998). Predictive reward signal of dopamine neurons. *J Neurophysiol* **80**, 1-27.

Scott MM, Marcus JN, Pettersen A, Birnbaum SG, Mochizuki T, Scammell TE, Nestler EJ, Elmquist JK, Lutter M. (2011). Hcrtr1 and 2 signaling differentially regulates depression-like behaviors. *Behav Brain Res* **222**, 289-94.

Seamans JK, Floresco SB, Phillips AG. (1995). Functional differences between the prelimbic and anterior cingulate regions of the rat prefrontal cortex. *Behav Neurosci* **109**, 1063-73.

Seo DO, Funderburk SC, Bhatti DL, Motard LE, Newbold D, Girven KS, McCall JG, Krashes M, Sparta DR, Bruchas MR. (2016). A GABAergic Projection from the Centromedial Nuclei

of the Amygdala to Ventromedial Prefrontal Cortex Modulates Reward Behavior. *J Neurosci* **36**, 10831-42.

Simon JJ, Skunde M, Walther S, Bendszus M, Herzog W, Friederich HC. Neural signature of food reward processing in bulimic-type eating disorders. *Soc Cogn Affect Neurosci* **11**, 1393-401.

Smith CJW, Mogavero JN, Tulimieri MT, Veenema AH. (2017). Involvement of the oxytocin system in the nucleus accumbens in the regulation of juvenile social novelty-seeking behavior. *Hormones and behavior* **93**, 94-8.

Somogyi P, Nunzi MG, Gorio A, Smith AD. (1983). A new type of specific interneuron in the monkey hippocampus forming synapses exclusively with the axon initial segments of pyramidal cells. *Brain Res* **259**, 137-42.

Sonntag KC, Brenhouse HC, Freund N, Thompson BS, Puhl M, Anderson SL. (2014). Viral over-expression of D1 dopamine receptors in the prefrontal cortex increase high-risk behaviors in adults: Comparison with adolescents. *Psychopharmacology* **231**, 1615-26.

Stefanik MT, Moussawi K, Kupchik YM, Smith KC, Miller RL, Huff ML, Deisseroth K, Kalivas PW, LaLumiere RT. (2013). Optogenetic inhibition of cocaine seeking in rats. *Addict Bio* **18**, 50-3.

Steketee JD. (2003). Neurotransmitter systems of the medial prefrontal cortex: potential role in sensitization to psychostimulants. *Brain Res Rev* **41**, 203-228.

Stryker MP. (2014). A neural circuit that controls cortical state, plasticity, and the gain of sensory responses in mouse. *Cold Spring Harb Symp Quant Biol* **79**, 1-9.

Suzuki S, Cross L, O'Doherty JP. (2017). Elucidating the underlying components of food valuation in the human orbitofrontal cortex. *Nat Neurosci* **20**, 1780-6.

Sweet LH, Hassenstab JJ, McCaffery JM, Raynor HA, Bond DS, Demos KE, Haley AP, Cohen RA, Del Parigi A, Wing RR. (2012). Brain response to food stimulation in obese, normal weight, and successful weight loss maintainers. *Obesity (Silver Spring)* **20**, 2220-5.

Taki K, Kaneko T, Mizuno N. (2000). A group of cortical interneurons expressing μ-opioid receptor-like immunoreactivity: a double immunofluorescence study in the rat cerebral cortex. *Neuroscience* **92**, 221-231.

Teffer K, Semendeferi K. (2012). Human prefrontal cortex: evolution, development, and pathology. 1st ed. Elsevier B.V.; 191-218.

Thanos PK, Roushdy K, Sarwar Z, Rice O, Ashby CR, Jr., Grandy DK. (2015). The effect of dopamine D4 receptor density on novelty seeking, activity, social interaction, and alcohol binge drinking in adult mice. *Synapse* **69**, 356-64.

Thomsen M, Caine SB. (2006). Cocaine self-administration under fixed and progressive ratio schedules of reinforcement: comparison of C57BL/6J, 129X1/SvJ, and 129S6/SvEvTac inbred mice. *Psychopharmacology (Berl).* **184**, 145-54.

Thomsen M, Caine SB. (2011). Psychomotor stimulant effects of cocaine in rats and 15 mouse strains. *Exp Clin Psychopharmacol*. **19**, 321-41.

Uddin LQ. (2014). Salience processing and insular cortical function and dysfunction. *Nat Rev Neurosci* **16**, 55-61.

Ursin H, Rosvold HE, Vest B. (1969). Food preference in brain lesioned monkeys. *Physiology and Behavior* **4**, 609-612.

Uylings HBM, Groenewegen HJ, Kolb B. (2003). Do rats have a prefrontal cortex? *Behav Brain Res* **146**, 3-17.

Ventura R, Cabib S, Alcaro A, Orsini C, Puglisi-Allegra S. (2003). Norepinephrine in the prefrontal cortex is critical for amphetamine-induced reward and mesoaccumbens dopamine release. *J Neurosci* **23**, 1879-1885.

Ventura R, Latagliata EC, Morrone C, La Mela I, Puglisi-Allegra S. (2008). Prefrontal norepinephrine determines attribution of “high” motivational salience. *PLoS One* **3**, 3044.

Ventura R, Morrone C, Puglisi-Allegra S. (2007). Prefrontal/accumbal catecholamine system determines motivational salience attribution to both reward- and aversion-related stimuli. *Proc Natl Acad Sci* **104**, 5181-6.

Verberne AJ, Lewis SJ, Worland PJ, Beart PM, Jarrott B, Christie MJ, Louis WJ. (1987). Medial prefrontal cortical lesions modulate baroreflex sensitivity in the rat. *Brain Res* **426**, 243-9.

Vertes RP. (2004). Differential projections of the infralimbic and prelimbic cortex in the rat. *Synapse* **51**, 32-58.

Vialou V, Bagot RC, Cahill ME, Ferguson D, Robison AJ, Dietz DM, Fallon B, Mazei-Robison M, Ku SM, Harrigan E, Winstanley CA, Joshi T, Feng J, Berton O, Nestler EJ. (2014). Prefrontal cortical circuit for depression- and anxiety-related behaviors mediated by cholecystokinin: role of DeltaFosB. *J Neurosci* **34**, 3878-87.

Vidal-Gonzalez I, Vidal-Gonzalez B, Rauch SL, Quirk GJ. (2006). Microstimulation reveals opposing influences of prelimbic and infralimbic cortex on the expression of conditioned fear. *Learn Mem* **13**, 728-733.

Vogt BA, Paxinos G. (2014). Cytoarchitecture of mouse and rat cingulate cortex with human homologies. *Brain Struct Funct* **219**, 185-92.

Volkow ND, Wise RA, and Baler R. (2017). The dopamine motive system: implications for drug and food addiction. *Nat Rev Neurosci* **18**, 741-52.

Walker F, Mock M, Feyerabend M, Guy J, Wagener RJ, Schubert D, Staiger JF, Witte M. (2016). Parvalbumin- and vasoactive intestinal polypeptide-expressing neocortical interneurons impose differential inhibition on Martinotti cells. Nature communications **7**,13664.

Wall NR, De La Parra M, Sorokin JM, Taniguchi H, Huang ZJ, Callaway EM. (2016). Brain-Wide Maps of Synaptic Input to Cortical Interneurons. *J Neurosci* **36**, 4000-9.

Wang Y, Gupta A, Toledo-Rodriguez M, Wu CZ, Harkram H. (2002). Physiological, molecular and circuit properties of nest basket cells in the developing somatosensory cortex. *Cerebral cortex* **12**, 395-410.

Warthen DM, Lambeth PS, Ottolini M, Shi Y, Barker BS, Gaykema RP, Newmyer BA, Joy-Gaba J, Ohmura Y, Perez-Reyes E, Guler AD, Patel MK, Scott MM. (2016). Activation of pyramidal neurons in mouse medial prefrontal cortex enhances food-seeking behavior while reducing impulsivity in the absence of an effect on food intake. *Front Behav Neurosci* **10**, 63.

Wolfe BE, Baker CW, Smith AT, Kelly-Weeder S. (2009). Validity and utility of the current definition of binge eating. *Int J Eat Disord* **42**, 674-86.

Xu H, Liu L, Tian Y, Wang J, Li J, Zheng J, Zhao H, He M, Xu T, Duan S, Xu H. (2019). A disinhibitory microcircuit mediates conditioned social fear in the prefrontal cortex. *Neuron* in press, corrected proof.

Yang CF, Chiang MC, Gray DC, Prabhakaran M, Alvarado M, Juntti SA, Unger EK, Wells JA, Shah NM. (2013). Sexually dimorphic neurons in the ventromedial hypothalamus govern mating in both sexes and aggression in males. *Cell* **153**, 896-909.

Yang Y, Raine A. (2009). Prefrontal structural and functional brain imaging findings in antisocial, violent, and psychopathic individuals: a meta-analysis. *Psychiatry Res* **174**, 81-8.

Yizhar O, Fenno LE, Prigge M, Schneider F, Davidson TJ, O'Shea DJ, Sohal VS, Goshen I, Finkelstein J, Paz JT, Stehfest K, Fudim R, Ramakrishnan C, Huguenard JR, Hegemann P, Deisseroth K. (2011). Neocortical excitation/inhibition balance in information processing and social dysfunction. *Nature* **477**, 171-178.

Zhang Y, Kerman IA, Laque A, Nguyen P, Faouzi M, Louis GW, Jones JC, Rhodes C, Munzberg H. (2011). Leptin-receptor-expressing neurons in the dorsomedial hypothalamus and median preoptic area regulate sympathetic brown adipose tissue circuits. *J Neurosci* **31**, 1873-84.

Zhou X, Rickmann M, Hafner G, Staiger JF. (2017). Subcellular Targeting of VIP Boutons in Mouse Barrel Cortex is Layer-Dependent and not Restricted to Interneurons. *Cereb Cortex* **27**, 5353-68.